NASA Contractor Repor

Large Deployable [illegible]enna Program

Phase I: Technology A[illegible]ssment and Mission Architec[illegible]

Craig A. Rogers and Warren L. S[illegible]

CONTRACT NAS1-18471
OCTOBER 1991

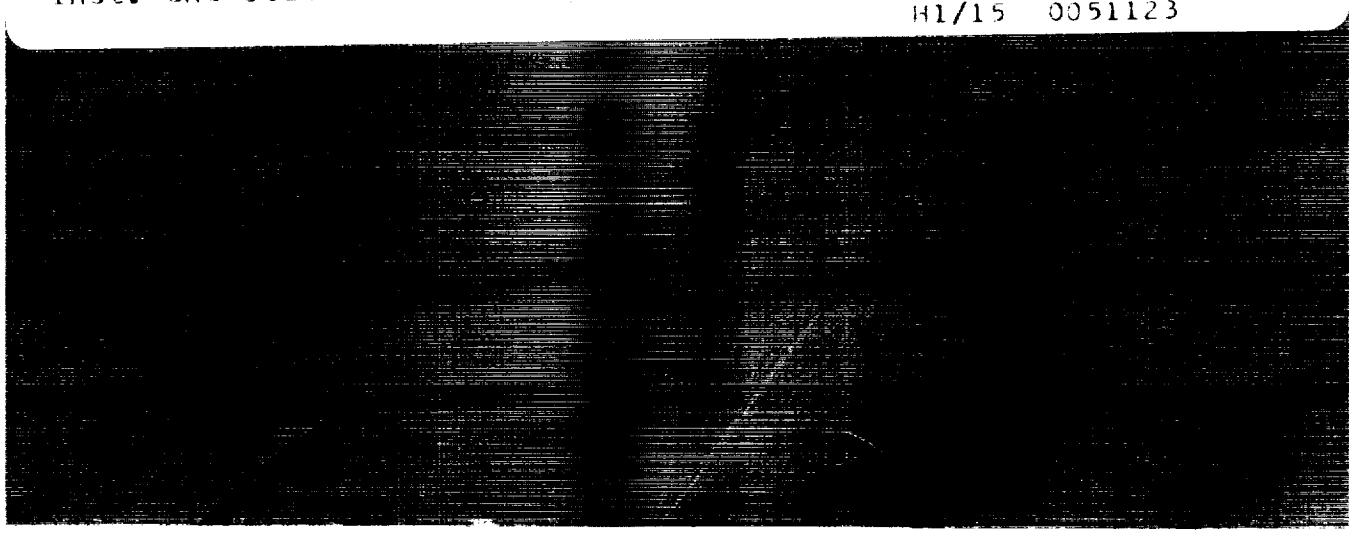

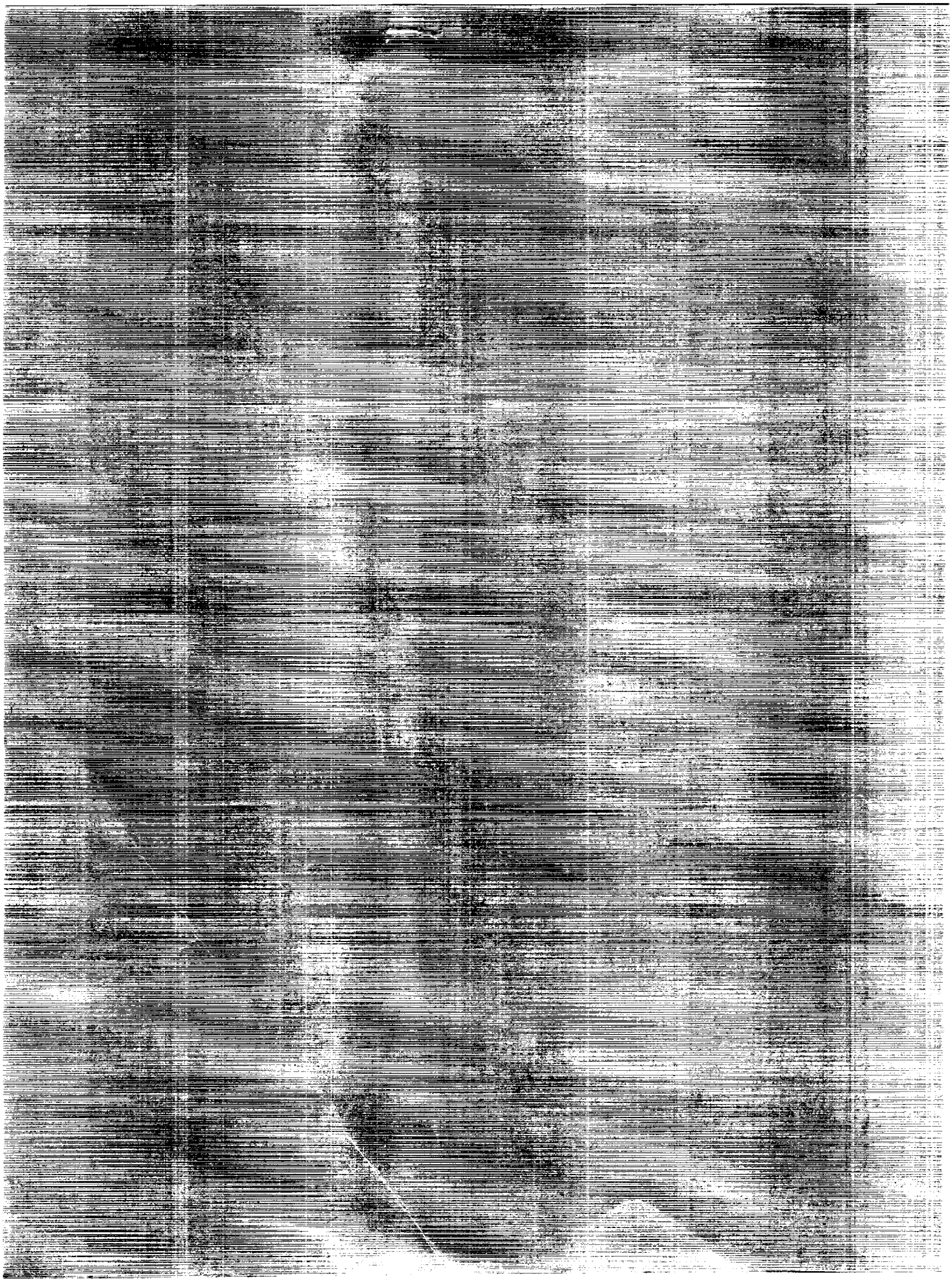

NASA Contractor Report 4410

Large Deployable Antenna Program

Phase I: Technology Assessment and Mission Architecture

Craig A. Rogers and Warren L. Stutzman
Virginia Polytechnic Institute and State University
Blacksburg, Virginia

Prepared for
Langley Research Center
under Contract NAS1-18471

National Aeronautics and
Space Administration
Office of Management
Scientific and Technical
Information Program
1991


INTENTIONALLY

TABLE OF CONTENTS

EXECUTIVE SUMMARY

The Large Deployable Antenna (LDA) Program was initiated to investigate and demonstrate the availability of critical technologies for passive microwave sensing which will be required for Mission to Planet Earth and for the NASA Office of Astronautics, Exploration and Technology (OAET) Global Change Technology Initiative (GCTI) which is scheduled for initiation in Fiscal Year 1991. The goal of GCTI "is to provide the technology needed to enable and enhance the long term observations, documentation and understanding of the earth as a system". Mission to Planet Earth, from the 1987 Sally Ride report to the NASA Administrator, is a concept referring to the endeavor of making long-term, space-based global observations for the purpose of understanding earth system processes.

The specific goals for the first phase of the LDA program were to:

- Review the technology state-of-readiness for large, precise, wide scanning passive radiometers up to 60 GHZ.

- Determine the critical technologies of the radiometer concepts presented to the study team and prioritize them.

- Develop preliminary mission architecture for each radiometer concept presented to the study team.

- Evaluate generic technologies to support large deployable reflectors.

The study team was composed of university and industry researchers and technologists with a wide range of skills and experience, including the following:

1. Principal Investigator: Dr. Craig A. Rogers, Department of Mechanical Engineering, Virginia Polytechnic Institute and State University
2. Dr. Warren Stutzman, Department of Electrical Engineering, Virginia Polytechnic Institute and State University
3. Dr. Harry Robertshaw, Department of Mechanical Engineering, Virginia Polytechnic Institute and State University
4. Mr. Mark Thomson, Astro Aerospace Company, Inc.
5. Dr. John Hedgepeth, Consultant, Astro Aerospace Company, Inc.
6. Mr. John Rule, Composite Optics, Inc.
7. Mr. Ed Derby, Composite Optics, Inc.
8. Dr. Brian Lilly, ANT Technologies, Inc.
9. Additional input was received from the Electromagnetic Advisory Panel convened by NASA Langley

The study approach involved determining basic operational parameters and configurations for a geosynchronous wide-scanning radiometer from which specific structural requirements were used as goals (rather than specifications) with which specific technologies could be evaluated.

The study team performed a detailed technology review, evaluated the feasibility and technology

readiness for a dual-reflector radiometer with a target size of 40 m for the main reflector. The team also developed a system design for a deployable radiometer scaled down to stow in a Titan IV launch vehicle. The study resulted in the following conclusions:

- The deployable dual-reflector radiometer configuration should be reduced from a 40-meter baseline to a 20-25 meter baseline.

- The largest deployable stiff dual reflector configuration which can be stowed in a Titan IV or Space Shuttle is approximately 20-25 meters (parent reflector) in diameter.

- A passively controlled 40-meter radiometer configuration requires a deep truss and thermal controls to satisfy the accuracy requirements at 40 GHz.

- Segmented 'stiff' reflectors about 3 m^2 have been designed to meet the surface accuracy requirements with an areal density of 2.4 kg/m^2.

- Several 'furlable' concepts have been developed using a gore or strip approach to deploying the reflector surface on the truss structure. The maximum width to satisfy the surface accuracy requirements is 12 m.

- Practically inextensible membrane reflectors may be possible for sizes up to 40 meters in diameter. However, several basic fundamental investigations are still needed to identify suitable materials; develop manufacturing techniques; design a reliable mechanical deployment scheme; quantify surface accuracy as a function of manufacturing variations, thermal stresses, edge distortions and deployment load variations; and suitability for ground testing.

- An active deployment scheme for stiff reflectors using shape memory alloys has been investigated and a detailed constitutive model formulated for further studies.

- Further study is needed in the following area:

    1. Detailed EM analysis of the baseline designs.
    2. Examination of alternative radiometric antenna configurations.
    3. Technology review and assessment of 20-30 meter antenna designs.
    4. Determination of remote sensing requirements for a 20-30 m antenna.

The study team also concluded that a specific mission focus is needed in order to efficiently and accurately determine the mission architecture and the state-of-readiness of the technology to support specific configurations. Upon selection of a mission focus, or determination of specific design goals, electromagnetic configurations can then be proposed for which specific structural and control requirements can be determined. With these specifications and requirements, a detailed technology assessment and point design can be completed.

1. INTRODUCTION

1.1 Mission to Planet Earth

In August of 1987, Dr. Sally K. Ride published "A Report to the Administrator" entitled, LEADERSHIP and America's Future in Space, which defined four potential U.S. space initiatives and evaluated them in light of the current space program and the nation's desire to regain and retain space leadership [1-1]. The Dr. Ride task group identified four candidate initiatives for study and evaluation, which they stated, "builds on NASA's achievements in science and exploration and each is a bold, aggressive proposal which would, if adopted, restore the United States to a position of leadership in a particular sphere of space activity." The four selected initiatives identified by the report are:

1. Mission to Planet Earth
2. Exploration of the Solar System
3. Outpost on the Moon
4. Humans to Mars

The technology program described in this report is in support of Mission to Planet Earth, a program (as described by the task group) that would use the perspective afforded from space to study and characterize our home planet on a global scale. Specifically, the mission is "an initiative to understand our home planet, how forces shape and affect its environment, how that environment is changing, and how those changes will affect us. The goal of this initiative is to obtain a comprehensive scientific understanding of the entire Earth System, by describing how its various components function, how they interact, and how they may be expected to evolve on all time scales. The challenge is to develop a fundamental understanding of the Earth System, and of the consequences of changes to that system, in order to eventually develop the capability to predict changes that might occur - either naturally, or as a result of human activity."

The principal concept of the Mission to Planet Earth is that data gathered over a decade or more from a space-based global perspective can be compared with data from earth-based observations to produce models for global change which are more comprehensive - and presumably more accurate - than any present-day models. Toward that end, the guiding principle behind the Mission to Planet Earth Initiative is the adoption of an integrated approach to observing the earth. Implementation of this OSSA (Office of Space Science and Applications) initiative has been proposed for Fiscal Year 1992 [1-2].

While current OAET (Office of Aeronautics, Exploration, and Technology) programs support OSSA's near-term missions, particularly the Civil Space Technology Initiative (CSTI), new technology efforts will be necessary to progress into the next era of earth observation, beyond the 5-year scope of CSTI [1-2]. To ensure availability of the technologies which will be required for the Mission to Planet Earth, OAET is developing a Global Change Technology Initiative (GCTI) for initiation in Fiscal Year 1991. The goal of this initiative is to provide the technology needed to enable and enhance the long-term observation, documentation, and scientific understanding of the earth as a system.

In July of 1988, an Ad Hoc Review Team on Space Technologies was formed to determine what

technologies must be developed in the near term to support Mission to Planet Earth. In their report entitled "Technology for the Mission to Planet Earth" they described the major space segments for the mission [1-2].

The three proposed mission classes that form the space segments for the Mission to Planet Earth are the Earth Observing System (EOS), the Earth System Explorer missions, and the advanced Geostationary Earth Science platforms. Each of these space segments described in detailed in the report "Technology for the Mission to Planet Earth" are given below.

EOS, a series of low earth polar orbit platforms, each containing multiple scientific instruments, is being planned to begin deployment in the mid-1990s. Subsequent launches will provide growth in the number and quality of remote sensing capabilities through the year 2000, and continuous operation of the system at full capacity until at least 2010. The EOS mission will create an integrated scientific observing system that will enable long-term multi-disciplinary study of the earth.

The second space segment is a proposed series of Explorer-class missions called Earth Probes, and the use of well-established instruments mounted on long-term platforms such as the space station. In addition to the powerful synergisms within EOS, there are some observing needs that require other low earth orbit (LEO) configurations or dedicated space craft.

The third possible space segment of a total system for global earth observation consists of advanced platforms in geosynchronous earth orbit (GEO). Foremost in the advantages these platforms will offer over other platforms is the capacity for high temporal resolution, limited only by instrument design and cost, to be brought to bear on the study of rapidly changing, global atmospheric phenomena. This type of orbit also would provide a fixed reference geometry for a given earth location, facilitating data analysis and interpretation; this advantage has been demonstrated by operational geosynchronous satellites, in service since 1974, which carry imager/sounder instruments providing high-resolution visible and infrared images of the earth. The infrared channels of the sounding instruments yield frequent temperature and moisture profiles over large areas of the earth. Another major advance would be passive-microwave sensing of regions of precipitation.

For the technology program described in this report, the current focus is on the passive-microwave sensing instrument for the geosynchronous earth orbit advanced platforms. The Ad Hoc Review Team on Space Technologies stated in their report that "the capability of microwave sounding is not now available because of the large antenna required for adequate spatial resolution at GEO altitudes." This specific technology need is the motivation for this program.

1.2 Technology Needs

The objectives of the Ad Hoc Review Team on Space Technologies was to determine what technologies must be developed in the near term to support Mission to Planet Earth. Along with another ad hoc group of the Committee on Space Research (COSPAR), they have identified the measurement of precipitation and soil moisture as high priority new technologies. These technologies have so far remained unobservable from space but should be developed to measure

global change parameters.

To determine the technology needs accurately, the science needs, priorities, and requirements must be defined. Once the science requirements are specified, specific mission and system planning is then possible. The technology review team identified a lack of coherent architecture as hampering their discussion of the Mission to Planet Earth and GCTI's support of it. "The committee felt hampered in their ability to assess OAET's GCTI plans because of insufficient mission and system planning and analysis." Adequate definition of architecture was viewed as prerequisite to their addressing many technology issues. NASA however, has had a basic assumption that full implementation of Mission to Planet Earth will include placing observation platforms in GEO. This assumption has influenced NASA's selection of key technologies to be emphasized in the GCTI.

NASA's scientists and technologists feel that a major advantage of GEOs for earth observing platforms is the ability to acquire continuous observations with high temporal resolution, i.e., to be able to stare at a scene. Earth system processes which require high temporal resolution observations also require high spatial resolution. Despite the substantially greater altitude of GEOs over the orbits of the EOS and the Explorer-class missions, the phenomena observed require the highest possible spatial resolution. This in turn means greater requirements for precision pointing and platform control.

Technology developments in precision pointing and vibration control for remote sensing instruments are important for the accurate pointing of multiple instruments and for large radiometric antennas. In the technology review teams' report they often used an 80 meter diameter antenna as a baseline for evaluating the technology issues. The goal of the GEO platform is to allow simultaneous and continuous observation of the earth by multiple instruments with minimal interference.

Advanced sensors and detector arrays would permit remote sensing across the electromagnetic spectrum from the microwave to the ultraviolet. Three regions of the spectrum, the submillimeter range (300 to 3000 GHz), the millimeter range (30 to 300 GHz), and the thermal infrared range (5 to 20 microns), are especially critical for understanding global climate change. The region from 1 to 200 GHz was cited as being particularly useful for metrology.

The technology review team also identified a particular need for large precision antennas. They made the following arguments concerning the technology needs for large antenna systems.

> "Large precision antennas would enable microwave sounding with adequate spatial resolution from geosynchronous orbit. Since it is estimated that about half of the earth's rainfall occurs in short-lived, small-scale storms, resolution corresponding to the size of these storms (10 km) is needed to provide complete rainfall monitoring data. Observations at 36 GHz with an earth footprint of 10 km require an antenna diameter of 40 meters. These large antennas would require precision shape correction and steering to allow coverage of the globe, either mechanically or through receiver array adjustments. Measurements above about 36 GHz require solid surface reflectors while lower frequency measurements can use large mesh reflectors. Unfilled aperture or interferometric techniques could provide an

alternative approach for the large antennas needed for frequencies less than 36 GHz. Special microwave-transparent structural materials may be necessary to achieve the instrument performance requirements. Array feeds will be required for effective offboresight pointing and scanning."

Another related technology need is advanced materials for both low earth and geosynchronous orbit environments. Technology research in long-life materials and structures will be aimed at developing and characterizing new structural materials for long-term operation. This research should include scaling up and characterizing promising new material systems into structural subelements for large precision platforms and reflector support structures; currently available materials may not provide the required specific stiffness and thermal stability for very large structures.

Conclusions: High priority items associated with the science aspects of the mission included the passive microwave remote sensing which resulted in a number of technology development needs, including advanced sensors and detectors, precision pointing and vibration controls, and advanced materials. All of these items have been made a part of the Large Deployable Antenna program.

1.3 LDA Program Objectives

The NASA Contract Task is entitled "Definition of Large Deployable Space Antenna Structure Concepts," a program involving the detailed definition, assessment, and selection of conceptual designs for a Large Deployable Antenna (LDA). The focus of this effort is technology readiness for the application of large modular reflectors to millimeter wave frequency (6 - 60 GHz) radiometers for future NASA Global Observation missions from the Earth Science Geophysical Platform (ESGP). Phase I of the program was oriented toward definition of the most feasible antenna concepts/designs for accomplishing the mission and evaluation of existing technology to support the mission. Phase II will consist of the development and testing of critical hardware components and selection of a point design, complete with preliminary engineering specifications and sketches. The specifications shall be of sufficient detail such that after the completion of this task, these specifications can be used to initiate a new procurement for follow-on development of a test article to demonstrate technology readiness.

For this effort, Virginia Tech has assembled a team of university and industry technologists which possess expertise in the areas of controls, structures, and electromagnetic technology. This team was charged with identifying suitable technologies, as well as innovative approaches to implementation of these technologies to the focus mission.

The primary objective of the LDA program is to demonstrate by means of ground test articles that the technology is available for a large-deployable wide-scanning radiometer. To this end, the focus of the Phase I and II efforts is to develop concepts and configurations for such a flight article, determine the state-of-readiness of the technology, evaluate and prioritize the critical technologies, perform trade studies and down-selection of alternate technologies, select test articles which will demonstrate the state-of-readiness and design such items to a degree that they can be specified in a future RFP.

The test article(s) requirements are straightforward to determine when the objective of the test articles is kept in mind. It is necessary to accommodate anticipated mission requirements associated with the critical component technologies. The plan for determining the test article requirements follows.

1. Evaluate all the radiometer configurations proposed by the EM Advisory Board

2. Determine the essential critical component technologies needed to be demonstrated in a ground-test article

3. Beginning with mission architecture specifications as compiled and iterated on by NASA-LaRC, Virginia Tech, the EM Advisory Board, determine the design specifications for each test article component, performance criteria, etc.

4. Circulate the selected design specifications to Virginia Tech who, in turn, will circulate to NASA-LaRC AMRB for comment and review

5. Develop test article configurations(s) that demonstrate the technologies selected in (2)

As a starting point, the following test article design goals in Table 1.3-1 and Fig. 1.3-1 were adopted. Please note that as the trade studies progress and designs begin to appear, that some of the parameters listed will be inconsequential. Likewise, there are many parameters that are presently missing from the list (e.g., control related parameters) which must be added.

The global mission requirements and specifications will be impossible to firmly determine until the science requirements have been agreed upon and set. A great deal of effort is being expended to determine the overall objectives of the radiometer instrument(s) and the necessary requirements and specifications. Because of the complexity of the instrument, the science and hardware requirements will be determined in a somewhat iterative fashion. Interaction between the electromagnetics, science and structural communities will be needed to achieve realistic and achievable design requirements and specifications.

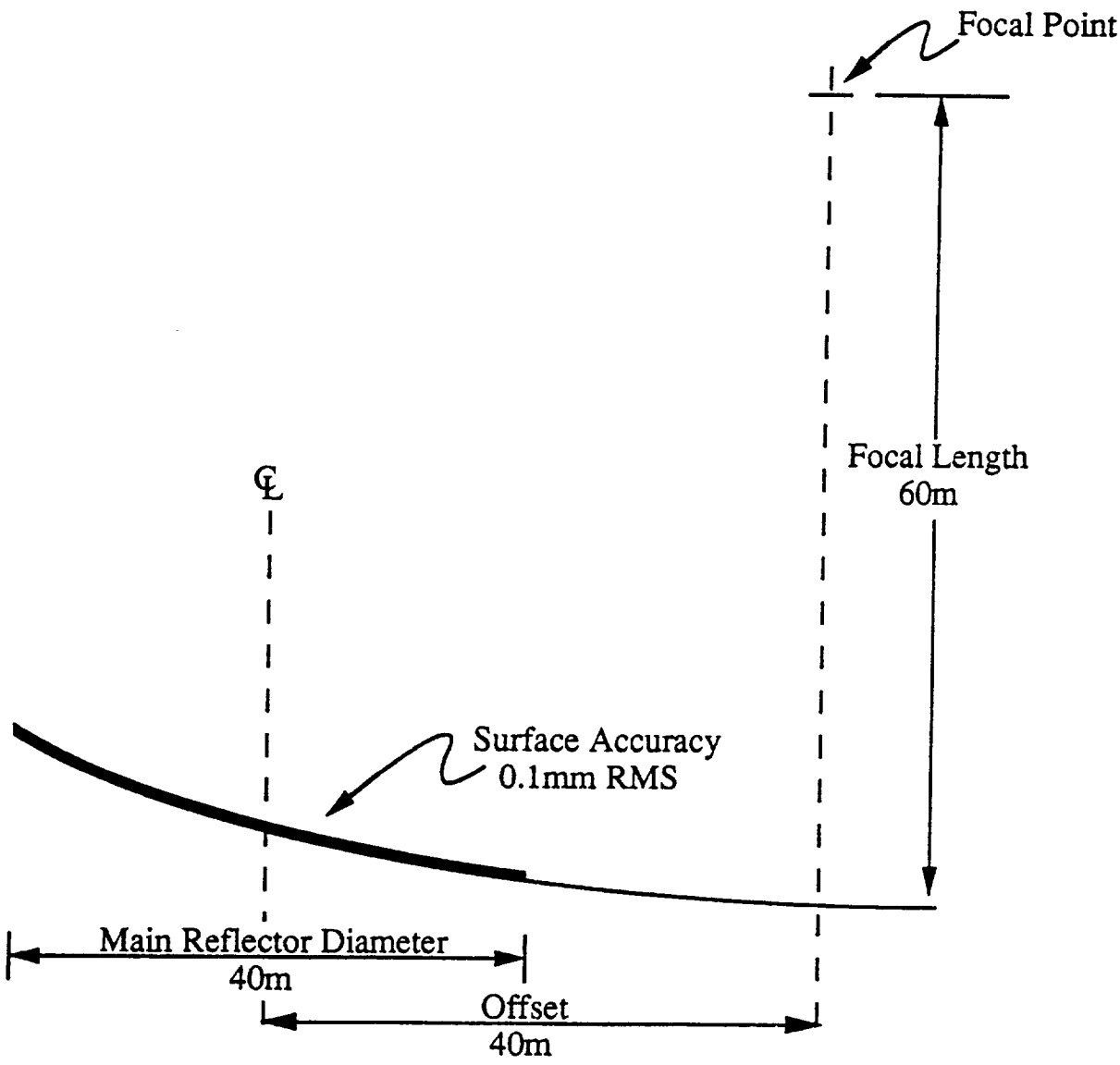

Figure 1.3-1. Initial Test Article Requirements

Table 1.3-1

Test Article Design Goals

Parameter	Goal
Frequency Range	6 to 40 GHz (60 GHz)
Bandwidth	Consideration for placement of at least two feed assemblies should be given to cover 6 to 40 GHz
Antenna Size	40 m (Circular Aperture)
Focal Length F/D	60 m 1.0 to 2.5 (present goal is 1.5)
Antenna Configuration	Dual Reflectors with an array feed
Offset	40 m (see Fig. 1.3-1)
RMS Surface Accuracy	0.1 mm
Reflector Surface	Lightweight Membrane, approx. 1 kg/m^2
Assembly	Deployable
Package Volume (Entire Instrument)	Titan IV (4.4 m x 15 m)
Thermal Differential	100°
Mechanical Scan	As required to achieve scan and steering. Goal is to minimize the mechanical motion of the main reflector, subreflector and feed system

2. MISSION AND ANTENNA REQUIREMENTS

NASA Langley hosted the Technology Workshop for Earth Science Geostationary Platforms in September 1988 [2-1]. At that workshop and subsequent EM Advisory Panel meetings, remote sensing issues for ESGP were discussed. Frequency channels from 6 to 220 GHz have been selected to observe these parameters. Some channels are at atmospheric windows (frequencies of low attenuation) allowing earth surface observation, while other channels are off window frequencies for vertical sounding through the atmosphere. Microwave sounding is used to determine temperature, water vapor and precipitation from the surface of the earth upward through the atmosphere. These data taken from geostationary orbit (GEO) permit observations of rapidly evolving meteorological events such as hurricanes. From GEO events can be tracked for long, continuous time periods - something not possible from LEO without a large constellation of satellites.

At the heart of the GEO microwave remote sensing problem is the radiometer design, especially the antenna system. From GEO very narrow antenna beams are needed for ground resolution. A resolution of 20 km is a long range goal at 6 GHz. This, of course, requires a large aperture antenna. Without preempting the design process we can quickly arrive at the classes of antennas that need to be considered. Arrays are high risk technology because of the large feed network which introduces loss and noise problems for the radiometer. For narrow beam microwave antennas, this leaves reflector antennas; there are, of course, many types of reflectors. Also, there could be a modest sized array used to feed the reflector.

A single antenna with multiple feeds to cover the necessary channels from 6 to 220 GHz seems out of reach for quite sometime. In addition, the EM Advisory Panel concluded that microwave components much above 60 GHz for use in the feed assembly and RF front ends is equally distant in the future. Therefore, we have redirected our attention to an upper frequency limit of 40 GHz (with a hopeful extension of similar technology to 60 GHz). It may turn out that resulting designs can be used from 6 to 220 GHz or it could be that two completely separate antenna systems eventually evolve, 6 to 60 GHz, and 60 to 220 GHz.

Table 2-1 gives design goals and characteristics of a 40-m diameter circular reflector antenna. A 40-m diameter was selected because it results in a 20 km ground resolution at midband (see line 3 of the table). Note that as frequency increases the 40-m antenna increases in electrical size (see line 1). This in turn leads to a narrower beamwidth (see line 2). Therefore, to accomplish complete global scan (± 8.6°) an increasingly large number of beamwidths of scan is required with increasing frequency (see line 4). The required wide scanning is perhaps the most challenging aspect of the design.

Another parameter of interest to the radiometer designer is that of beam efficiency (the ratio of power in the main beam to that in the entire pattern solid angle). Beam efficiency is affected by system configuration and surface roughness. Since surface accuracy is a strong determinant of candidate mechanical approaches, a basic feel for the numbers must be introduced early on. Table 2-2, part a, gives physical distances for two electrical lengths of RMS surface errors. Part b gives beam efficiency values for typical reflector illumination for the cases of a perfectly smooth reflector and the same random surface error cases. The beam efficiency calculations were based on the null locations for the smooth reflector (M.C. Bailey, NASA LaRC). Remote sensing

engineers would like to have about 95 percent beam efficiency [2-1]. The table reveals that on the order of λ/50 surface accuracy is required which is about 0.1 mm for our 40 (60) GHz antenna.

The parameter values for the baseline antenna design shown in the previous chapter (Fig. 1.3-1) were arrived at from remote sensing requirements described above, constraints on technology development in the future, subcontractor review, NASA input, and EM Advisory Panel review. The dual offset reflector with an array feed is not "the" design, but one which is rather simple in structure and has some evidence of providing electronic scan capability.

Table 2-1
Design Goal and Characteristics of a 40-meter Reflector in GEO

	Frequency					
	6	10	18	22	31	60
Main Reflector (wavelengths)	800	1,333	2,400	2,933	4,933	8,000
Half power beamwidth deg x 10^{-2}	8.16	4.90	2.72	2.22	1.32	0.82
Ground resolution (km) (23dB beamwidth)	60.2	36.1	20.0	16.4	9.7	6.0
Beamwidths of scan for ±8.6°	±105	±175	±316	±388	±652	±1054
Surface error required in mm for λ/50 RMS	1.00	0.60	0.33	0.27	0.16	0.10

Table 2-2
Characteristics of a 40-meter Circular Reflector Antenna

a. RMS Surface Error

f	λ	λ/20		λ/50	
(GHz)	(mm)	mm	mils	mm	mils
6	50	2.50	98	1.0	39
37	8.1	0.41	16	0.16	6.4
50	6.0	0.30	11.8	0.12	4.7
220	1.5	0.075	3.0	0.03	1.2

b. Beam Efficiency

Smooth Reflector	λ/20 Surface Error	λ/50 Surface Error
98%	~70%	~93%

3. REFLECTOR FUNDAMENTALS AND CANDIDATE CONFIGURATIONS

Conventional antenna design consists of these steps: (1) Performance specifications are developed for the application at hand (communications, radar, or radiometry), (2) Electrical design, (3) Mechanical design and construction, and (4) Measurement of electrical and mechanical performance. This is a serial process with each step being completed before the next. In this project these steps have not been performed in a serial fashion. The research and development effort has been ongoing while remote sensing requirements evolve. Also, electrical and mechanical designs were performed at the same time. This was necessary because of the nature of the program; it is complex and pushes the state-of-the-art in many technology components. This requires that the steps be performed iteratively. That is, as the mechanical implications of a particular electrical configuration reveal an inferior design, remote sensing goals must be relaxed or electrical design changed.

This section identifies reflector fundamentals and candidate configurations from which the antenna design was initiated.

3.1 Overview

The ESGP design problem holds many challenges but the two elements associated with the antenna design that are most challenging are: i) its large size and ii) its required wide scanning. These would also be challenges for earth-based antennas. Therefore, the design process must be tempered with a goal of simplicity to facilitate launch and long life in space.

It is important then to have clearly in mind the fundamental trade-offs in the design of large space reflectors for wide scanning. Scanning can, of course, be accomplished by slewing the entire reflector assembly, as is usually done on the ground. However, mechanical motion creates many problems in space. Drives and controls are required. Momentum compensation for antenna motion is required; this is a major problem on ESGP which also carries laser and other experiments that require a stable platform.

Figure 3.1-1 illustrates scanning fundamentals. A flat reflector offers undistorted scanning. The penalty is that it provides no focusing and a large array feed is required to collect the arriving waves. The reflector merely acts to redirect the incoming waves. At the other extreme (Fig. 3.1-1c) a parabolic reflector sharply focuses a plane wave arriving parallel to the axis of the reflector. However, for waves arriving from directions other than along the axis of the parabola, rapid performance degradation such as gain loss and pattern distortion occurs. The parabola offers the best aperture efficiency but with the poorest scan properties. The spherical reflector of Fig. 3.1-1b is a compromise. It focuses (but not to a point) and has scan capability. Its aperture efficiency is lower than that of the parabola.

With the reflectors of Fig. 3.1-1 scanning is achieved in the ways illustrated in Fig. 3.1-2 for the case of no main reflector motion. The most elementary method is to physically move the feed antenna (or array feed). Electronic scanning (either switched or phased) is the alternative that offers instantaneous beam positioning and even multiple beam possibilities. Mechanical motion can be avoided by switching between fixed feeds as illustrated in Fig. 3.1-2b. A full array feed

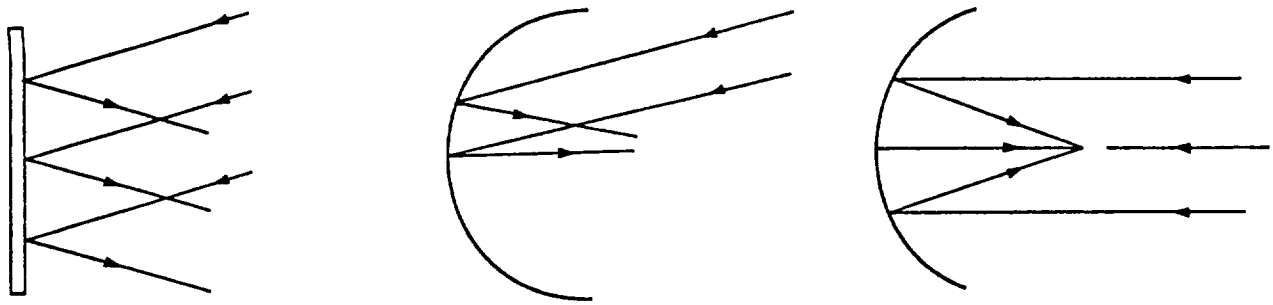

a) Flat reflector:

Full scanning, no focusing

b) Spherical reflector:

Partial scanning, partial focusing

c) Paraboiic reflector:

Limited scanning, focused

Figure 3.1-1. Scanning Properties of Reflectors

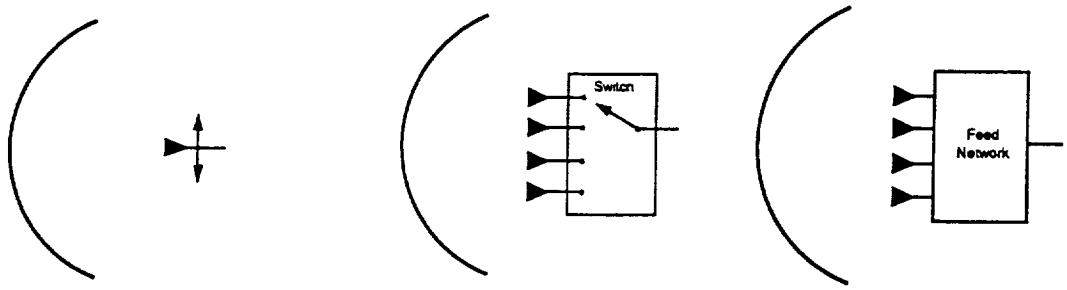

a) Movement of the feed assembly

b) A switched feed

c) Full array feed

Figure 3.1-2. Implementation of Scanning without Movement of the Main Reflector

(Fig. 3.1-2c) is the best solution (assuming no motion) in that the appropriate elements can be properly amplitude and phase weighted to compensate for scan degradation (as well as main reflector surface distortions).

The full spectrum of scanning methods available are represented in Fig. 3.1-3. For reasons mentioned above, full mechanical slewing is to be avoided if possible. The electronic-scan approach illustrated in Fig. 3.1-2 will require a very large array and associated feed network. We are, therefore, left with using a hybrid approach or with finding a clever electronic scan configuration. There is no clear cut answer to our design problem in the literature we have reviewed.

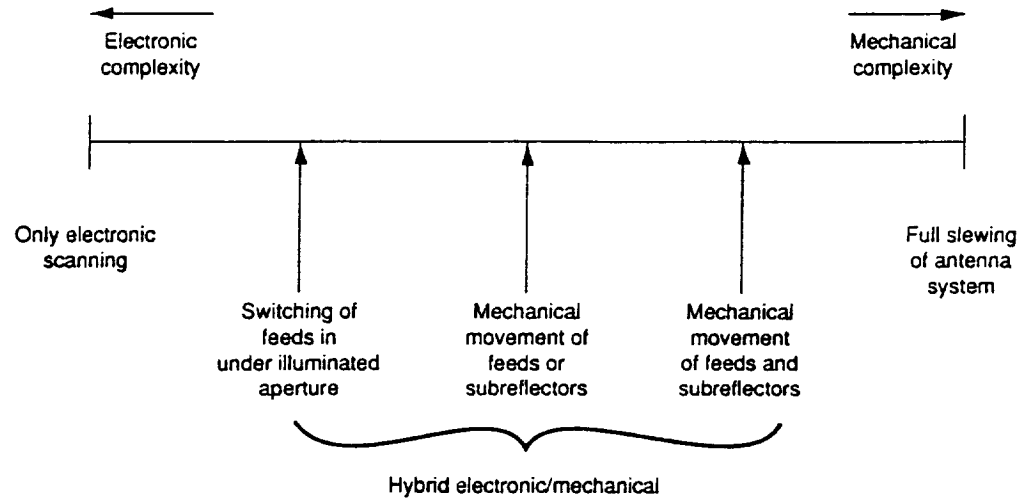

Figure 3.1-3. The Trade-offs in Scanning Reflector Antenna Systems

3.2 Main Reflector Shapes

There are a few classical main reflector shapes that are in common use. In this section we summarize the fundamental types.

The paraboloidal reflector of Fig. 3.2-1 is the most popular because it focuses incoming (on-axis) plane waves to a point (the focal point). This leads to high gain (high aperture efficiency). Scan properties are summarized on the figure.

The parabolic torus of Fig. 3.2-2 has a circular cross-section in azimuth and parabolic cross-section in elevation. With the penalty of reduced aperture efficiency multiple feeds may be placed in the azimuth plane along the focal circle and separate simultaneous beams can be obtained from each feed.

The parabolic cylindrical reflector of Fig. 3.2-3 has a straight cross-section in azimuth and parabolic cross-section in elevation. A linear array feed along the axial focal line can be phase steered to scan the beam.

The spherical reflector of Fig. 3.2-4 has been used in applications where scanning is more important than aperture efficiency. For example, the Arecibo 1000-foot diameter spherical reflector which is stationary achieves scan by feed displacement. Potential for wide angle scanning may be worth the costs associated with a reflector larger than a paraboloid for the same resolution.

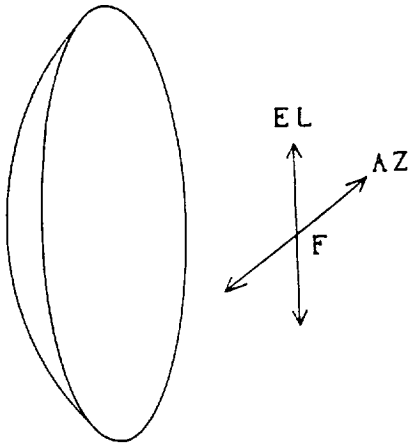

•Scanning in AZ and EL accomplished by linearly displacing feed (or feed switching) in the plane through the focal point F.
•Phase errors induced in the aperture during scan cause gain loss and pattern degradation.
•Arrays may be used to correct aperture phase errors, however, this requires amplitude and phase weighting and arrays can be large.

Figure 3.2-1. Paraboloidal Reflector

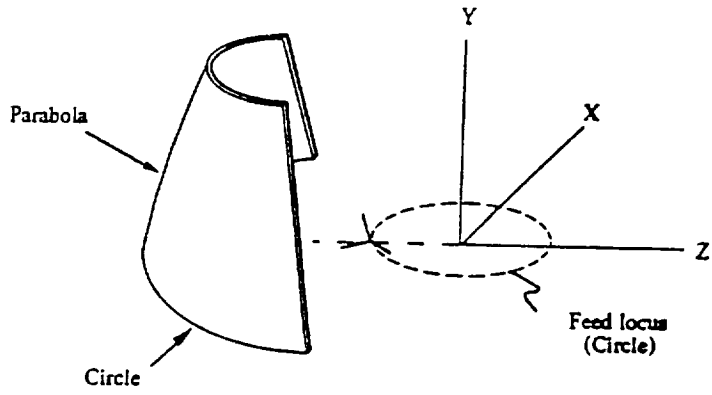

•Scanning in AZ accomplished by feed movement (or feed switching) along paraxial focal arc with no scan induced gain reduction or beam degradation.
•Scanning in EL identical to parabolic case.
•Cylindrical phase errors in AZ plane degrade performance.

Figure 3.2-2. Parabolic Torus

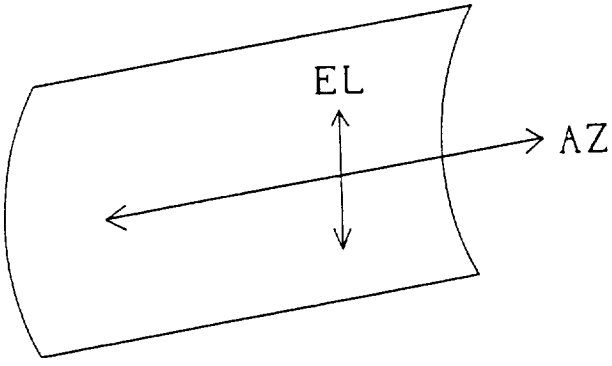

•Undistorted scanning in AZ accomplished by phase tilting a linear array feed.
•Scanning in EL identical to parabola.

Figure 3.2-3. Parabolic Cylindrical Reflector

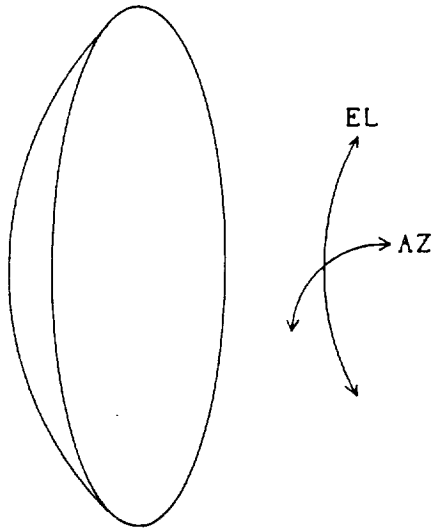

•Scanning in AZ and EL accomplished by feed movement (or feed switching) along paraxial focal sphere with no scan induced gain reduction or beam degradation.
•Spherical phase errors degrade performance.

Figure 3.2-4. Spherical Reflector

3.3 Candidate Configurations

After an extensive literature search accompanied by contacts with companies involved with reflector antenna development, several candidate configurations were selected. The candidates represent the range of possible configurations available including all reflector shapes and different scanning methods with the promise of wide scan capability. They are summarized in Table 3.3-1.

Table 3.3-1
Candidate Configurations

1. Switched Feed or Moveable Feed

   1.1 Bifocal Dual Reflector
   1.2 Tri-Reflector (Foldes Type 2)
   1.3 Gregorian Corrected Spherical Reflector
   1.4 Parabolic Torus

2. Partial Mechanical, Electronic Scanning

   2.1 Array-Fed Tri-Reflector (Foldes Type 1)
   2.2 Array-Fed Dual Reflector (Foldes Type 3)
   2.3 Cylinder with partial movement

3. Electronic Scanning

   3.1 Dual Parabolic, Array-Fed, Gregorian Reflector
   3.2 Array-Fed Dual Reflector (Foldes Type 3)
   3.3 Array-Fed Cylindrical Reflector

Diagrams of the configurations are given in the following figures (Figs. 3.3-1-10).

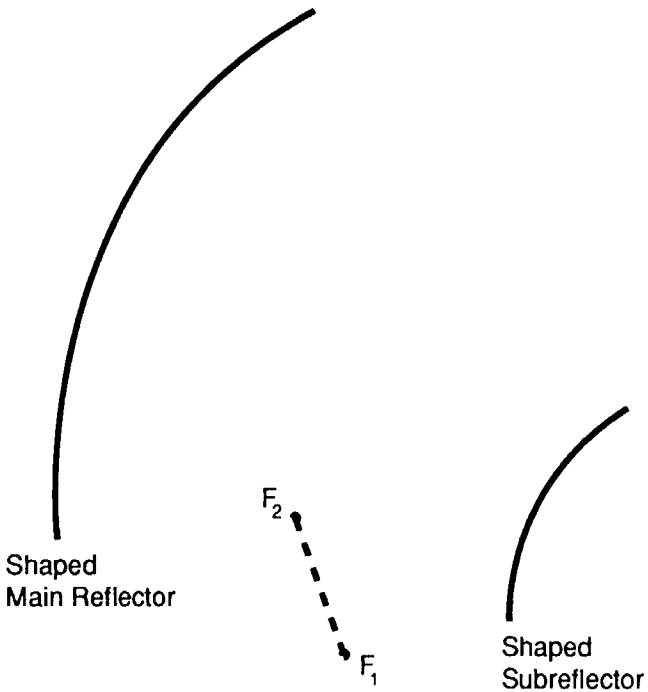

Scanning in elevation accomplished by:

- Switched feed elements located between focal points F_1 and F_2.
- Combination of translation and rotation of single feed along path between F_1 and F_2.

Figure 3.3-1. 1.1 Bifocal Dual Reflector

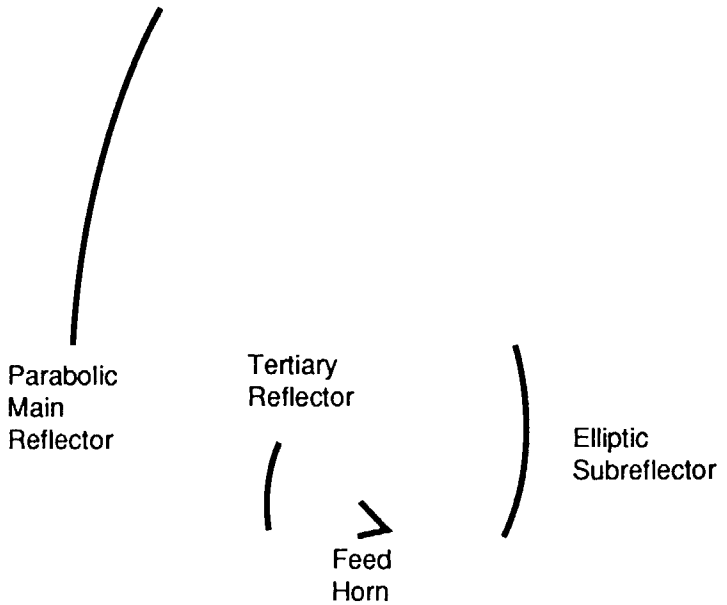

Scanning in elevation accomplished by translation and rotation of feed horn and tertiary reflector as a rigid unit.

The Foldes Type 5 tri-reflector is similar to this, however, a smaller subreflector is used. The subreflector must be moved in order to intercept the rays for different directions of the scan.

Figure 3.3-2. 1.2 Foldes Type 2 Tri-Reflector

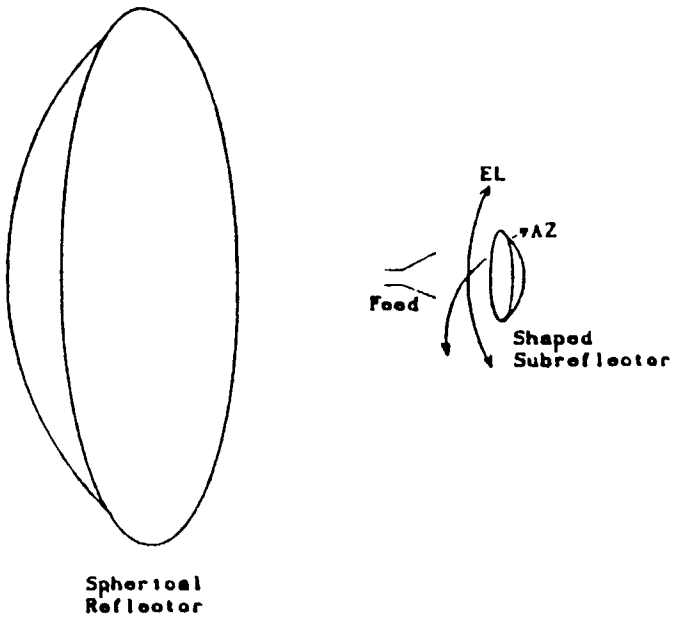

Scanning in azimuth and elevation accomplished by translation and rotation of feed and shaped subreflector along focal surface as a rigid unit, or switched feed array.

Figure 3.3-3. 1.3 Gregorian Corrected Spherical Reflector

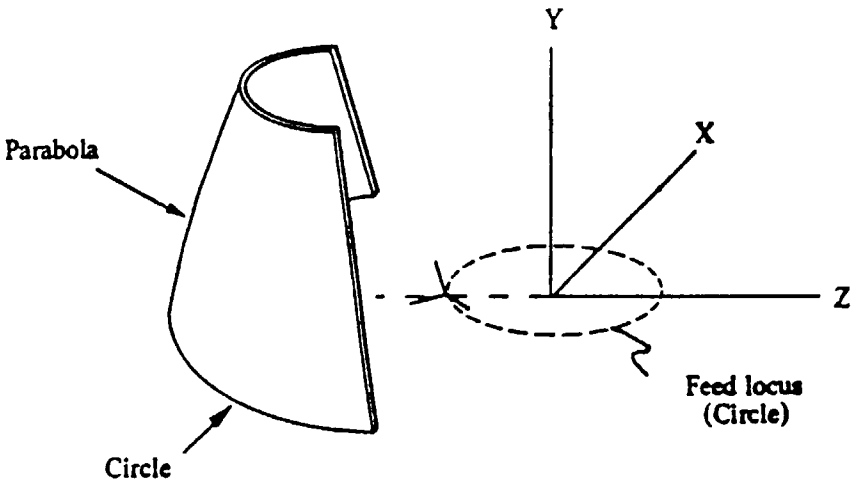

Scanning in azimuth accomplished by rotation and translation of feed along focal curve, or switched feed array.

Figure 3.3-4. 1.4 Parabolic Torus

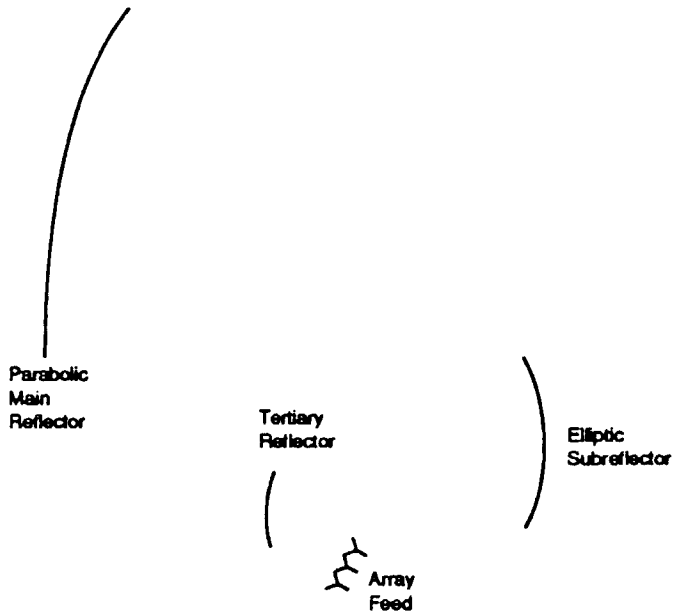

Small angle scanning and compensation for slow varying reflector surface errors accomplished by small phased array.

Large angle scanning in elevation accomplished by translation and rotation of feed array and tertiary reflector as a rigid unit.

Figure 3.3-5. 2.1 Foldes Type 1 Array-Fed Tri-Reflector

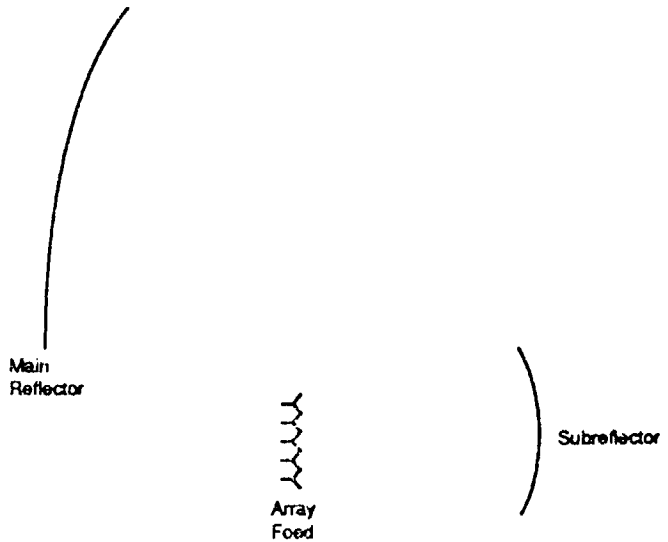

Small angle scanning and compensation for slow varying reflector surface errors accomplished by medium sized array.

Large angle scanning in azimuth and elevation accomplished by slewing of entire structure as a rigid unit.

Figure 3.3-6. 2.2 Foldes Type 3 Array-Fed Dual Reflector

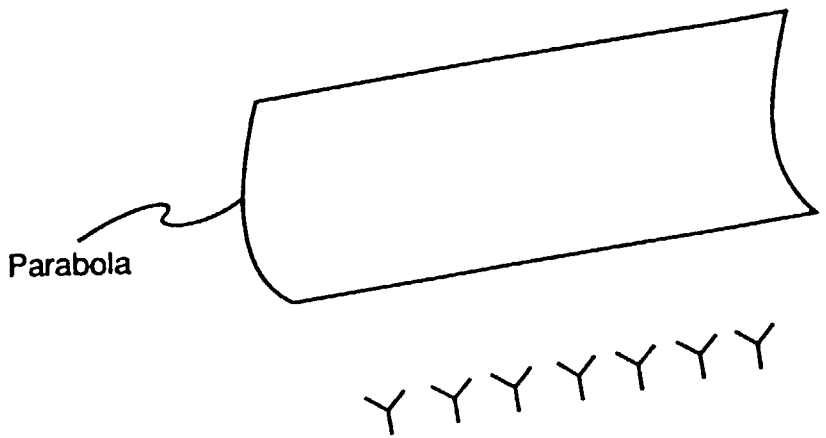

Scanning in azimuth and compensation for slowly varying reflector surface errors accomplished by linear phased array.

Scanning in elevation accomplished by tilting entire structure as a rigid unit.

Figure 3.3-7. 2.3 Cylinder with Partial Movement

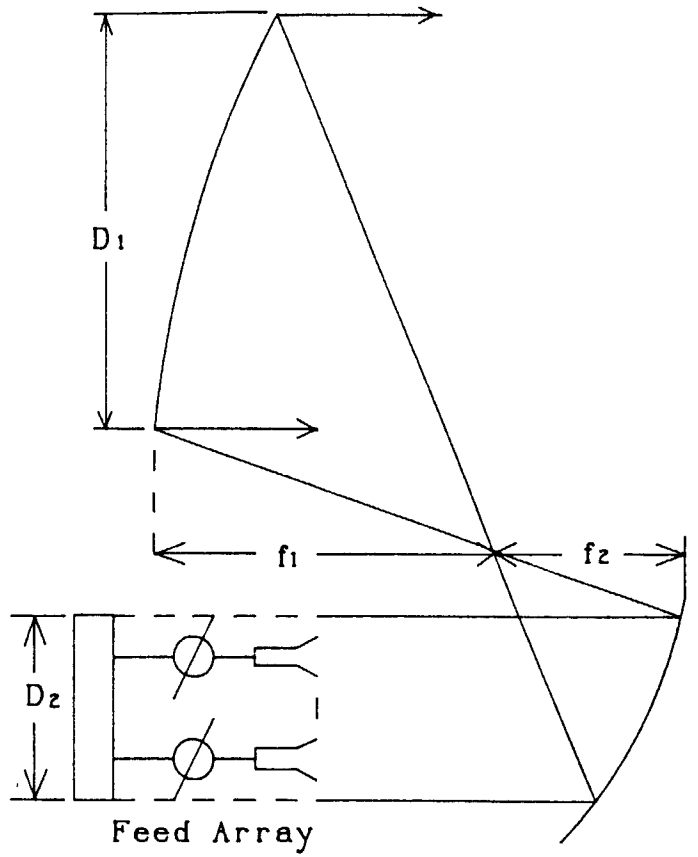

Scanning in azimuth and elevation, and compensation of slowly varying reflector surface errors accomplished by large phased array.

Figure 3.3-8. 3.1 Dual Parabolic, Array-Fed Reflector

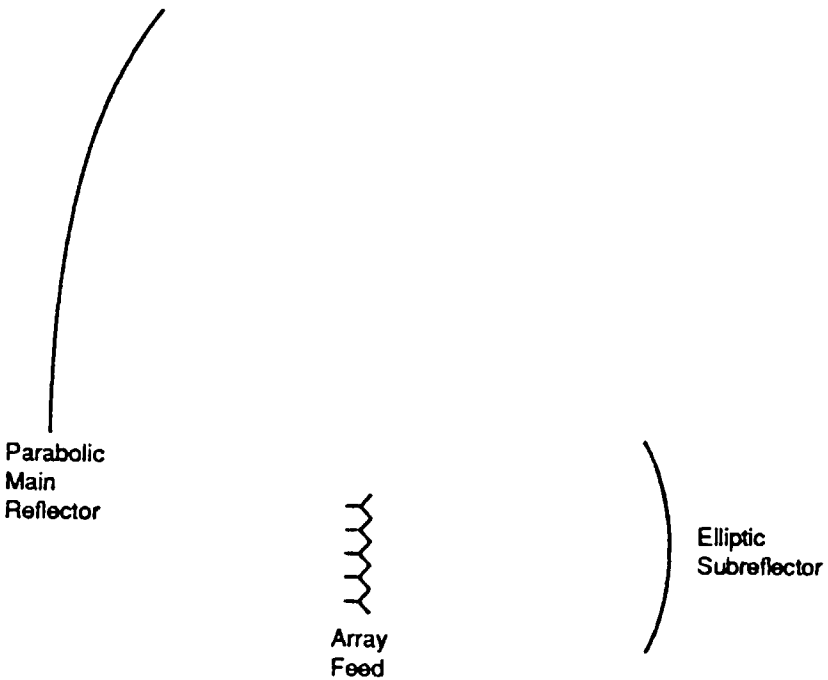

Scanning in azimuth and elevation, and compensation for slowly varying reflector surface errors accomplished by large phased array.

Figure 3.3-9. 3.2 Foldes Type 4 Array-Fed Dual Reflector

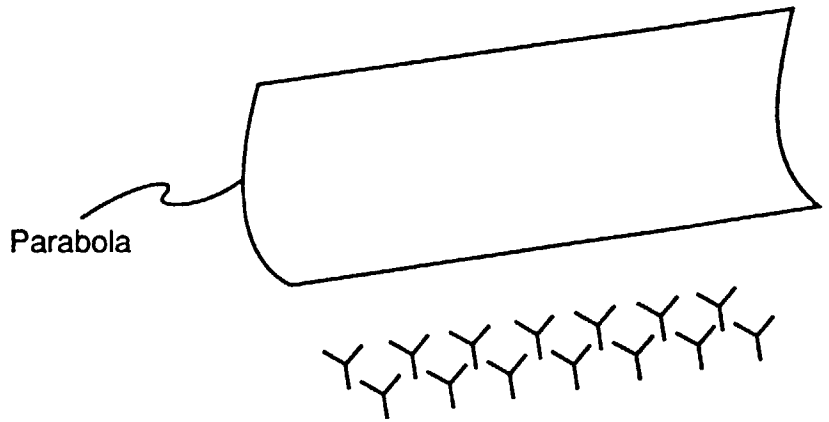

Scanning in azimuth and elevation, and compensation of slowly varying reflector surface errors accomplished by large phased array

Figure 3.3-10. 3.3 Array-Fed Cylindrical Reflector

4. DESIGN AND PERFORMANCE EVALUATION

4.1 Overview

Phase I of the "Definition of Large Deployable Space Antenna Structures Concepts" program has been oriented towards definition of the most feasible antenna concepts/designs for accomplishing the objectives of the LDA and evaluating the existing technology to support such an instrument. This chapter will discuss the technologies evaluated and physical designs considered for the LDA. Technologies considered range from current state-of-the-art, i.e. pactruss and furlable reflector surfaces, to the more exploratory concepts, i.e. practically inextensible membrane antennas.

Many of the technologies discussed in this chapter have been evaluated based upon their inclusion in preliminary physical designs of conceptual LDA configurations. This is to say that each technology of interest has been included into a LDA design that best utilizes its unique performance characteristics and is judged by the design goals listed in Table 1.3-1. In the case where the technology was judged not to meet the stated performance requirements an attempt was made to determine the maximum size of the antenna or component that would enable the technology to be utilized or further studied.

This chapter contains several novel design approaches to accommodating large deployable space structures. In each case, the technology warrants further study and will have utility in future space missions. However, not all the technologies described in this chapter will be carried into Phase II because of the specific performance requirements as described in Chapter 1.

4.2 Deployable Trusses

4.2.1 *Deployable Truss Technology Overview*

The Phase I LDA study has progressed with the assumption that an area truss structure will be required for precise support of a reflector surface that is composed of a segmented rigid or semi-rigid solid surface. One may ask if a truss is even necessary, since supporting structures for reflector surfaces are often integrated with the reflecting surface itself. Indeed, this approach is used for the small solid dishes flying on communication satellites. The simplicity of this approach is attractive and the resulting structure can be made dimensionally stable enough to be used at extremely high frequencies. Ingenious concepts have been devised for deploying larger dishes by hinging between adjacent segments as in the TRW Sunflower [4.2-1] and the Harris Hexagonal Panel [4.2-2] concepts shown in Figs. 4.2-1 and 4.2-2. Integrated-structure, or panel-only, concepts also use well established fabrication techniques and appear to be of low risk. They are, however, structurally "thin," so that small fabrication or thermally induced errors in individual parts grow into large distortions for large sizes. In addition, such structures are difficult to test in a one-g environment. Their flexibility combines with the gravity loading to produce deflections that are large in comparison to those acceptable for the present application. It is therefore difficult to passively achieve the desired accuracy, either by fabricating the component parts with enough precision or by "trimming" the structure by adjustments based on measurements obtained during ground testing.

The experience and information obtained by studies and tests over the past two decades have

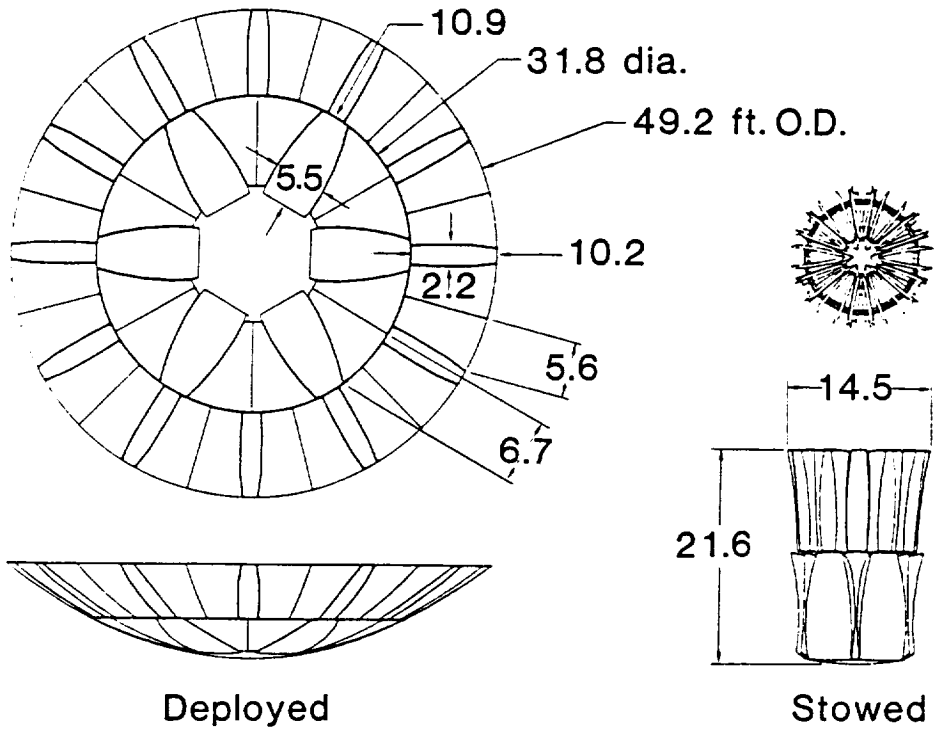

Figure 4.2-1. TRW Sunflower Deployable Reflector Concept

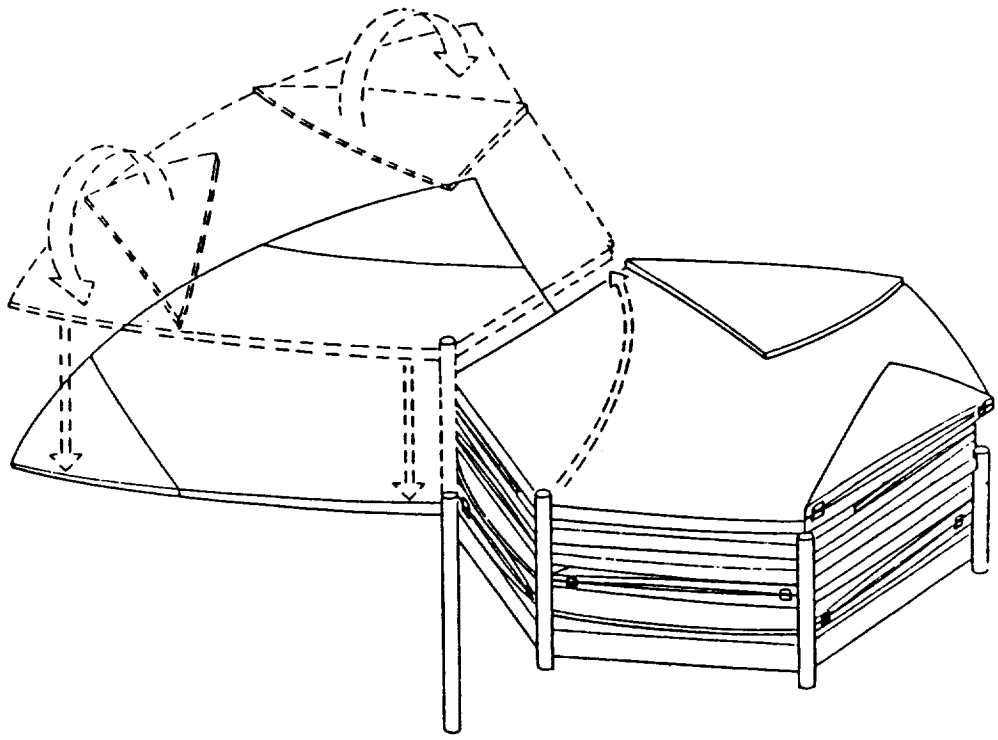

Figure 4.2-2. Harris Hexagonal Panel Deployable Reflector Concept

shown that structural configurations that are "deep" are much more suitable for large high-precision surfaces than are the "thin" ones. See Refs. [4.2-3, 4, 5, 6 and 7]. Not only is this notion intuitively obvious, but also detailed analyses have shown that very high precision is achieved with careful fabrication. A simulation of a 20-meter-diameter tetrahedral-truss structure constructed from 2-meter struts which have random lengths with an RMS variation of 20 micrometers, showed an expected RMS surface error of 43 micrometers. The worst of 100 cases had an RMS surface error of 72 micrometers. Furthermore, analysis of the deflections caused by testing in a one-g field showed an RMS error of about 100 micrometers; gravity compensation should be able to decrease that by an order of magnitude.

Numerous concepts for remotely deploying precision antennas with solid reflector surfaces exist. As previously mentioned, several concepts have been devised for deploying large dishes by hinging between adjacent segments or panels that have integral but structurally thin support. One antenna with a deep-truss support structure flew on the SEASAT spacecraft. The 10.75 meter long synthetic aperture radar antenna is supported by a deployable truss. A feature of this truss that is crucial to the LDA application is that the radiating panels are stowed and deployed while attached to the truss. This structure, which supported an L-band antenna (λ = 20 cm) was accurate to better than 2.5 mm maximum deflection. This was achieved and demonstrated by careful efforts; the robustness of the configuration simplified analysis, integration and testing. A similar deployable truss concept has been studied for possible use with reflector antennas. One of these is shown in Figs. 4.2-3. This arrangement has the advantage that it allows the doubly curved panel segments to nest, thereby saving package volume.

Single-fold truss-stiffened concepts are useful only for diameters smaller than the available package length, approximately 10 to 15 meters, depending on the launch vehicle configuration. For larger reflectors, it will be necessary to divide the reflector surface in both directions. This poses a severe problem because double fold truss geometries are notoriously difficult to breakdown and stow with rigid reflector panels attached. Stowage of flexible mesh reflector surfaces integrally with deep, double fold truss structures has been demonstrated by General Dynamics using their Geo Truss [4.2-8-11] and by Martin Marietta with the Box Truss [4.2-11-15]. Autonomous deployment of rigid, doubly curved panels onto a deep support truss has yet to be accomplished, however, a concept for achieving this is proposed later in the report.

The supporting truss can be stowed separately, and the panels can be assembled to the deployed truss by a robot. Research is in progress at Langley Research Center on such robotic assembly. Another concept for constructing large segmented reflectors in remote locations employs individual modules, each consisting of a panel and its associated support truss section. It is shown in Fig. 4.2-4. These are stowed in a deployment canister which moves around the periphery of the reflector surface, deploying modules and locking each to its neighbors. The development of this intelligent canister would require some effort but seems to be easier than using a robot. Use would be made of the fact that each module would be hinged, so far as possible, to its neighbors. The hinging would aid in control of the canister motions.

One concept for the deployable truss which is being extensively studied for various high-precision applications is the Pactruss shown in Fig. 4.2-5. The deploying truss in this concept is very strongly synchronized and offers reliable deployment with a few actuators. The design of the Pactruss is flexible in that its geometry can be altered to make it compatible with

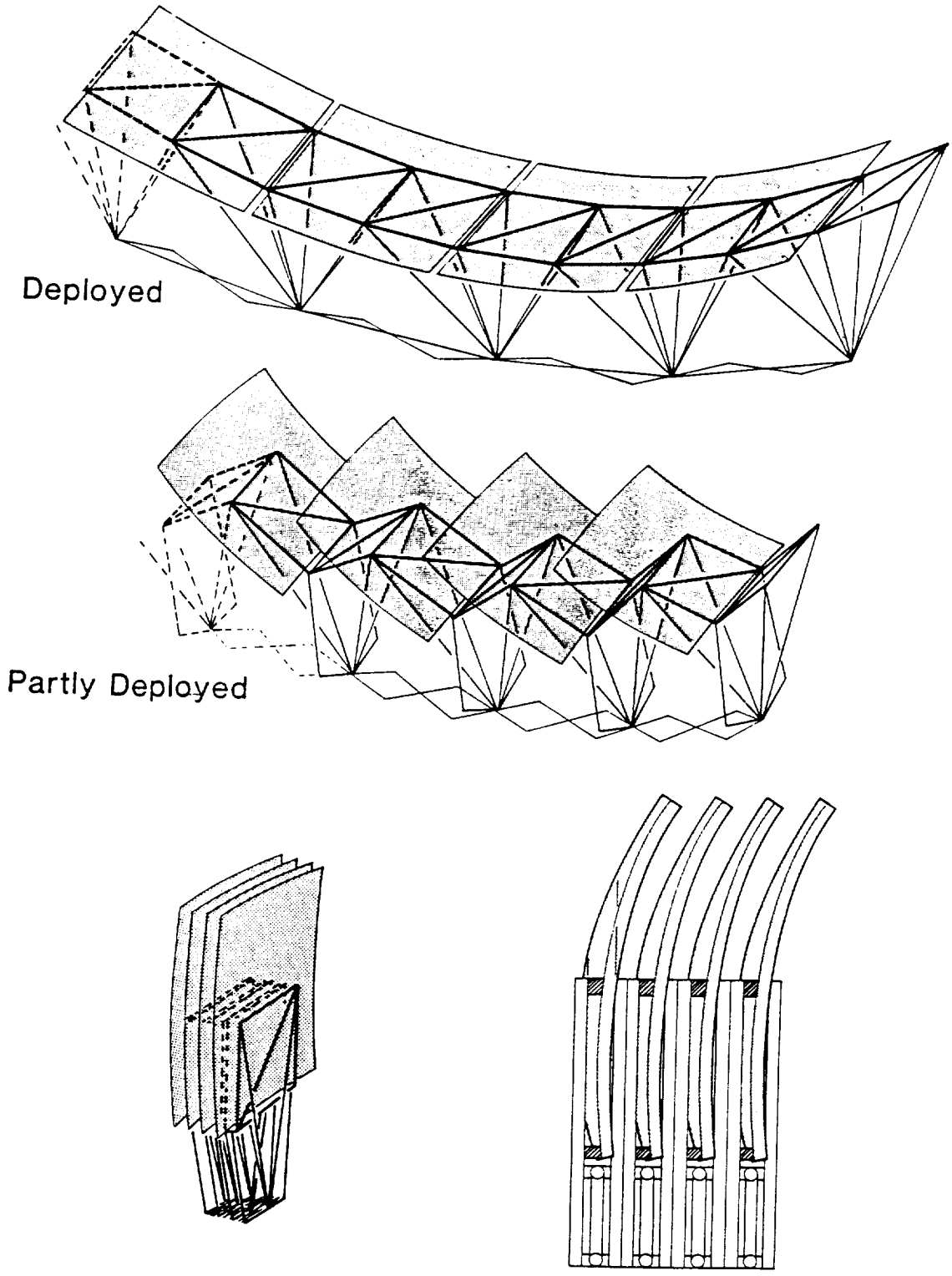

Figure 4.2-3. Synchronously Deployable Concept B (Crest) for Stiff Panel Reflectors

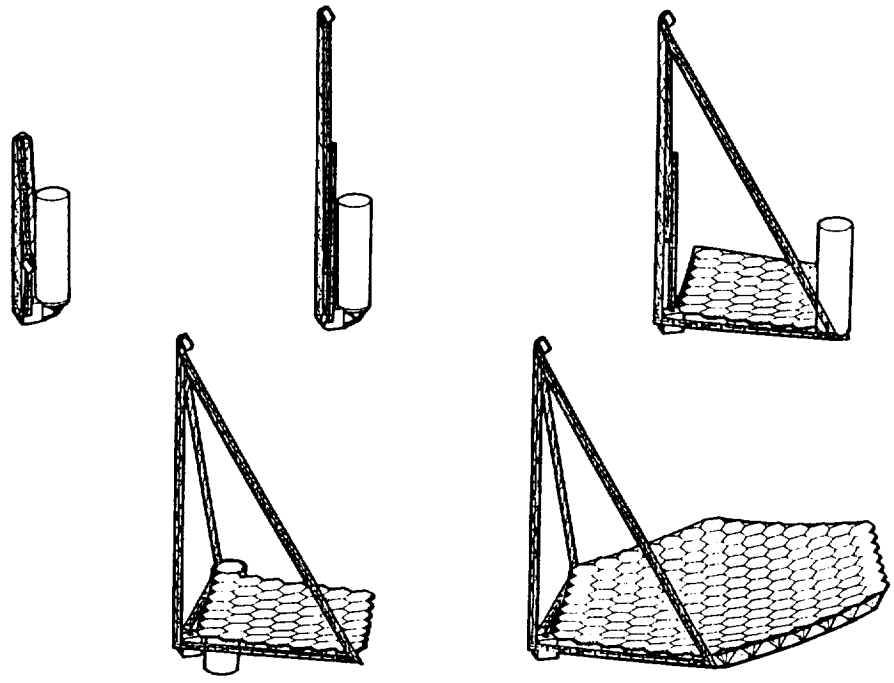

Figure 4.2-4. Sequentially Deployable Segmented Reflector

various types of reflector geometries. The square form of the Pactruss, shown in Fig. 4.2-6, is compatible with rectangular stiff panel segments or flexible strips of furlable reflector material. The triangular, or more correctly, the parallelogram form of the Pactruss is shown in Fig. 4.2-5. This version is compatible with the geometry of hexagonally shaped stiff panels if the parallelogram units on the surface of the truss are tilted 60 degrees as shown in the figure. Figure 4.2-7 depicts a hybrid Pactruss which is composed of six single-fold radial beams and six double-fold Pactruss segments. The hybrid configuration will stow around a central body such

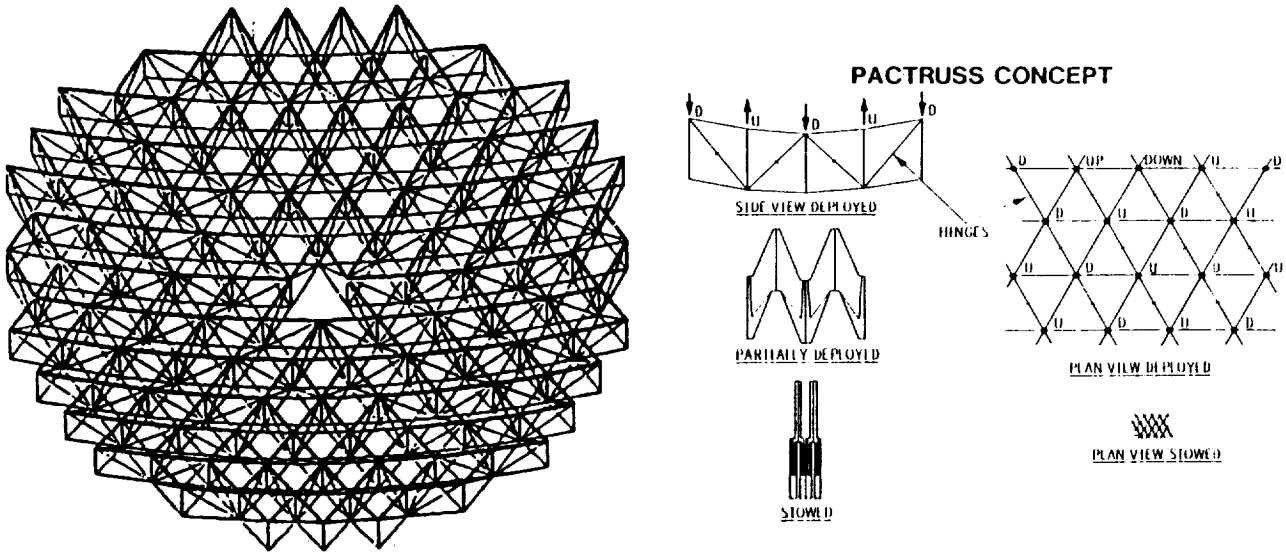

Figure 4.2-5. Pactruss Concept with Triangular Form

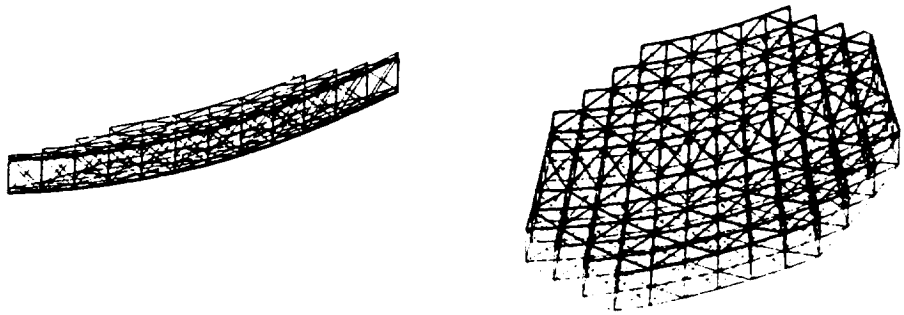

Figure 4.2-6. Views of Pactruss for Offset Paraboloid

as a feed structure or cryogenic equipment, and is compatible with hex-panels. See Ref. [4.2-16] for descriptions of recent evaluations of precision applications.

4.2.2 *Ring Truss Technology Review*

Several types of ring structures have been developed for the support of membrane reflectors which are held in the proper configuration by distributed forces. Some of these designs are reported below.

The inflatable torus type is not a truss but it does support the reflector membrane surface with a rim that carries a compression load. The assembly is deployed by slow inflation and is intuitively very reliable. Examples of inflatable trusses include the ECHO passive satellite, a 100-foot-diameter balloon, which was launched early in the space age. Its shell was composed of a thin sandwich with Mylar-film face sheets and an aluminum foil core. More recently, technology work in Europe has been underway since the early 1980s developing a Kevlar-epoxy composite surface which is cured and hardened on orbit after inflation. See Refs. [4.2-17] and [4.2-18].

Inflatable structures, while being vigorously promoted for lower frequency antennas, are generally viewed as being inapplicable for the high frequencies being considered herein. The available suitable materials lack the long-term dimensional stability and super-low coefficient of thermal expansion needed for very high precision. In addition, inflatable antennas, once fabricated, are difficult to "tune up," even during ground testing. Adjustments in orbit seem to be impossible.

Another ring-type structure that is capable of supporting a membrane reflector surface is the wire wheel. As shown in Fig. 4.2-8, the wire wheel is composed of a folding ring that is deployed by stays or spokes. The spokes also load the ring in compression in its deployed state to provide the appropriate stiffness and precision. The folding ring approach has been utilized in the design of the hoop-column antenna structure at Langley Research Center.

A deployable folding ring without wires was developed by Astro for Rockwell in the late 1970s. The ring segments stow in a radial fashion and are deployed by a circumferential scissors

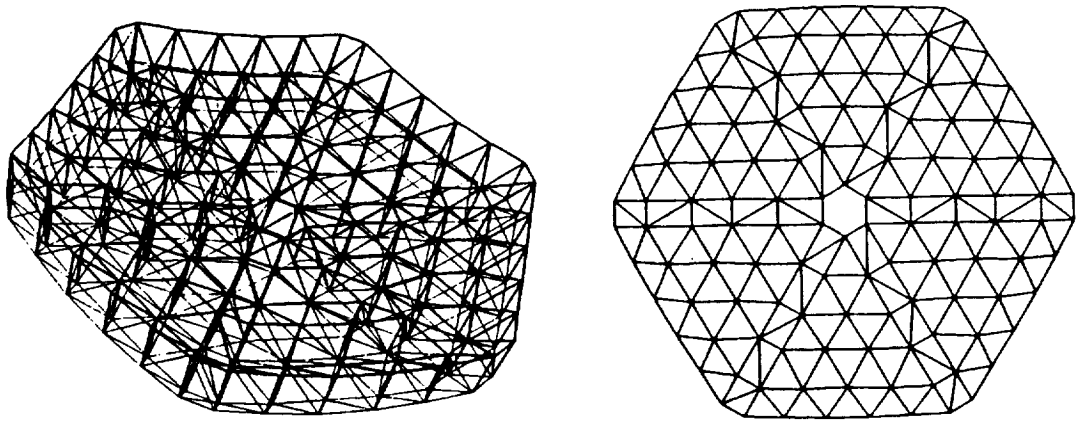

252 Nodes
1014 Struts
264 Redundants

Stows around a central body

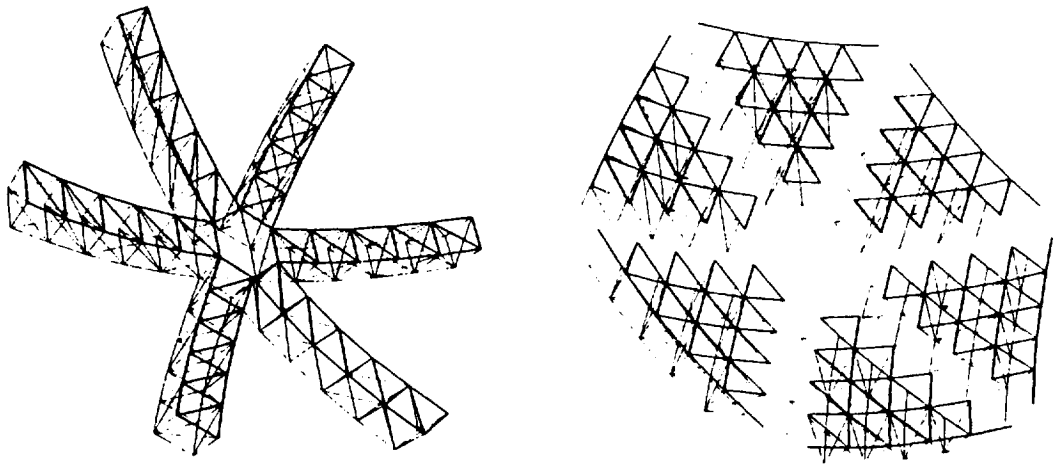

Singlefold beams

Pactruss

Each beam and Pactruss sector is unique for an offset configuration.

Figure 4.2-7. Five Ring Hybrid Pactruss

mechanism. The ring segments are space frame structures which can be no longer than the launch vehicle payload bay radius.

4.2.3 *Evaluation of Deployable Truss*

A simple two-dimensional analysis has been performed to estimate the structural depth that will

be required for the 40-meter-diameter LDA configuration to passively maintain the required accuracy. The derivation of the equation used for this analysis was based on the lattice rectum equation for the rise height of a shallow, circular arc. The final form of the equation is:

$$h = \frac{\Delta\varepsilon L^2}{8(\Delta\delta)} \tag{4.2-3}$$

where: h is the beam (truss) depth
$\Delta\delta$ is the rise height
L is the length of the arc segment
$\Delta\varepsilon$ is the strain differential between the outermost surfaces of a beam (truss)

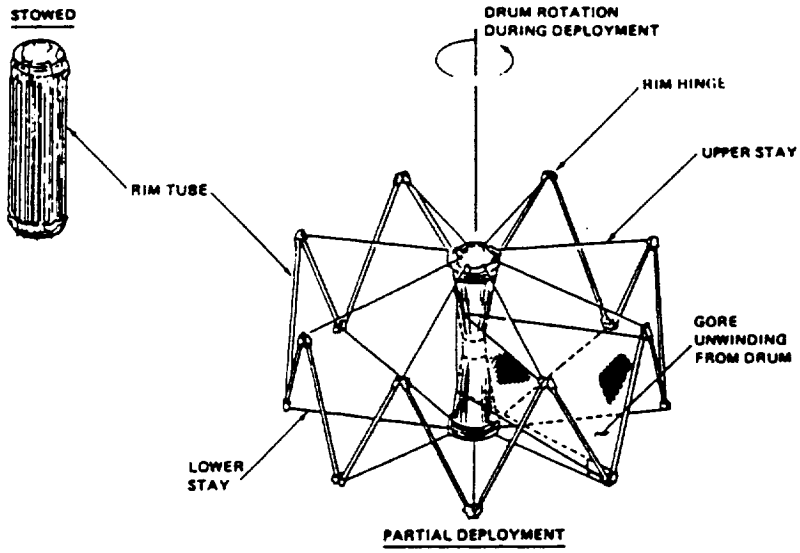

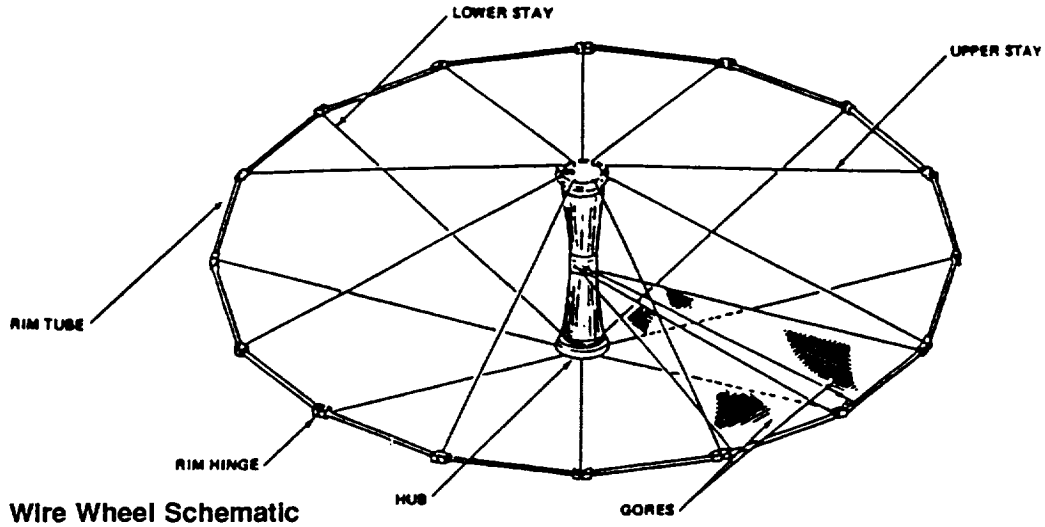

Figure 4.2-8. Wire Wheel Schematic

For the required LDA configuration, $\Delta\delta$ can be set to 0.3 mm. This is because experience has shown that a specific RMS accuracy (0.1 mm in this case) can be achieved if the maximum deviation from the ideal feature is approximately three times the RMS value. This is approximately valid whether the deviations are due to gross changes in curvature or more localized undulations of the surface.

Shown in Fig. 4.2-9 is the relationship of the strain differential $\Delta\varepsilon$ to the required structural depth, h, for the LDA to maintain a maximum deformation $\Delta\varepsilon$ of 0.3 mm.

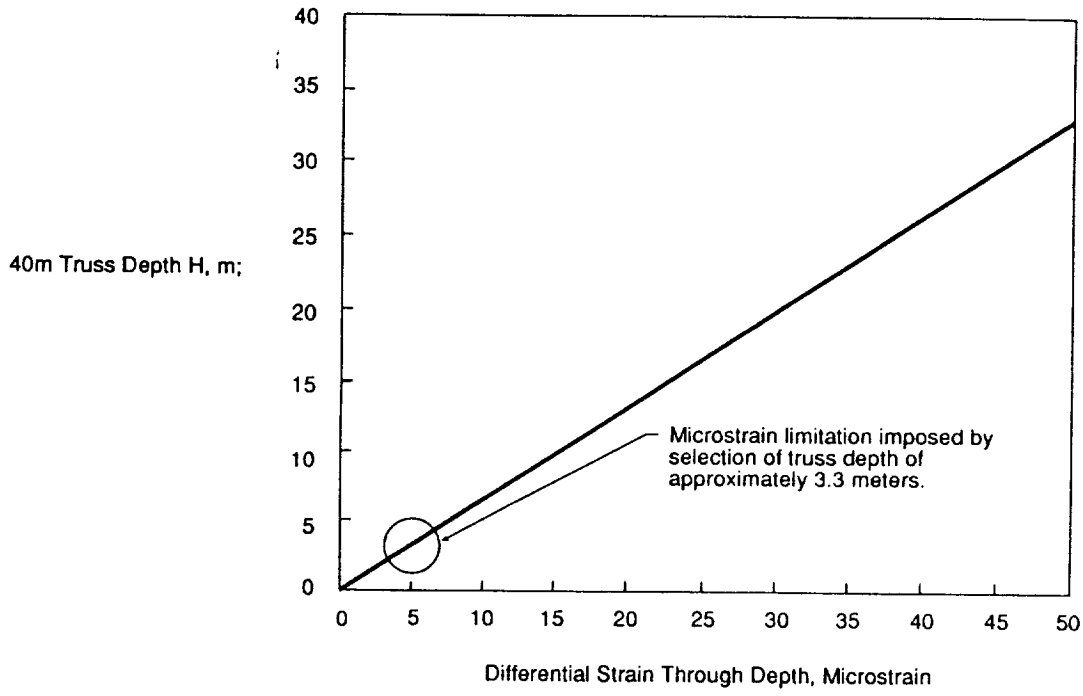

Figure 4.2-9. Truss Depth and 4.0 m Panel Thickness vs. Microstrain to Limit $\Delta\delta$ to 0.3 mm

The value of $\Delta\varepsilon$ that is chosen represents the maximum strain differential that is anticipated through the depth of the structure for any reason. This value will be a combination of the maximum thermal distortion between the truss front and back, fabrication imperfections such as length errors, and scatter in the CTE of the composite material. Experience has shown that 5 microstrain is a reasonable value for $\Delta\varepsilon$, although achievement of this value may require extensive thermal insulation of the structure due to the 100°C maximum thermal differential stated in the LDA baseline requirements list. With the maximum $\Delta\varepsilon$ set to 5 microstrain, structural depth is approximately 3.3 meters.

Therefore, the structural configuration required is a truss with a minimum depth of 3.0 to 3.5 meters. This depth is required to insure that the LDA requirements for passive accuracy control can be maintained. A truss of this depth will be composed of members that are shorter than the 4.4-meter-diameter of the STS or Titan launch vehicles, which, incidentally, will prove to be convenient for packaging.

4.2.4 *New Truss Concepts for the LDA*

New truss concepts that are compatible with the LDA performance requirements have been generated. At least one new truss has been conceived for each of three reflector concepts: rigid panel segments, furlable semi-rigid reflector strips and a ring truss for one-piece membrane type reflector surfaces.

As explained in Section 4.2.3, a truss structure of 3.0 to 3.5 meters depth is required for the 40-meter-diameter LDA configuration. These characteristics dictate that the structure will be highly articulated. Such a structure must be very strongly synchronized during deployment to achieve high reliability. The truss must be doubly folded since its diameter exceeds all of the payload dimensions of the Titan IV or any other current launch vehicle. It must also deploy into a doubly curved configuration so that additional structural elements such as standoffs need not be used to create a parabolic shape for support of the reflector. Finally, the truss should be very stiff to promote achievement of the proper precision.

The truss concepts, described in the following sections, are, in general, based on the Pactruss. The Pactruss can be designed to simultaneously satisfy the needs for reliable, highly synchronized deployment, double-fold packaging geometry, deployment into doubly curved area trusses and high stiffness. In addition, the Pactruss is very flexible in that its geometry is readily altered to accommodate a variety of reflector geometries.

4.2.4.1 Truss Concepts for a Segmented, Rigid Panel LDA Reflector: The Pactruss has been studied in some depth as part of NASA's Precision Segmented Reflector (PSR) program. In the PSR capacity, the Pactruss supports hexagonally shaped reflector panels of optical precision on three points. This panel configuration dictates a triangular Pactruss geometry such as that shown in Figs. 4.2-7. The PSR approach to attachment of the hex-panels to the truss, however, requires extravehicular activity by Astronauts or advanced robotic assembly techniques.

Hexagonally shaped panels do not readily lend themselves to autonomous deployment techniques. One method has been described in Ref. [4.2-2] and is shown in Fig. 4.2-2, but this approach is not appropriate for deployment onto a backup truss. Additionally, deployment into five rings of 130 or more segments is required since panels will be about 4.0 meters in diameter and the aperture is 40 meters. The mechanical complexity would be staggering. The task might more reasonably be accomplished with the mechanized canister approach depicted in Figs. 4.2-5; however, this approach was also considered to be too complex.

Due to the limitations of hex-panels, rectangular panels have been chosen for further study of the 40-meter LDA with rigid, segmented reflector panels. Rectangular panels can be accordion-folded and deployed into long rows on tracks built into the surface of a rectangular geometry Pactruss such as that shown in Fig. 4.2-6. A minimum of 13 rows and columns of 3.1 meter square panels would be required to fill the 40-meter-diameter LDA aperture. Two rectangular geometry Pactruss configurations that are appropriate for the LDA requirements have been conceived and are shown in Figs. 4.2-10 and 4.2-11.

A concept for deployment of square panels onto the truss is shown in Figs. 4.2-12(a-d). This

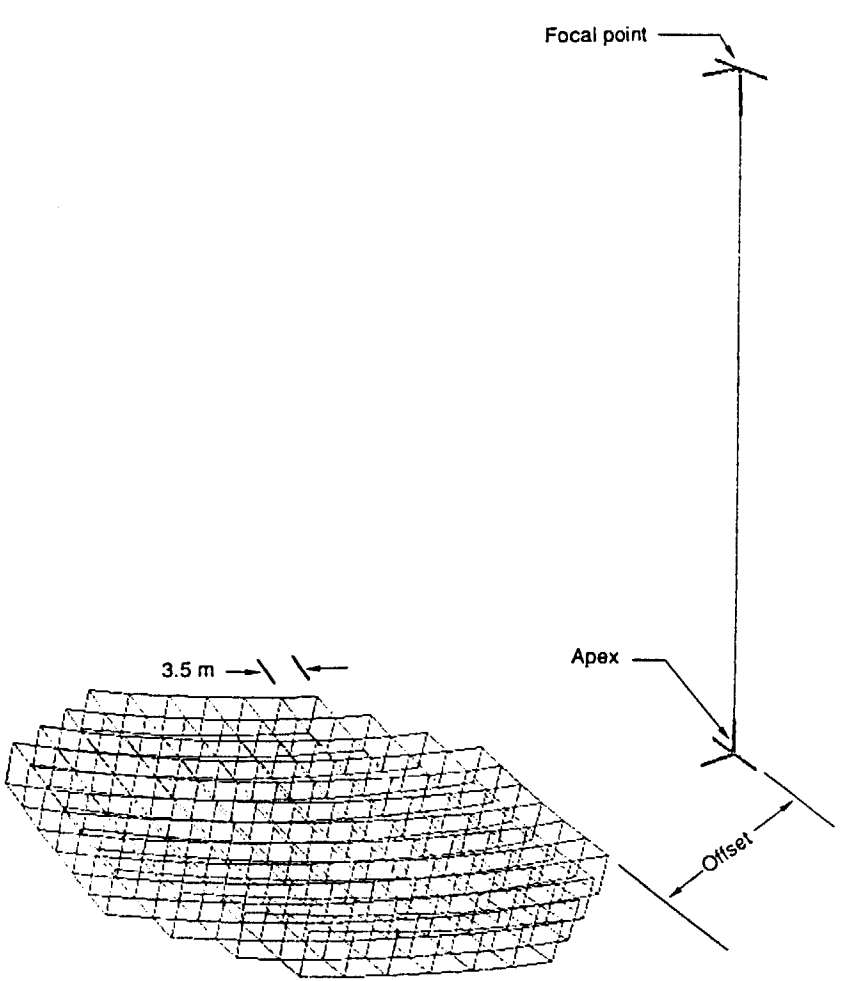

Figure 4.2-10. Pactruss for Rectangular Rigid Panels - 45° Orientation with Axis (diagonal members omitted for clarity)

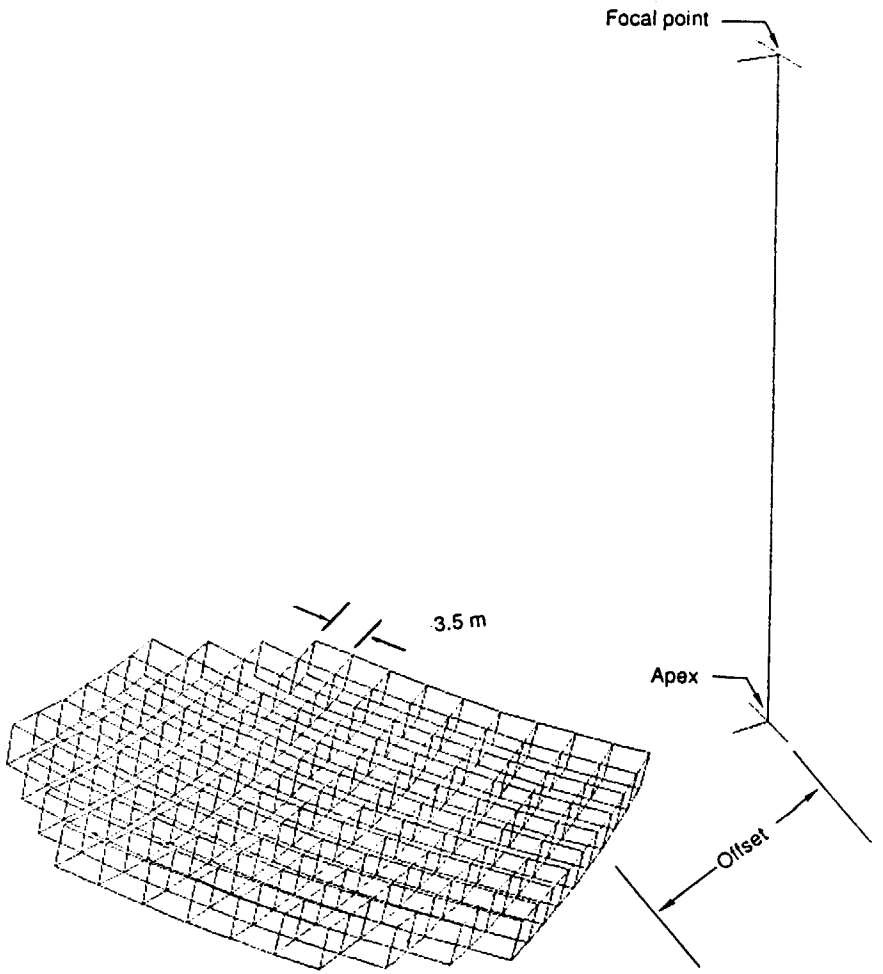

Figure 4.2-11. Pactruss for Rectangular Rigid Panels - Orthogonal Orientation with Axis (diagonal members omitted)

deployment concept is however not appropriate for a 40 meter aperture, because the panel stack width must be less than the payload maximum diameter of 4.4 meters. If the package shown in Fig. 4.2-12(a) is rotated 90 degrees so that a larger panel stack height is possible, the stowed

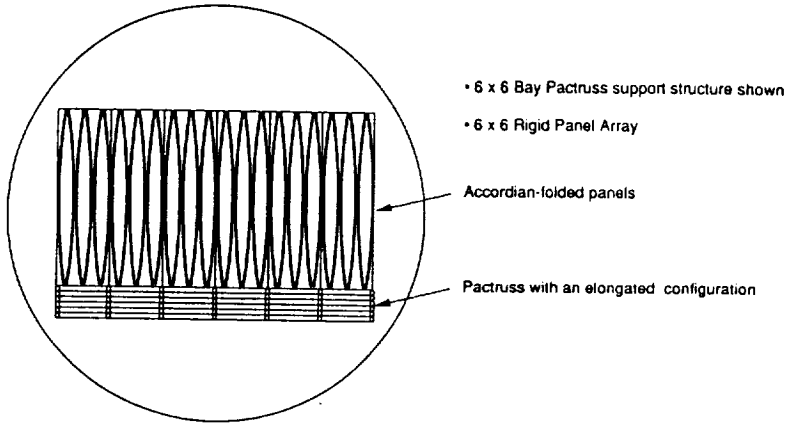

Figure 4.2-12(a). Square panel deployment concept - stowed

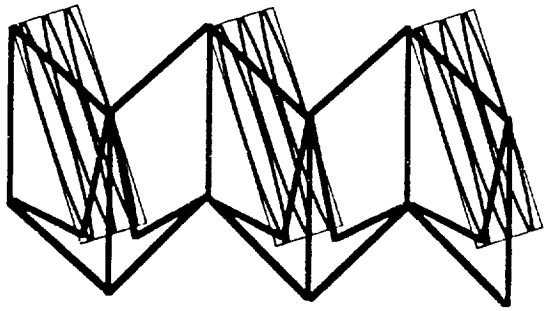

Figure 4.2-12(b). Square panel deployment concept, partially deployed

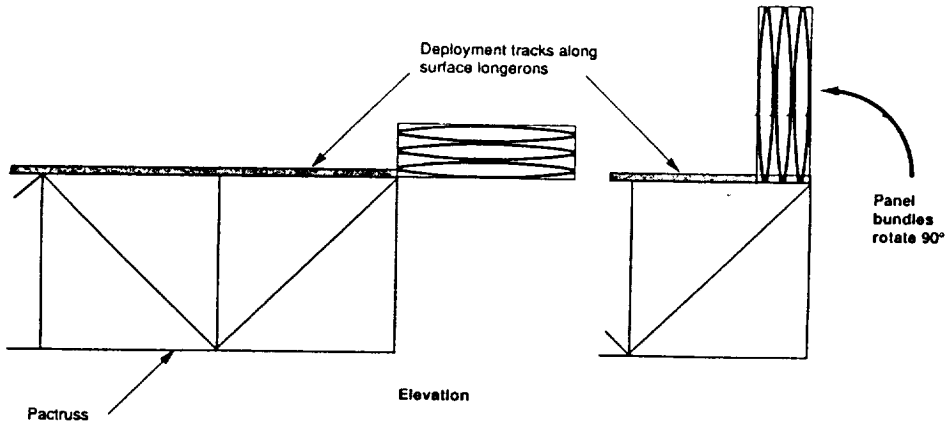

Figure 4.2-12(c). Panel deployment concept, Truss deployment complete

Pactruss is then limited to less than the allowable payload diameter. A stowed Pactruss is about 2 times as long as its deployed depth. If the panels are rectangular, the payload cross-section will be utilized more efficiently and the panel stack height limit is the length of the payload bay. The concept provides the possibility of truly autonomous deployment with relative simplicity. Deployment of the Pactruss synchronously unfolds the bundled rows of panels as shown in Fig. 4.2-12(b). Once this is accomplished and the Pactruss is fully deployed, the bundled rows are lined up along one edge of the truss, panels parallel to the truss face. They must then be rotated to be perpendicular to the truss face as shown in Fig. 4.2-12(c). The panels may then be unfolded accordion style in tracks on the truss face as shown in Fig. 4.2-12(d).

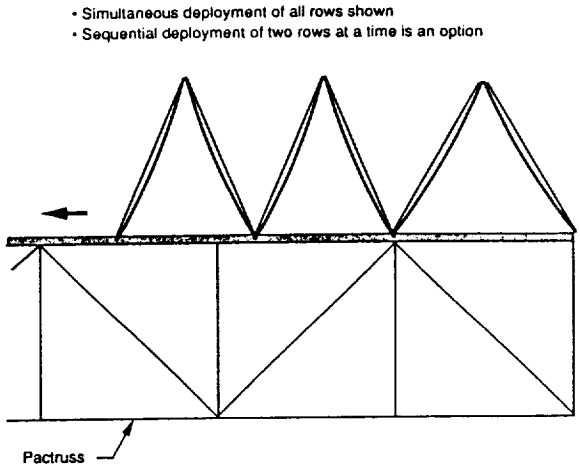

Figure 4.2-12(d). Square panel deployment concept, Reflector deployment

Figure 4.2-13 shows how the Pactruss would be stowed separately from the 3.1 meter square panels in the launch vehicle. Although autonomous deployment of this configuration is probably

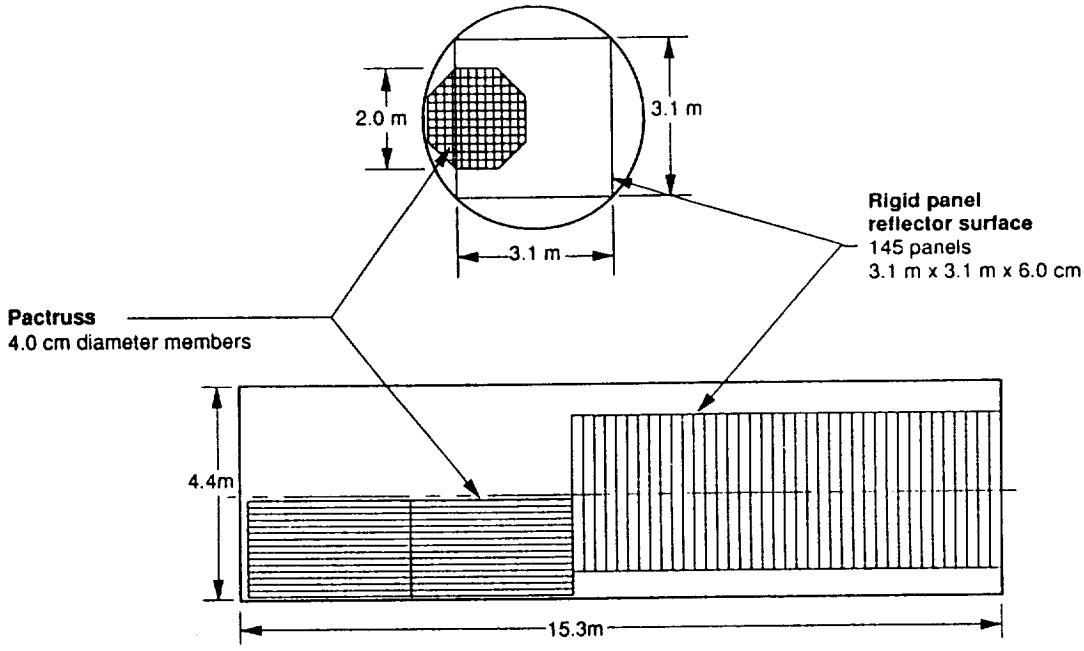

Figure 4.2-13. Primary Reflector Stowed on Titan IV

impractical, the figure illustrates that a 40 meter diameter rigid paneled primary reflector with 6.0 centimeter thick panels will fit into a Titan IV with little volume remaining for other constituents of a complete radiometer space craft such as the secondary reflector, feed and feed support structure, bus and solar arrays. Composite Optics has indicated that 3.1 meter square panels would require a shell and rib structure of about 12 centimeters thickness. The stack height of 145 panels 12 centimeters thick alone exceeds the maximum payload length of a Titan IV in the geosynchronous launch capability. Obviously, a 40 meter diameter segmented, rigid panel instrument will not be feasible until one of the following situations applies:

1. New launch vehicles such as HLLV are available
2. Orbital assembly from several launch vehicles is deemed acceptable
3. Materials with several orders of magnitude greater strain accuracy/stability are available.

4.2.4.2 Truss Concepts for Furlable Reflector Strips: The furlable reflector concept was originally conceived by Composite Optics, Inc. (COI) as a one-piece dish that can be rolled into a cigar-shaped bundle for stowage. For the LDA configuration, the reflector must be cut into 40-meter-long strips that can be rolled onto parallel tracks built into the supporting truss after its deployment.

The rectangular geometry Pactruss designs described in the previous section and shown in Figs. 4.2-10 and 4.2-11 are appropriate for the deployment of long, narrow, furlable strips. The rectangular truss configuration, however, requires that each furlable reflector strip have a unique figure whether it occupies a row or a column in the surface pattern of the truss. It would be desirable to have only one type of furlable strip, such as a gore, that is repeated throughout the aperture. Therefore, only one mandrel would need to be made for fabrication of all the furlable strips.

A plan view of a gored truss geometry for an offset aperture is shown in Fig. 4.2-14 The truss would be made from adjacent tapered beams that are identical except in length. The long edges of the beams radiate from the apex of the parent parabola. The design of a gored truss is aided by an aperture geometry that is significantly offset. This keeps the truss edges from converging together to one point at the apex. It may be possible to design such a truss using Pactruss geometry; however, other geometries may be found to be appropriate upon careful review of the gored approach to deployable truss design.

Stowage of the Pactruss with furlable strips is much more efficient than with rigid panels. The furlable packages can be attached to the outer longeron struts which stow vertically in the launch vehicle as shown in Figs. 4.2-15. Figure 4.2-15 depicts furlable strips that are one truss bay wide. When the truss is deployed, the bundles of furlable strips end up in the proper position for deployment by rolling out onto tracks or ruling surfaces built onto the truss face. More detailed concepts for actual deployment of furlable strips onto a truss are discussed in forthcoming sections of this report.

4.2.4.3 Ring Truss Concept for a Membrane Reflector: A new concept for a ring truss has been designed using Pactruss geometry and is shown in Fig. 4.2-16 with its deployment sequence. The PacRing, like the Pactruss, is highly synchronized during deployment and is capable of high precision without the guy wires or spokes often associated with ring trusses.

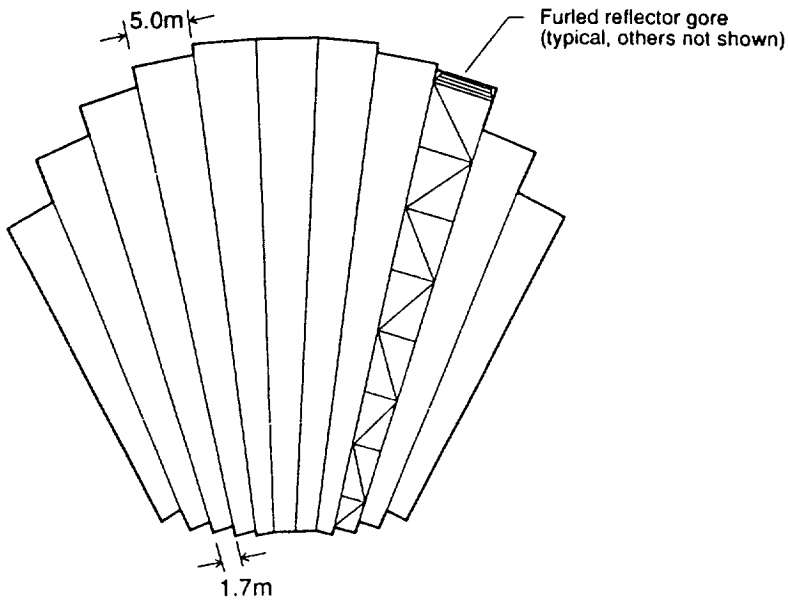

Figure 4.2-14. Gored Truss Plan View Concept

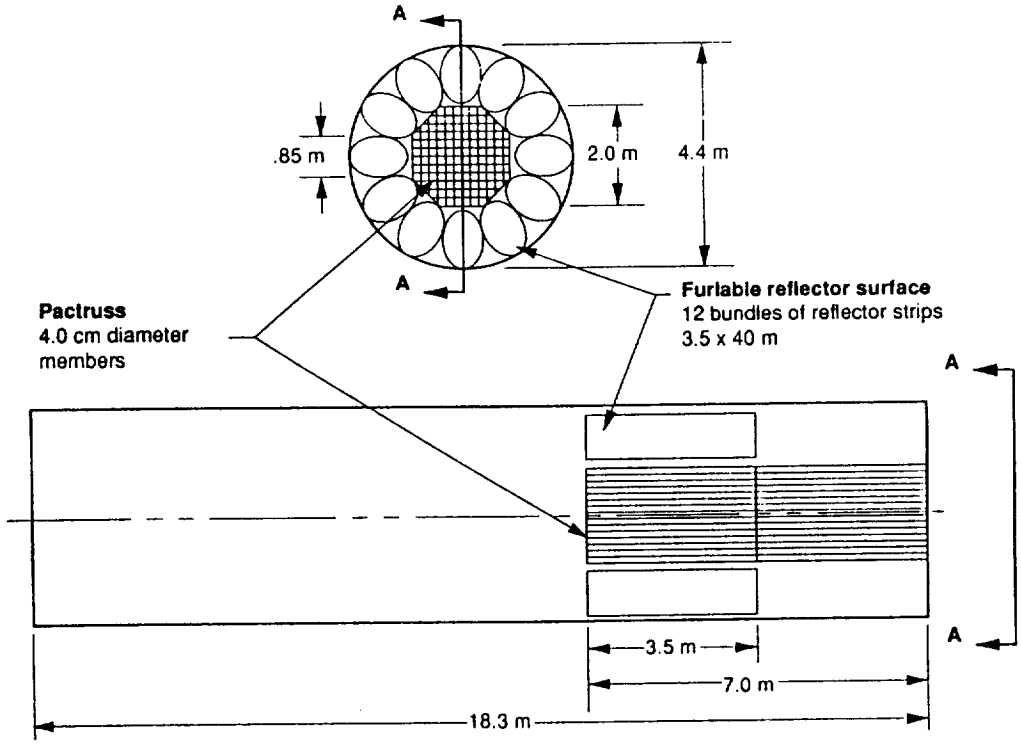

Figure 4.2-15. Primary Reflector Stowed on Titan IV

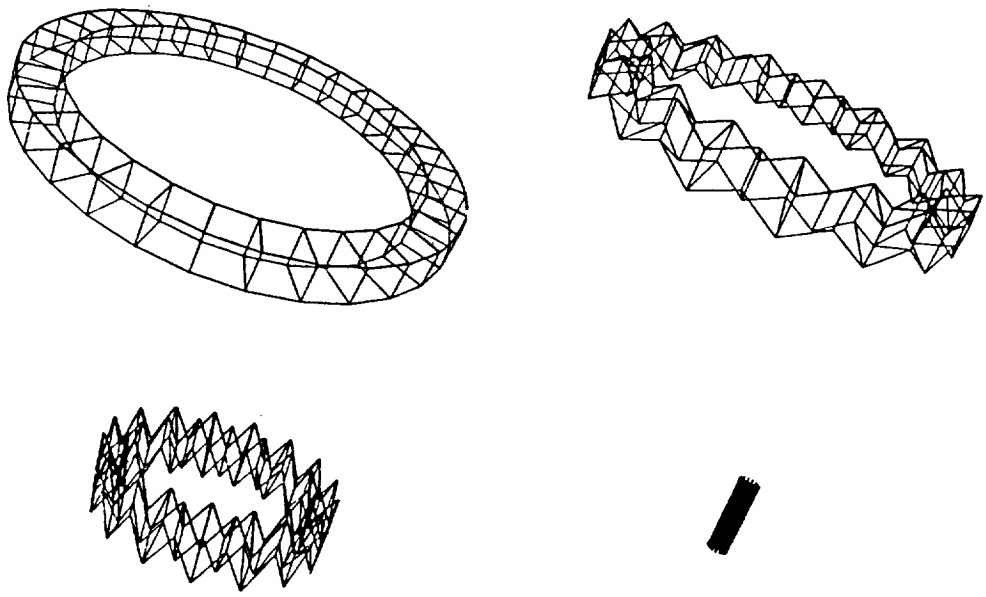

Figure 4.2-16. Pacring Support for Deployable Membrane Antenna

4.2.5 *Selected Radiometer Structural Configuration*

The conclusion of the reflector studies by the various contractors is that only a rigid paneled radiometer can achieve the required surface precision for the 40 m diameter aperture. Packaging studies of the rigid paneled configuration concluded that a 40 m diameter aperture will not stow within a Titan IV.

Therefore parametric studies were conducted with the rectangular paneled truss configurations described in Section 4.2.4.1. It was determined that the maximum aperture diameter possible within the other constraints of this study is approximately 28m. The maximum aperture configuration, when stowed with the feed and secondary, occupy about 14m of the Titan IV payload bay. The deployed radiometer is depicted in Fig. 4.2-17 and it is shown stowed in Fig. 4.2-18.

4.3 Reflector Surfaces

4.3.1 *Rigid Facets*

Various concepts for large deployable antennas (LDA) have been developed. Two deployable surfaces commonly used are either a continuous mesh or an assembly of rigid, continuous surface facets. For upcoming remote sensing applications, reflector apertures of up to 40 meters and frequencies on the order of 40 GHz are desirable. For these targeted frequencies, mesh surfaces have inadequate reflectance characteristics which drives the design to a continuous solid surface. Surface accuracies for adequate performance at 40 Ghz need to be on the order of .1 mm RMS.

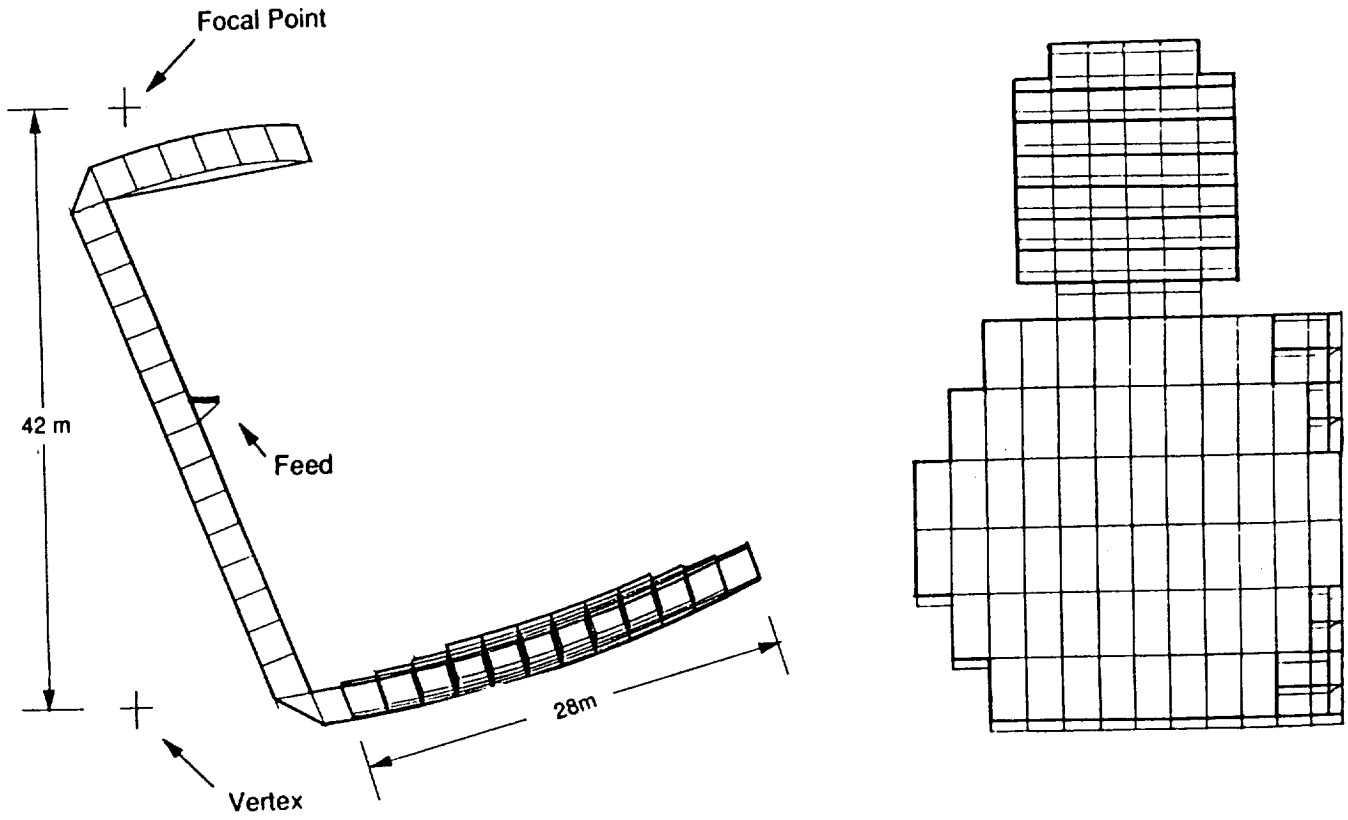

Figure 4.2-17. 28 meter LDA radiometer spacecraft structural Concept

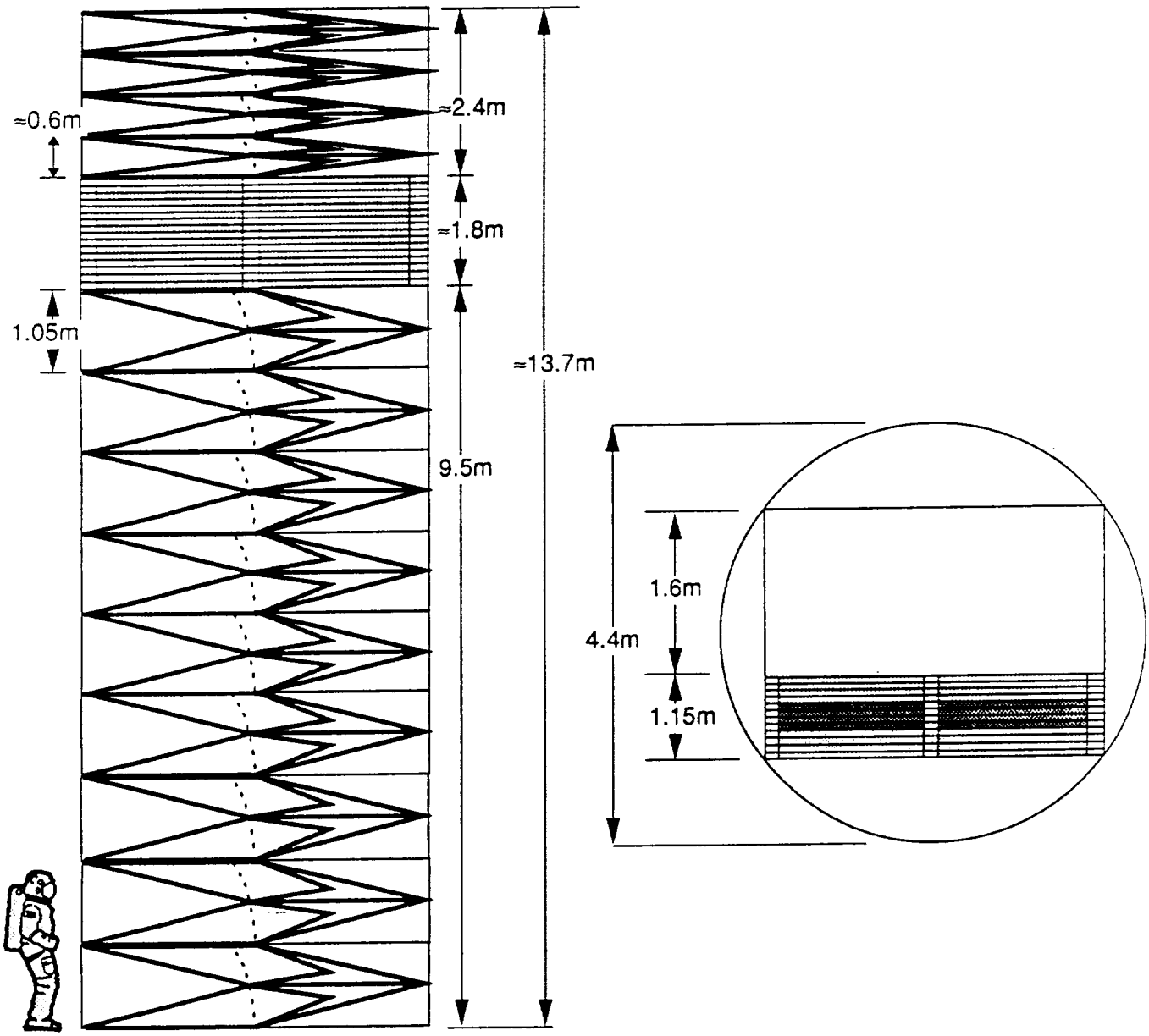

Figure 4.2-18. 28 meter radiometer structure stowed in Titan IV

Composite Optics has manufactured many continuous-surface reflectors that are of the following four types.

1. The single-surface, honeycomb-shell-stiffened reflector used on the Advanced Communication Technology Satellite (ACTS) receive and transmit reflectors.

2. The single-surface, membrane-stiffened reflector used on the Direct Broadcast Satellite (DBS).

3. Dual-shell-stiffened Kevlar gridded reflectors as used on the Ford Superbird, Anik E, Spacenet, Satcom, and GSTAR Satellites.

4. Gridded-shell-stiffened hyperbolic subreflectors with a Kevlar front shell and a graphite/epoxy- stiffened back shell.

Sizes of these reflectors range from 1.0 to 3.3 meters in aperture with areal densities ranging from 2.5 to 6.1 kg/m^2. The manufacturing of rigid continuous surface reflectors which are produced from low-density graphite/epoxy has evolved to the point where achieving surface accuracies of better than 0.1 mm RMS is feasible.

At Composite Optics, Incorporated, (COI), the most recent demonstration of this kind of accuracy has been the 3.3-meter transmit antenna for ACTS where the accuracy achieved was 0.06 mm RMS. Attaining this type of surface accuracy involves employing a highly accurate plaster master mold, from which a high temperature thermally stable graphite/epoxy mold is replicated. After reducing the manufacturing induced thermal stresses in the graphite/epoxy mold, it is used for lay-up of the antenna reflective skins or shells.

A backup support rib structure is also created and the cured skin or shell is laid on it and mapped. The final accuracy of the shell and backup rib structure can be adjusted during manufacturing to achieve surface accuracies of 0.070 mm RMS for 2.2 m reflectors and 0.053 mm RMS for 3.3 m reflectors.

The areal weight of many graphite/epoxy reflectors can vary significantly by the design approach. The ACTS reflector designs exhibit areal weights of 3.4-3.8 kg/m^2. These designs use a graphite skin/Nomex honeycomb shell bonded to graphite skin/Nomex honeycomb rib support structure. Compare this design approach to the COI design used on the DBS. This design uses a .015"-thick graphite/epoxy skin bonded to a backside rib support structure as shown in Fig. 4.3-1. This design yields a much reduced areal density of 2.2 kg/m^2, yet maintains a surface accuracy of 0.11 mm RMS.

4.3.1.1 Design Evaluations: The Astro Aerospace deployment concept shown in Fig. 4.3-2 shows both the stowed and the deployed arrangements for a rigid-facet surface attached to the Astro Pactruss. This concept utilizes square, rigid-facet segments which deploy sequentially on the truss. The stowed arrangement shows the rigid facets to be packaged by stacking one rigid facet on the next as closely as possible.

With this deployment concept, two antenna aperture sizes of 40 meters and 15 meters were

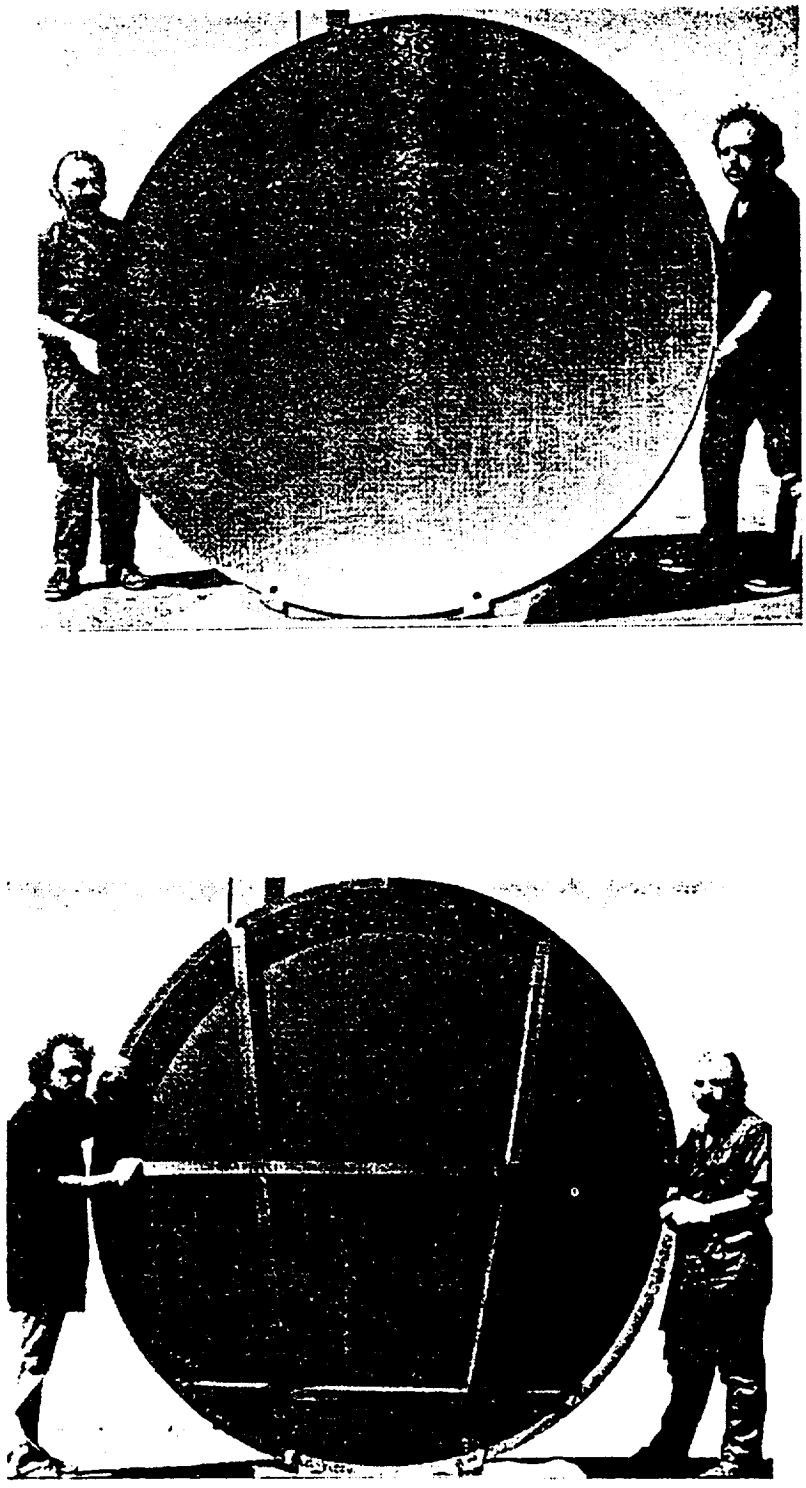

Figure 4.3-1. 2.1 Meter skin stiffened antenna for Direct Broadcast Satellite (DBS)

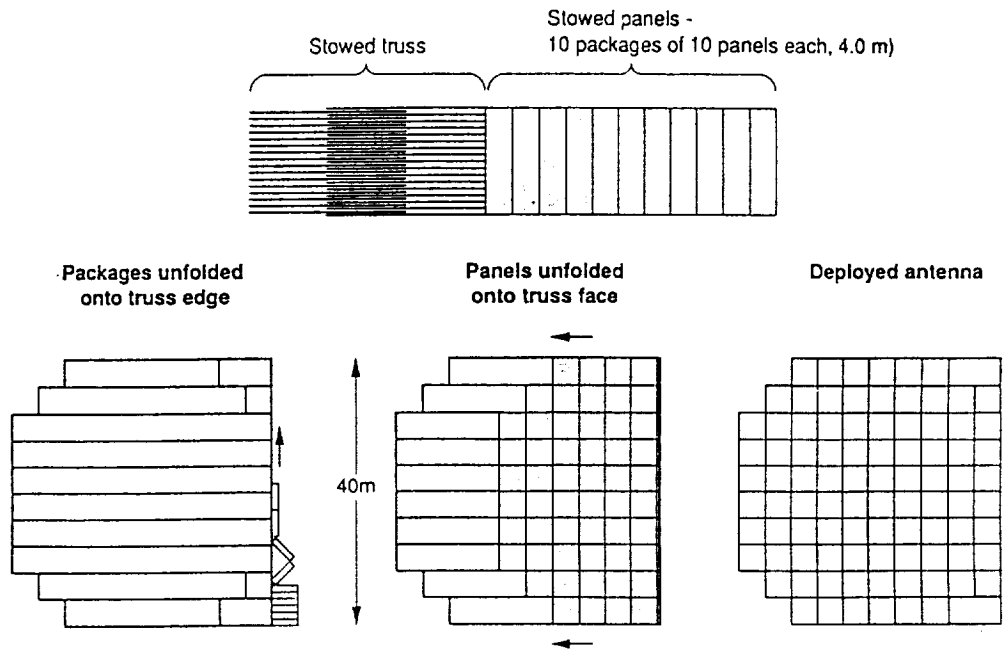

Figure 4.3-2. Deployment Concept for Rigid Panels

investigated. For these aperture sizes, a 3.1-meter and 2.0-meter square facet was baselined for the 40-meter and 15-meter-aperture reflectors, respectively.

The goals for the rigid facet design were a minimum thickness facet and areal density while maintaining facet surface accuracies of 0.1 mm RMS. Minimizing the facet thickness enables more condensed packaging and stowage within the launch vehicle. The total thickness of the facets includes the depth of draw which is dictated by the F/D and the thickness of the facet required to maintain the surface accuracy requirements.

Feasibility of meeting a minimal areal density was also investigated. For the 40-meter-aperture antenna, a 1.0 kg/m^2 areal density was targeted to maintain a reasonable overall total launch weight. As-manufactured surface accuracies for the rigid facets were baselined at 0.1 mm RMS for performance requirements of this LDA application.

A simple finite element model was set up to represent the rigid facet concepts for both the 2.0- and 3.1- meter square facets. A total of 40 "CQUAD4" plate elements were used to model the reflective shell and 44 "CBAR" element used for the backside rib structure. The four support points were all modeled to be simply supported. A 1-g load was assumed to compute the surface standard deviation in order to size the reflector to meet the targeted surface accuracy. Several iterations were performed on both configurations. The results were as follows.

Figure 4.3-3 shows the resultant design concept for the 3.1-meter square facet having a 1.9-cm-(.75-inch) thick shell consisting of 0.25 mm-(0.01 inch) thick graphite/epoxy skins laid up in a quasi-isotropic orientation onto 1.9 cm-thick core. For the purposes of this sizing analysis, aluminum core properties were used in the finite element model. The backside rib structure consists of a perimeter ring stiffener with two separate ribs crossing through the center. These ribs have a cross-section of a box beam with a 1 mm (.04 inch) wall thickness and cross-section

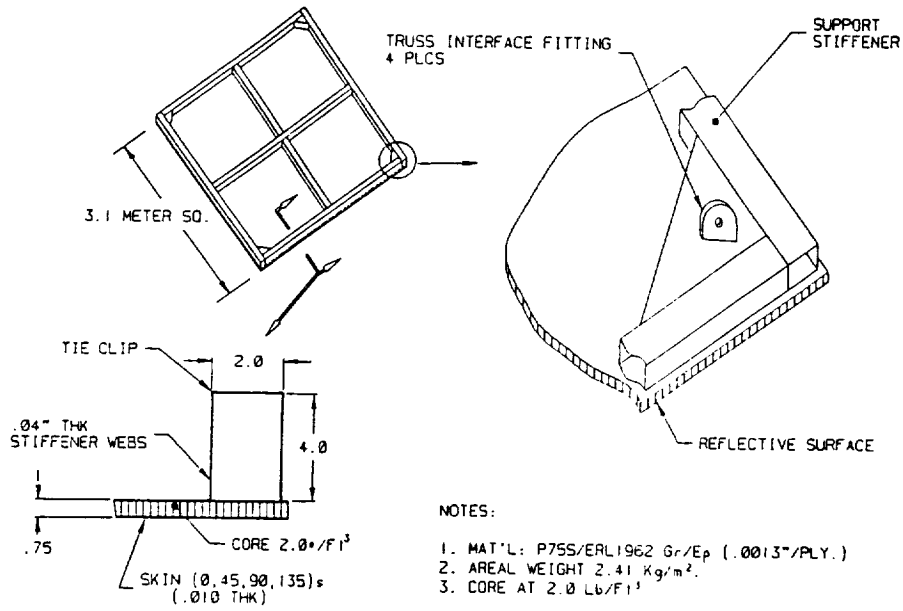

Figure 4.3-3. 3.1 Meter square facet shell stiffened concept

dimensions of 5 cm (2 inches) wide and 10 cm (4 inches) deep. This deep box beam section was required to meet the surface accuracy target with the four-point simply supported attachment.

The resultant areal density calculations for this configuration as follows:

	Weight	
Item	3.1-Meter	2.0-Meter
Shell skins (2)	8.3	3.5
Shell core	5.9	1.6
Backside ribs	7.9	4.6
Tie clips	0.8	0.5
Interface fittings	0.2	0.2
Total Weight (Areal Density)	23.1 (2.4 kg/m^2)	10.4 (2.6 kg/m^2)

The 2.0-meter square facet was of the same design as the 3.1 meter facet in Fig. 4.3-3. It had a 1.3mm-(.5 inch) thick shell consisting of .25mm-(.01 inch) thick quasi-isotropic graphite/epoxy skins bonded to a 1.3cm-(.5 inch) thick core.

The same modeling techniques were used on this concept as on the 3.1-meter square facet. The backside rib structure was the same as the 3.1-meter concept except the cross-section was smaller with 3.8 cm x 3.8 cm (1.5 in. x 1.5 in.) box beam. The wall thickness of the box beam members were .2 cm (.08 inch) thick. The resultant areal density for the 2-meter panel was 2.6 kg/m^2.

For each of the two concepts, the total facet thickness was computed which includes the amount of draw for each case. The amount of draw varies depending where on the antenna the draw is desired. For these purposes, the maximum draw on the antennas was used in the overall

thickness determination which is at the location closest to the vertex. The total panel thicknesses are summarized as follows for each concept.

	3.1-Meter Square Facet	2.0-Meter Square Facet
Maximum Draw	1.96 cm	2.18 cm
Shell Thickness	1.90 cm	1.27 cm
Rib Thickness	10.16 cm	3.81 cm
Total Thickness	14.02 cm	7.26 cm

The results of these preliminary studies show that attaining areal densities of 1.0 kg/m^2 are too optimistic. However, areal densities of 2.0 kg/m^2 seems feasible. Based on the areal densities of previous COI reflectors, areal densities of 2.0 kg/m^2 offer improvements over many of the current reflector designs. Panel thicknesses may also require reduction, especially in the case of the 3.1-meter concept. These preliminary antenna sizing studies results are based on the listed design criteria which are very sensitive to the results obtained.

1. A four-point interface to the truss

2. Quasi-isotropic graphite/epoxy laminates

3. Aluminum core properties.

When considering these baseline design criteria, several further iterations could be performed in future studies to optimize the rigid facet design, thereby producing a reduced areal density and thinner panel design. These include:

1. The interface attachment to the truss is presently a four-point attachment with one point at each of the corners of the rigid facet. There could be considerable improvement to the panel design if an increased number of attachments were feasible. One option could be a six-point attachment with three truss interfaces along each edge, thereby giving additional support at the center of the panel. Another option would be a center truss interface support where the center of the panel would be supported. Additional supports seem to offer the most benefit to reduced areal weight and panel thickness.

2. The design concepts shown baseline the P75 high- modulus graphite/epoxy fiber system which is a 75- million-modulus fiber. This fiber selection is ideal due to its near-zero CTE characteristics when laid up in a quasi-isotropic orientation. The baseline concepts assume all laminates (shell and ribs) are quasi-isotropic. However, further optimization is possible where the backside rib structure could be designed using a more directionalized orientation or using higher-modulus graphite/epoxy material (e.g., P100 or P120). This would benefit the design since the cross-sectional properties of the box beam ribs could be reduced.

3. The core selection is another area requiring further investigation. In place of aluminum core, COI could propose a quasi-isotropic tri-cell core made of the same parent

graphite/epoxy material as the shell skins. This benefits the structure by offering a more uniform sandwich CTE. The core can also offer improved core shear modulus which improves the sandwich stiffness. In addition, it is anticipated that the core density could approach 1.5 lb/ft^3, thereby reducing the areal densities of the rigid facets. Figure 4.3-4 shows COI's graphite/epoxy tri-cell core and its possible use in applications such as these.

4. Additional design options could be studied which are similar to those shown in Figs. 4.3-5 and 4.3-6. These options require further analysis in future studies. They represent viable alternatives requiring investigation.

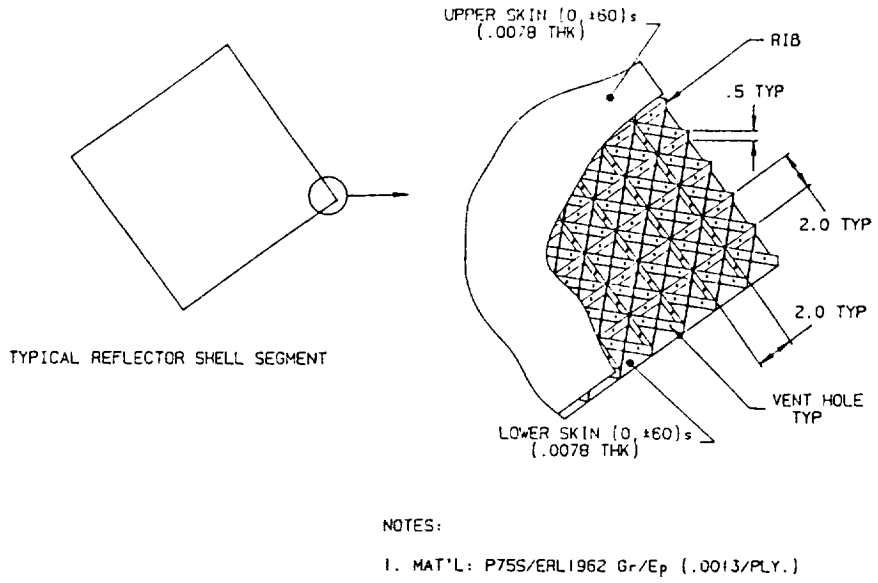

Figure 4.3-4. Tricell sandwich design concept

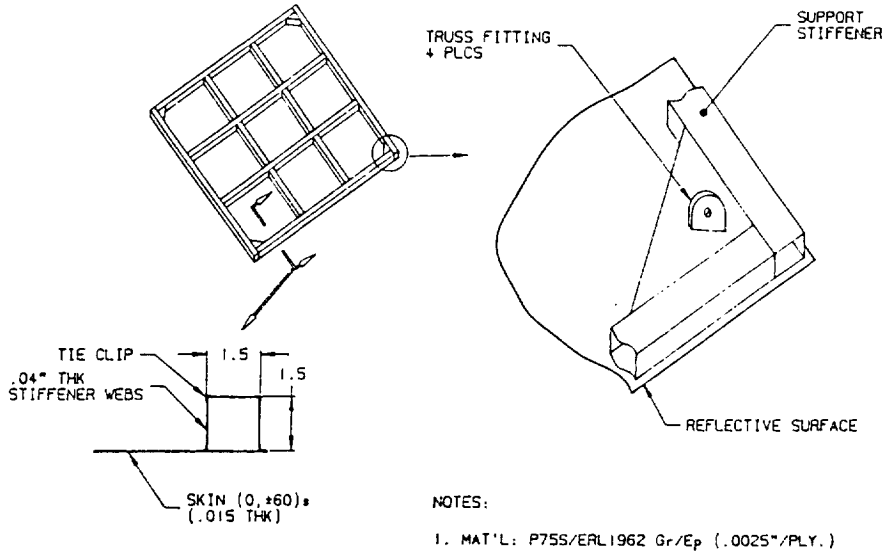

Figure 4.3-5. Shell stiffened concept 2

Figure 4.3-5 shows a membrane-stiffened reflector similar to the Direct Broadcast Satellite (DBS) reflector manufacturing at COI (see Fig. 4.3-2). Figure 4.3-6 shows a rigid facet panel design whereby discrete ribs from the inner core are enclosed by a top and bottom facesheet. The discrete ribs can be individually optimized to meet the requirements. This approach is similar to that used on thermally stable space-based optical bench designs.

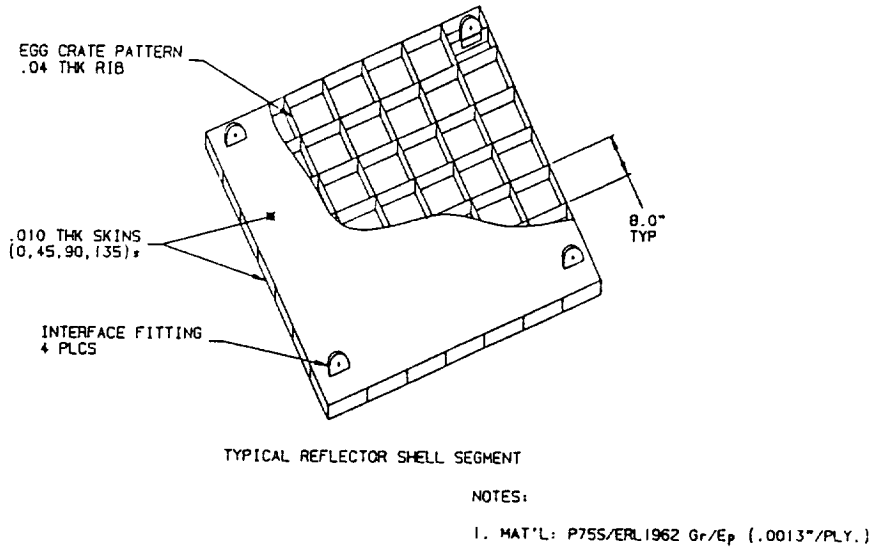

Figure 4.3-6. Egg crate shell design concept 2

4.3.1.2 Manufacturing Considerations for Rigid Facets: The baseline design of the rigid facets assumes use of elevated-temperature-curing graphite/epoxy composite systems typically requiring a 250°F or 350°F cure with vacuum bag or autoclave pressures. Since elevated curing is required, a parabolic mold tool is required that can withstand the temperatures without degradation to the surface accuracy.

The tooling approach used to develop the parabolic mold tool shape is briefly described in Section 4.3.1. A master mold is fabricated of plaster to surface accuracies of below .025 mm RMS. From this master mold, a graphite/epoxy production mold is replicated which is used as the mold in which to lay up the final reflector hardware. This mold is thermally stable and capable of withstanding the temperature extremes required to cure the space-based reflector hardware material. These are the tooling requirements employed at Composite Optics. Other variations on this approach are feasible, especially for reflector sizes less than 1.5 meters. These include primarily the use of low-expansion metal or bulk graphite tooling as the master mold. However, for aperture sizes in excess of 1.5 meters where surface accuracy requirements of .2 mm RMS or better are required, the thermally stable high-temperature composite mold approach is preferred.

This was the approach on the recent ACTS reflectors which has final as-manufactured surface accuracies of 0.076 mm RMS for a 2.2-meter-aperture, solid-surface reflector and .053 mm RMS for a 3.3-meter-aperture reflector. It is anticipated that the same surface accuracies can be attained for the 2.0-meter and 3.1-meter square rigid facet segments for the LDA application.

While this tooling approach is successful and could be used, it does require a large number of high temperature and master molds for the baseline concept of 15 or 40-meter aperture. The baseline approach requires a separate mold tool for each 2 or 3-meter square rigid segment due to the variations in the parabolic geometry of each segment which comprise the entire aperture.

The number of mold tools can be greatly reduced. Since the radial parabolic geometry is the same, a set of four (4) master molds can be fabricated so that each square reflector segment can be manufactured by rotating the segment to the appropriate angle. This approach again is identical to the one typically used at COI and the same surface accuracies could be attained as was achieved on ACTS.

4.3.2 *Furlable Surfaces*

With the need for high-frequency, large-aperture antennas, COI has developed a unique approach to a deployable continuous surface that can be furled into a cylindrical bundle. COI designed and manufactured a one-meter reflector surface that can be rolled into a semi-cylindrical volume for storage and then allowed to unroll and register against a deployable substructure (an underlying truss structure) to reform the fabricated parabolic shape. The result is a continuous surface that can provide surface accuracies of acceptable quality for aperture diameters of up to 15-meters.

COI fabricated a one-meter furlable reflector surface that deploys on a rigid support frame as a proof-of-concept (Fig. 4.3-7). The reflector furlable surface was manufactured from six-ply P75S/930 graphite/epoxy on a high-temperature graphite/epoxy mold. The support structure is made of the same graphite/epoxy laminate and consists of a perimeter support ring with a two-inch-square cross-section and a diameter slightly smaller than the one-meter skin. The

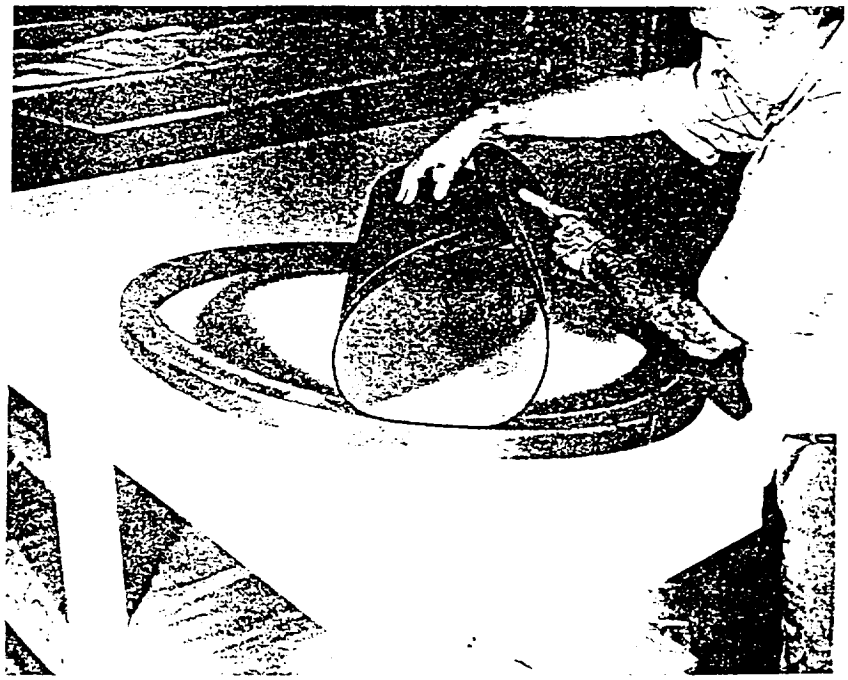

Figure 4.3-7.

support structure also employs a curved beam across the center of the support ring with the same cross-section as the ring so that, when the skin is resting on the perimeter ring, it will also rest on the curved beam.

Two sets of restraints were used. The first set holds the furled skin on the support ring at two points on the center beam. One point allows for rotation and the other allows for rotation and radial translation. The second restraint supports the unfurled skin on the perimeter support ring by using a flexible magnetic strip on the inside upper edge of the ring (Fig. 4.3-8) and orients the surface to be parallel to the surface of the deployed skin. An additional ferrous flexible magnetic strip was bonded to the backside of the skin which mates to the magnet in the support ring during deployment.

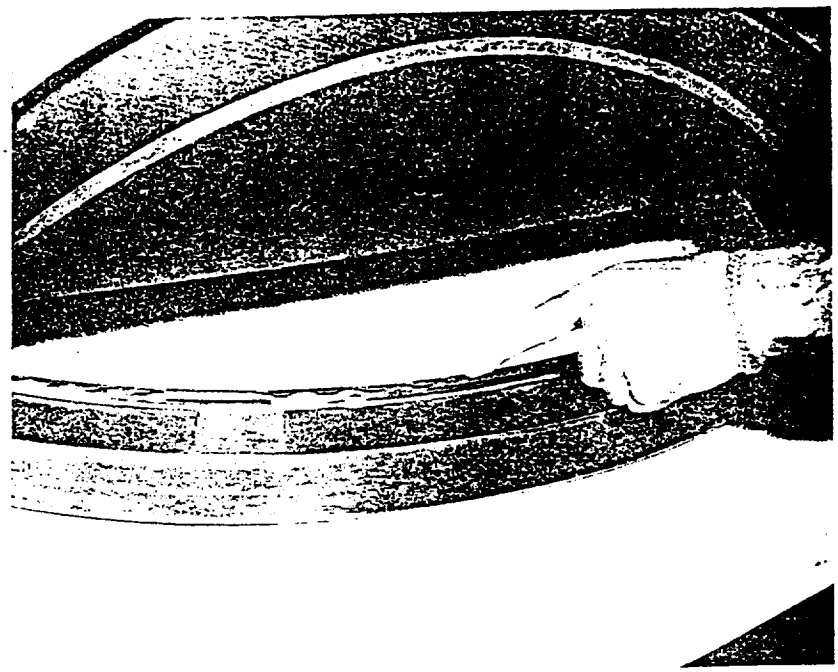

Figure 4.3-8.

This restraint method provides retention of the skin to the support structure and also aids in the deployment process by the magnetic force of attraction between the unfurling skin and support ring.

4.3.2.1 Preliminary Analysis: In an effort to support the preliminary design configurations for large-aperture, furlable reflector surfaces, preliminary material evaluation/sizing analyses have been conducted for a number of aperture sizes ranging from five (5) to forty (40) meters. Results of these analyses are presented in the following sections. In addition to the detailed analysis of the furlable reflector surface, preliminary analysis concerning minimum roll diameters for which the reflector surface may be rolled for subsequent storage will be discussed.

Material Properties: In order to meet the performance requirements of the LDA program, a high-modulus graphite/epoxy material system (i.e., P75S/ERL1962) has been selected for preliminary evaluation. Lamination of the P75S/ERL1962 material system in a quasi-isotropic laminate configuration results in:

1. A near-zero CTE in the plane of the material ($\alpha = \pm 0.1 \times 10^{-6}/°F$),

2. A laminate configuration capable of seeing temperatures as low as -250°F without microcracking, and

3. A relatively stiff configuration (i.e., frequency requirements) with an in-plane modulus of approximately 14.5-15.5 MSI

Minimum Effective Roll Diameter: The fundamental concept behind the furlable reflector surface is that of rolling the reflector surface as a whole or as segments into cylindrical canisters for storage during launch. Once in orbit, the reflector surface can be unrolled and allowed to register against a deployable substructure to re-form the fabricated parabolic shape.

An analysis was performed to determine the minimum roll diameter for the furlable antenna surface. The analysis considered the amount of stress in the plies that may initiate fracture of the laminate, creep in the laminate while rolling the surface, and a preferred roll direction for which the laminate provides the minimum roll resistance. The analysis also assumed a flat reflector surface. The minimum diameter to which a 0.010-inch-thick quasi-isotropic P75S/ERL1962 laminate can be rolled is 13.0 inches. A smaller diameter roll may initiate fracture in the laminate or have high amounts of creep. By increasing the laminate thickness from 0.01 to 0.015 inches, the minimum roll diameter increases to approximately 20.0 inches.

Work up to this point has been restricted to preliminary evaluation of a single "flat" laminate configuration being rolled in a specific direction. Further analysis should be performed to determine alternate laminate configurations, long term creep effects and stress in the rolled laminate.

4.3.2.2 Panel Sizing Analysis: Analysis of the appropriate panel sizes for two Pactruss design configurations was performed: a gored truss and a square truss. The panel size for the different configurations was chosen based on an the RMS surface accuracy of the overall antenna surface under a 1-g loading condition. The surface accuracy was determined by measuring the Z displacements of the individual nodes forming the reflector surface.

Gored Truss: Initially, a gored truss configuration, such as that shown in Fig. 4.2-14, was evaluated for various aperture sizes ranging from five (5) to forty (40) meters. In order to evaluate the various design configurations, a finite element model of a representative gore section for each of the configurations was constructed. For the purpose of the current study, the individual gore sizes evaluated were assumed to be a linear function of the focal length. Simply supported boundary conditions were assumed for all four sides of the gore section. A facesheet thickness of 0.01 inches was assumed for all subsequent analyses.

Resulting RMS surface accuracies for the various gore sizes varied from 0.0024 to 0.0389 inches for the 10 to 40 meter apertures respectively for the 1-g load in the Z direction. It can be seen from these results, that in order to meet the design goal of 0.1 mm (.00393 in.) RMS surface accuracy, a maximum aperture size of approximately 12 meters would be required (based on linear interpolation for the 1-g loading condition). The maximum acceptable aperture size might be increased by the addition of circumferential attachment points at mid-span of the gore section.

It is estimated that apertures in the range of 15-16 meters might be feasible.

Square Pactruss Design: An alternate Pactruss concept that has been proposed by the Astro Aerospace Corporation and is presented in section 4.2.4.2 is the "rectangular geometry Pactruss". Preliminary sizing analyses conducted by the Astro Aerospace Corporation for the "rectangular geometry Pactruss" have resulted in bay sizes on the order of 3.0 meters for a 40-meter aperture reflector, and 2.0 meters for a 15-meter aperture reflector.

Finite element analysis of representative segment sizes were conducted for reflector apertures of 10 meters to 40 meters. Boundary conditions consisted of assuming all four edges of the facet to be simply supported. The resulting RMS surface accuracies once again indicate a maximum aperture of approximately 15 meters for meeting current surface requirements.

Future work should be directed toward more detailed evaluation of support conditions (i.e., fixed vs. simply supported, continuous or discrete); the effect of support truss inaccuracies on the resulting RMS surface accuracy; and affects of mismatch in CTEs between the reflector surface and the truss structure on RMS surface accuracy as well as resulting attachment loads.

4.3.3 *Deployment of Furlable Surfaces*

COI performed deployment tests on the one-meter furlable antenna with the configuration described in Section 4.3.2.

Three successful deployments onto a support structure with magnetic restraints (as described in section 4.3.2) were done with the reflective surface up. Additional deployments were performed in a vertical, on-edge position which resulted in complete deployment. The reflector was then tipped beyond vertical to test whether the magnetic forces in this design were adequate to overcome the 1-g gravitational effects. It was discovered that a 10° position beyond vertical was the point at which complete deployment did not occur.

COI then mapped the one-meter furlable reflector to determine surface accuracy and focal length after a series of deployment repetitions. Mapping was done at sixty (60) points on the reflector surface using electronic theodolites. The reflector was deployed twice and mapped after each deployment. In addition, another map of the surface was performed where a .050" x .5" shim was intentionally placed at one interface between the skin and perimeter support ring to detect the sensitivity of surface accuracy and focal length. Table 4.3-11 shows the results of these maps.

The mapping results show very close correlation of surface accuracy (RMS) and focal length. The map that was performed with the .05" x .5" shim was to demonstrate sensitivity on surface accuracy and focal length of localized anomaly. The results showed a doubling of best-fit RMS with a slight reduction in best-fit focal length. The effect on the skin caused by the intentional shim is a very localized effect.

Table 4.3-11
Mapping Results of COI One-Meter Furlable Reflector

Initial Surface	RMS: 0.0047"
	Focal Length: 24.110"
After First Deployment	RMS: 0.0042"
	Focal Length: 24.100"
After Second Deployment	RMS: 0.0039"
	Focal Length: 24.102"
After Deployment with 0.05" x 0.5" shim at one Point Along Perimeter Magnetic Interface	RMS: 0.0068"
	Focal Length: 24.068"

4.3.3.1 Design Evaluation: The application of the furlable skin concept to large-aperture antennas was investigated with a number of different design concepts. Many critical parameters were foreseen for deployment of furlable skin antenna segments. Some are listed here.

1. Deployment of furlable skin segments requires support to the underlying truss structure. This support may be point contacts, perimeter support, or a combination of both.

2. Controlled deployment of the furlable segments is preferred because precise placement and lock-down is guaranteed. Furlable segments require positive engagement force magnetic surfaces or other proposed lock-down methods.

3. Deployment of furlable segments need accurate placement to maintain a maximum gap of 1 mm between furlable segments and to maintain overall antenna surface accuracy without skin surface-to-truss interface anomalies.

4. Furlable segments need to have provisions for lock-out to the truss and lateral engagement lock-out in order to maintain their relative position on the truss over long periods of time.

A number of different deployment concepts were developed for the LDA application.

The deployment of the furlable skin is a secondary deployment after full deployment of the underlying truss. It involves unfurling the reflector skin bundle onto the truss by controlling the unrolling of the rolled bundle. Important to all of the different techniques that were studied for deploying the furled surface is the proper positioning of the edges of each of the furled segments.

The unfurling process can be accomplished by restraining the unrolling of the furled segment with a canister as shown in Fig. 4.3-9 or with a restraining cord as shown in Fig. 4.3-10. The edges of the segment are deployed with the use of movable tracks at each radial edge or by a zipper concept attaching the edges of the unfurling segments to the truss. A number of other techniques were also investigated.

Many different configurations of the furlable segments can be employed for covering the whole surface of the reflector. The segments can be unfurled inward to a central vertex or from an offset vertex as shown in Fig. 4.3-11. Different unfurling concepts provide different types of tooling configurations which can minimize the complexity of the manufacturing.

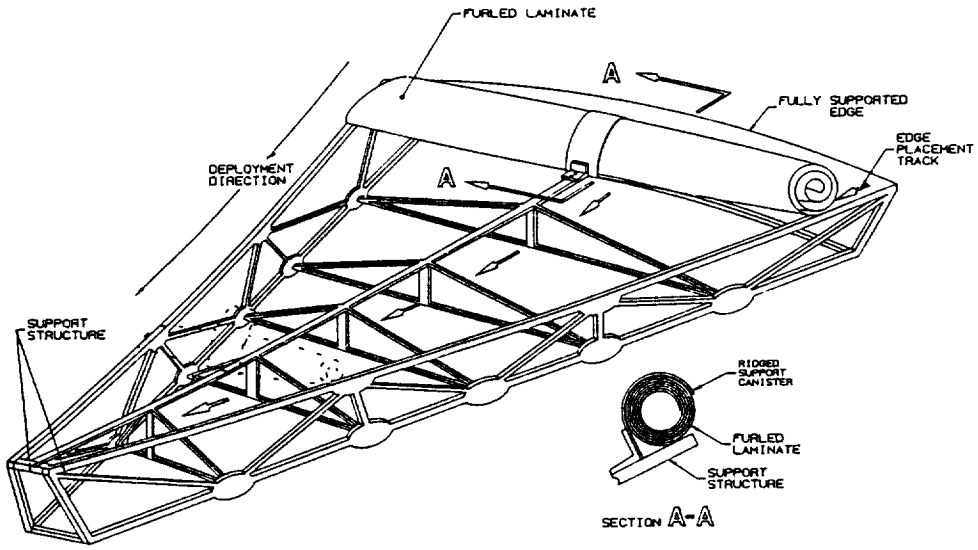

Figure 4.3-9. Canister support concept

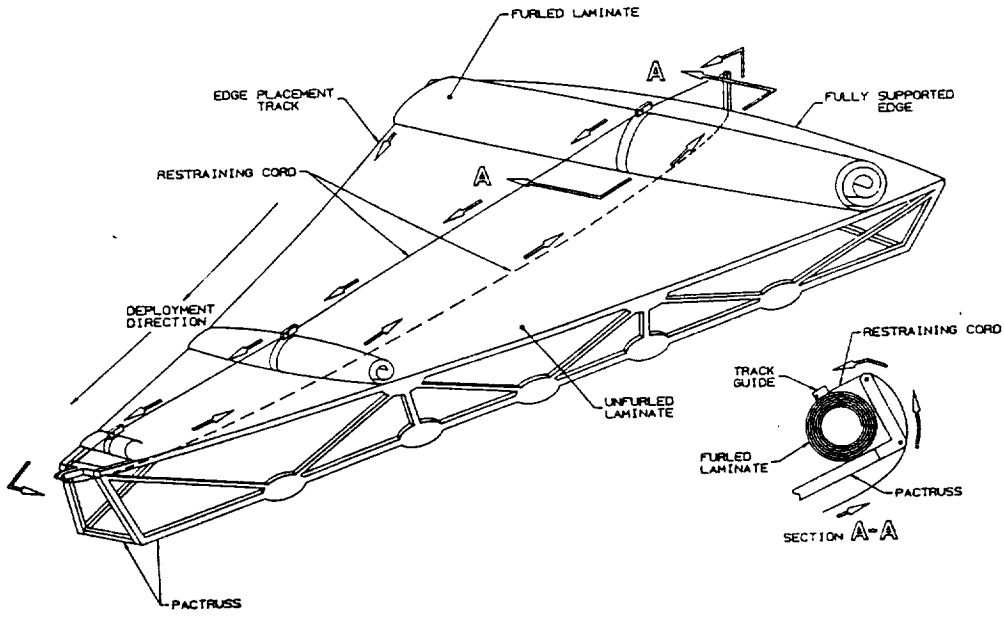

Figure 4.3-10. Restraining cord concept

4.3.3.2 Manufacturing of Furlable Segments: The manufacturing of the furlable segment reflector using existing technology is feasible using the same tooling approach as described in Section 4.3.1.1 for the rigid facet concept. In the case of the furlable segments, however, it is advantageous to maintain large roll-out segments similar to those shown in Figure 4.3-11.

The manufacturing approaches possible for the furlable segments include using master plaster molds as in the rigid facet concept but of much larger dimensions. The different rectangular furlable segments can be accommodated by rotating each appropriately on the mold. Another

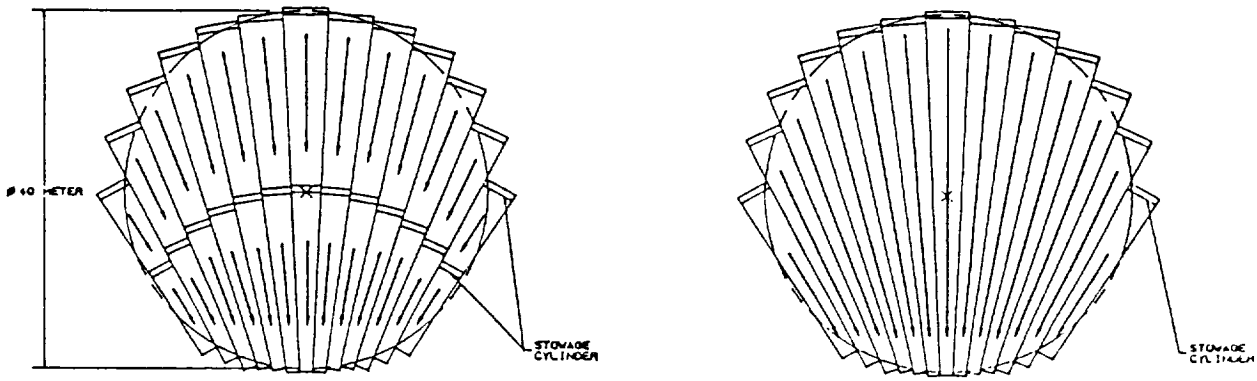

26–SEGMENT RADIAL FACET

13–SEGMENT RADIAL FACET

4.3-11. Furlable segment radial deployment concept

method involves making master molds that form the segments that are all identical and simply radiate outward from the offset vertex. This requires two master molds and can be used only for the gored segment approach. A third concept involves making a single master mold to represent the entire reflector aperture. The master mold could be machined in segments as shown in Figure 4.3-12 on a large numerically controlled machining center and spliced together to form the entire aperture.

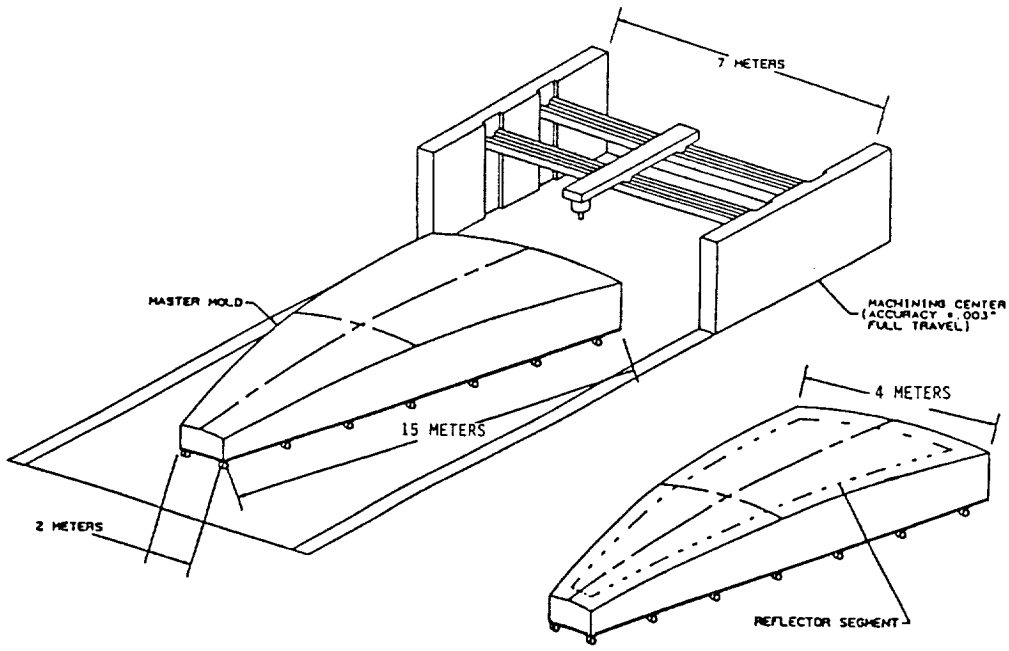

Figure 4.3-12. Master mold machining concept

With this approach, it is proposed to use composite materials that cure at either room temperature or a slightly elevated temperature (180°F), allowing the reflector surfaces to be laid up directly on the master mold. Some of the advantages of using a room temperature cure include:

1. Lay up of reflector on master mold omitting the production of a high-temperature mold. Higher accuracy of the final reflective surface is the result since this option requires only one replication and no thermal stress relieving. Reflector surface accuracies are expected to replicate very closely to the surface accuracy of the master mold.

2. No Special Facilities for heating and pressurizing the curing laminates. Since room-temperature-curing materials are used, the mold size does not necessarily have to be restricted to accommodate for standard size ovens or autoclaves so large mold sizes can be accommodated. One large master mold can serve as both lay-up mold and assembly tool.

3. Surfaces Can Be Cut/Mapped/Reworked: Once a master mold segment is cut to the proper parabolic shape, it can be mapped using one of several techniques (photogrammetry, theodolites, machining center) and reworked or recut if unsatisfactory.

4. Considerable costs savings are possible with this approach.

4.4 Membrane Reflectors

Several membrane reflector antennas have been developed as possible solutions to the problem of placing large antennas in space. They are low in weight and package volume and can be self deploying. The foremost problem with this type of antenna has been the limitations with regard to geometric precision. Part of the problem stems from the fabrication method whereby a limited number of film gores are pieced together to approximate the ideal geometry [4.4-1-4]. For certain designs, the imperfect geometry is improved because the deployment load assists in correcting the shape [4.4-1-4]. In other words, the shape becomes a function of the applied load, the elastic (extensible) properties of the membrane, and the initial shape of the reflector. All three factors may not be well defined or easy to maintain. Under laboratory conditions surface precision of 1 mm RMS for a 3.5 meter antenna and .1 mm RMS for a 1 meter antenna have been reported [4.4-1]. The mass density of membrane reflectors including supports and electronics is typically 0.4-0.5 kg/m^2.

4.4.1 *Practically Inextensible Membrane Reflector*

Concept Description: A membrane is called inextensible if both normal and shearing in-surface strains can be assumed zero (i.e., no stretching). Thus, an inextensible membrane is perfectly rigid in terms of surface stretching and perfectly flexible in bending. Such a membrane lacks elastic deformability but possesses kinematic deformability, much like a multi-degree-of-freedom mechanism with absolutely rigid members. As a consequence, if an inextensible membrane is smoothed of folds (stabilized) the geometric shape is guaranteed to be precisely that of the fabricated shape.

Although theoretically a membrane is modelled as perfectly flexible, in reality it possess a finite bending stiffness, D, which for an isotropic material is given by:

$$D = Et^3/12(1-\nu^2) \qquad (4.4\text{-}1)$$

Here E is the modulus of elasticity, t is the membrane thickness, and ν is the Poisson ratio of

the material. Efficient storage and deployment require minimizing the bending stiffness of the membrane which can be achieved by reducing its modulus of elasticity and thickness. This, however, is in apparent conflict with the inextensibility requirement since the extensional stiffness of the membrane,

$$B = Et \tag{4.4-2}$$

is also a function of E and t. Comparing Eqs. (4.4-1) and (4.4-2) shows that, for an isotropic membrane, the best compromise is to reduce membrane thickness. An inherent limitation in this approach is the strength requirement of the membrane. The proposed concept achieves the desired combination of membrane inextensibility with bending flexibility by creating a custom-tailored composite material. It is comprised of extensionally stiff, strong fibers and a flexible matrix which results in a rugged continuous (seamless) membrane.

4.4.2 *Membrane Design and Material Selection*

Space environments place extraordinary demands on material performance, especially for polymer materials. Membrane design and material selection are primarily concerned with two interrelated aspects: mechanical properties, and functional performance (electrical). The most important mechanical considerations for the membrane include:

1. Practical Inextensibility
2. Coefficient of Thermal Expansion
3. Creasing
4. Extreme Temperatures
5. Ultraviolet Degradation
6. Vacuum Exposure

Looking at the first consideration, a membrane is considered to be practically inextensible if the material elastic deformations are within a prescribed tolerance for a given range of external loads. This tolerance is usually specified as a fraction of the operational wavelength. As the antenna size or focal length to diameter ratio increases the requirement of practical inextensibility becomes more difficult to achieve.

To determine the maximum external (deployment) load that the membrane can support yet still remain practically inextensible, requires the selection of fibers and the determination of the fiber/matrix volume fraction, fiber layout, and the membrane thickness. One approach in determining these membrane parameters is to require that the membrane have a zero coefficient of thermal expansion (CTE).

To this end, an extensive analysis was performed using existing theories in the literature to determine an appropriate combination of materials that would satisfy the above requirements. The proposed concept for the membrane materials is a result of that analysis.

The analysis investigated specifically: silicone elastomer, glass filler and Kevlar fiber. This combination was analyzed in detail to produce a zero CTE material that could be produced in a quasi-isotropic lay-up. The analysis then continued, to determine if the combination could satisfy the requirements of practical inextensibility and good creasing resistance. It was found

that the silicon elastomer with reasonable amounts of glass filler ($V_f = 20-50\%$) combined with Kevlar at volume fractions of 40% to 60% could provide quasi-isotropic composites with zero or near zero CTE. Furthermore, the material was found to have very adequate membrane stiffness and creasing resistance. The silicone elastomers, fluoroelastomers, and the silicon-flouroelastomers in general have demonstrated good resistance to harsh environments [4.4-5,6] and have had previous applications in space.

4.4.3 *Deployment Alternatives*

Mechanical Deployment: Numerous antennas have been designed and built in an effort to obtain a precision geometry by manipulating an extensible (mobile) surface, such as a mesh, through the use of precision length strings or cords attached to this mesh [4.4-7-9]. These designs become particularly difficult or possibly unrealistic as the operational frequency increases.

The philosophy behind the proposed mechanical deployment concept is opposite to previously attempted designs. A highly elastic medium which is not of precision length is attached to a practically inextensible precision molded surface (composite membrane) and by simply engaging the elastic medium (which is fairly easy), the membrane is reliably stabilized. A prototype which successfully demonstrates this concept has been built and analyzed (Fig. 4.4-1). The shortcoming of this prototype was poor storage volume, however the problem can be remedied by utilizing a different elastic medium.

The stabilization method is illustrated in Fig. 4.4-1b. The structural skeleton of the system involves four main components: a compression pole (1) which doubles as a waveguide; a conical fabric skin (2); a system of 12 thin ribbons (3) radiating from the top of the pole; and a compression ring (4) at the junction of the straps and the fabric cone. The flexible parabolic membrane (5) has its edge attached at the same junction, and the space between the membrane and the conical skin is filled with a very low density, elastic material (6) adhered to both surfaces. This material may be an array of highly elastic "strings" which need not be precision length members.

In the process of deployment, the central pole is extended thereby inducing tension in the skin and ribbons, and compression in the ring. Tension in the skin has two extremely useful effects. First, due to the skin stretching (however slight), it produces some tension in the elastic medium, and more importantly, in the reflecting membrane, so that the membrane is now taut. Second, the skin itself is now quite stiff (due to prestress) and will resist any tendency of the reflecting surface to wrinkle. Thus, the parabolic membrane is reliably stabilized: its inextensibility prevents any deflection along the external normal, while the skin and the elastic medium restrict deflections in the opposite direction. Additionally, any factors which attempt to distort the membrane geometry (e.g. thermal gradients) are resisted by the action of the elastic material.

The design of a 40 meter test article which utilizes this deployment technique is shown in Drawing 1. The contour ring is likely to be a truss structure or "pacring". The RMS surface accuracy of a 40 meter diameter pacring using conventional fabrication techniques was computed to be 0.64 mm RMS. A ring with an accuracy of 0.64 mm RMS is sufficiently accurate to attain the mission requirement of .1 mm RMS, because a flexible material will only have localized geometric distortions. Unlike a rigid reflector, a membrane is very forgiving to local

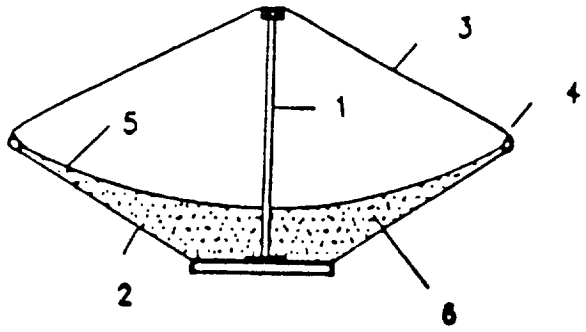

Figure 4.4-1(a and b). Photograph of the mechanical deployment prototype (a), and Drawing of the mechanical deployment prototype (b)

disturbances. It is expected that these imprecisions would only affect a zone within 1-2 cm of the edge which is trivial for a 40 m antenna.

Alternate Deployment Techniques: An attractive alternative to mechanical deployment is to use an electrostatic field to prestress the membrane. An inextensible membrane is particularly well suited for this because the electrostatic field does not have to be very uniform or well controlled. With an inextensible membrane which already has the desired shape, only a slight attractive force is required. Once the deployed membrane has biaxial tension everywhere the correct shape is guaranteed.

A second alternative would utilize a solidifying polymer or foam. The rear of the membrane would have a small pouch. The front of the reflector would have a temporary film pressure chamber which has an initial pressure P_1. A solidifying foam can be injected into the rear pouch with a pressure always less than the film chamber pressure P_1. Once the foam is solidified the front film is no longer necessary and the membrane is reliably stabilized.

4.5 Motion and Controls

4.5.1 *Introduction*

This report discusses the technology issues related to moving the subassemblies of the Large Deployable Antenna (LDA) Point Designs as presently envisaged. The needed motions are briefly reviewed, some present and proposed spacecraft antenna motions are discussed, present motion technology is reviewed with an eye toward specific actuators with a general discussion of some drive train considerations, some vibration reduction issues (antenna surface motion excepted) are discussed, finally, some conclusions are made about the impact of these issues on the LDA project.

4.5.2 *LDA Motion Requirements*

Foldes reported the needed motion characteristics for the top four (of ten) candidate antenna geometries in a trade study. These have also been selected as candidate antenna configurations for the LDA program. Additionally, a fifth concept has been proposed by Foldes in a personal communication with the authors. Three of these concepts involve mechanical motion of the feed, one of the concepts involves complex motion of the subreflector and one of the concepts involves electronic scan using stationary optics.

The motion requirements can be classified into the areas of: ranges of motion required, accuracy required, and speed of response required. The speed of response required has not been determined at this time. Hedgepeth [4.5-1] has analyzed the kinematics of two scan schemes (raster scan and spiral scan). Using his assumptions the required maximum accelerations (α) and maximum angular velocities (Ω) are: $\alpha = 10^{-6}$ rad/sec^2, and $\Omega = 10^{-1}$ rad/sec.

The range of motion and accuracy required of the five Foldes point designs are abstracted in Table 4.5-1 below.

In the Foldes type 1,2 and 3 point designs the motion requirements are composed of linear and angular motions. The linear motion required in Types 1 and 2 is ±.83 m ±2.6 cm. The angular motions required of the Type 1-3 point designs range from ±7.3° to ±21° with needed accuracies of ±0.006 for each case. As an aside, the linear motion tolerances given in Table 4.5-1 for axial motion of the feed are not typical of the required lateral motion tolerances of ±0.3 cm.

The differences in the requirements are primarily the masses involved. This mass difference will have a significant influence on the types of components chosen for the motion system. The masses included in Table 4.5-1 include the approximate counterweight masses to be used to reduce transmitted forces to the rest of the spacecraft.

Table 4.5-1: Motion Requirements for Foldes Point Designs

Antenna Config.	Motion Required	Accuracy	Mass Involved
Type 1	Feed: Axial–±.83 m Angle-±21°	±2.6cm ±0.006°	380kg
Type 2	Feed: Axial–±.83 m Angle–±21°	±2.6cm ±0.006°	39kg
Type 3	Feed: Angle–±7.3°	±0.006°	1221kg
Type 4	None Required	Same	N/A
Type 5	Subr: Axial–±.48 m Radial–±.83 m Azim.-±90° Tilt–±5°	±0.4cm ±0.4cm ±0.04° ±0.04°	145kg

The Type 4 point design has electronic scan capabilities and requires no mechanical motion of the subassemblies of the LDA. The Type 5 point design requires a complex, four degree-of-freedom (DOF), motion of the subreflector. There are two angular and two linear motions required. The angular tolerances are not as strict as those required for feed motion; however, the linear tolerances are similar to the lateral motion tolerances for the feed assembly.

4.5.3 *Antenna Motion Systems*

A partial review of systems, both proposed and tested, that are intended to be utilized for producing motions of antennas for pointing and scanning is given in this section. Many of these systems fall under the classification of gimbals. Most of the literature reviewed here contains studies on systems that have a lower mass than the proposed LDA Point Designs; however, the concepts and approaches may be useful for this project.

Emerick [4.5-2] reports experimental studies (at Ford Aerospace) with an antenna waveguide comprised of a set of steerable RF mirrors. The masses involved were low. The demonstrated pointing accuracy was 0.01°. The torsional stiffness of the actuator was high (over 5000 in-lb/deg). No speed of response information was reported.

Lightsy and Baer [4.5-3] report the analysis (at NASA-Goddard) of a proposed scanning instrument for the second generation GOES satellite with a needed scanning rate of 0.16 deg/sec. The accuracy needed is 1 microradian. The mass to be moved is approximately 18 kg.

Heimerdinger [4.5-4] reports experimental studies with an antenna pointing mechanism. The device had a direct-drive, ball-bearing supported configuration. The accuracy was reported to be in the range of ±0.004° with angular speeds of 0.1 deg/sec. The mass used in this two axis device was 6.3 kg. The total range of motion was ±4°.

Wiktor [4.5-5] discusses the development and laboratory testing (at JPL) of a reactionless precision pointing actuator dubbed the "reactuator" being used as the baseline actuator for the Mariner Mark II class of spacecraft. This actuator has a built-in reaction wheel that is operated in conjunction with the gimbal so that only a small (or zero) reaction force is felt by the spacecraft during motions. Digital resolvers with high accuracy (±29μrad) give position

information. Two-phase, 16-pole brushless dc motors are used to provide torque for the motion. Nickel iron lamination material is used to reduce the cogging torques. Experimental results in a laboratory breadboard of the system set up to reject disturbances from the spacecraft yielded disturbance rejection of greater than 20dB. The particulars of the disturbance frequencies were not given by Wiktor; however, position disturbance responses were reported to be 7 μrad RMS. The mass driven, the range of motion, and the achievable pointing accuracies were not reported.

Hughes Aircraft is marketing a two-axis gimbal with a pointing accuracy of ±0.047° with a range of motion of ±77° (From P. Conley, Hughes Aircraft). The specified inertias to be used in this device are 60 kg-m^2. The torsional stiffness is reported to be 13,000 kg-m/rad. This devices uses conventional bearing technology instead of flexures or magnetic bearings as described below.

Hubert [4.5-6] reports the development and experimental studies with an antenna pointing mechanism that uses a deformable element instead of bearings for a two-axis actuator. Four (two redundant) linear actuators are used to drive the motion through the ±1.5° range of motion for each axis. Accuracies of motion were 0.0015°. Speed of response can be inferred from the experimental time response data and should be at least 2 Hz with an unreported mass loading.

The Annular Suspension and Pointing System (ASPS) developed by NASA in conjunction with Sperry Flight Systems (now Honeywell) a two-axis gimbal to perform rough pointing in series with and a magnetically supported, fine-pointing gimbal. This system was designed to perform precision pointing of large payloads [4.5-7]. The unit is designed for payloads in excess of 600 kg, seemingly well suited for some of the masses involved in the LDA. It was designed to move through ±60° and rotations for the two axes with a pointing accuracy of ±0.1 arc-seconds (2.8×10^{-5} deg). The system featured coarse and fine control loops. Subsequent experimental results with the magnetic suspension portion of this system yielded accuracies less than ±1 arc-second.

Takahara [4.5-8] reports the development and laboratory testing (by Toshiba) of an Antenna Pointing Mechanism (APM) intended to drive a subreflector. This mechanism uses a unique tetrahedron-shaped magnetic suspension system with six degrees of freedom. They demonstrated 0.002 deg pointing accuracies over a ±1.5° range with a 2 kg mass in the laboratory using laser measurements. The speed of response based on the closed-loop data presented is limited to approximately 1-2 Hz. The linear stiffness of the magnetic joint was 200 N/mm. This stiffness will affect the ability of the mechanism to accelerate the masses involved.

4.5.4 *Actuator Technology*

Wide use of permanent magnet motors has been made in projects of this type. The technology in this area is sound and expanding rapidly. Highlights are: New research magnets (up to 35-40 mega gauss Oersteds maximum energy product), PWM control amplifiers, an overall increase in product life and reliability, and a significant reduction in torque ripple (or cogging) by motor design and careful design of digital controllers.

Emerick [4.5-1] reported using Schaeffer Magnetics rotary actuators. These actuators feature permanent magnet stepping motors with high ratio harmonic drives which provide zero backlash. They also reported using an inductively coupled rotary-absolute position transducer with the

capability of 2^{19} bits per revolution.

Wyn-Roberts [4.5-9] reports a so-called Digital Position Actuator (a dc brushless motor with trapezoidal flux distribution) constructed for ESA with space-approved components that is capable of indexing to an accuracy of ±0.0028°.

Lorell [4.5-10] reports the design and testing, by Lockheed, of a precision, wide-dynamic-range actuator for positioning and controlling optical systems. The basic active unit in this system is a voice-coil type actuator with a force offloading system operating with a small time constant to relieve the static power requirements of the voice coil actuators. Flexural members are used to eliminate bearings and the resulting friction. A four-bar linkage is utilized to give a mechanical advantage to the actuator. Experimental results in a laboratory environment, using analog electronics resulted in a positioning accuracy of 20 nm (RMS) with a mechanical range of 2 mm.

Adaptive Truss Actuators: Implementation of the two DOF motion for Types 1 - 2 may be accomplished with separate rotary and linear actuators configured serially; however, the implementation of the four DOF motion for Type 5 is not as clear. There are clear problems in analysis and mechanical complexity with stacking four actuators in series. This application seems well-suited to the use of a variable geometry truss (also termed an adaptive truss).

The concept of utilizing a variable geometry truss (a truss with variable length members actuated by motors) to produce motions or perform robotic tasks has been investigated at NASA Langley Research Center (Rhodes[4.5-11], Warrington[4.5-12]); at VPI&SU (Reinholtz [4.5-13], Lovejoy [4.5-14], and Robertshaw [4.5-15]); and in Japan (Natori [4.5-16]). These actuators operate with the individual member actuators working in parallel. They have been shown to be able to have high number of degrees-of-freedom with a small increase in flexibility. The kinematic relationships (both forward and inverse) have been worked out so that the needed motions can be isolated or done simultaneously. The concept still needs development and needs to have some space-qualified, high-precision experiments performed; however, the potential is high for these actuators to perform the motions needed by the Type 5 LDA point design.

Linear Motors: Although most applications in space call for conventional rotary motors, the use of linear motors and drive systems is a feasible option. The characteristics of linear type motors is much the same as their rotary counterpart. The main differences come into the commutation and feedback control of the device. The linear motors require smaller increments in the spacing of poles to eliminate cogging effects found in poles spaced outside the overlap of the magnetic fields.

4.5.5 *Power Train Considerations*

Bearings and gearing will play an important role in the actuation of the LDA subsystems. Bearings (more generally, the support structure) must allow motion with a minimum of friction which can degrade the pointing performance of the system.

Lowenthal [4.5-17] discusses the problems with rolling element mechanical bearings for use in gimbals. The problems mentioned are formidable with conflicting performance specifications of high precision and low friction in the face of high temperature gradients (which affect bearing

dimensional stability) and low speeds (which affect bearing lubrication).
The flexural bearings or magnetic bearing systems discussed earlier (Hubert [4.5-6], Geirsson [4.5-18], Cunningham [4.5-7], Lorell [4.5-10], and Takahara [4.5-8) have an advantage in bearing characteristics and therefore better pointing precision. The disadvantage is in complexity (magnetic bearings must have an active control system), range of motion (flexural bearings move against an effective linear spring), and cost.

Traction drives or roller actuators for space applications are discussed by Williams [4.5-19] and Steinitz [4.5-20]. The promise of high stiffness and zero backlash spurred this research. Steinitz reports a drift of approximately 30 arc-seconds (0.0083°) over a 24 hour period with a load of 1980 in-lb (223 N-m) for a roller actuator.

The smooth transference of motion through the gear train of the actuator structure is important. A few design considerations are zero backlash, high stiffness, and smooth operation. Simplicity is another very important element in a high reliability application. One option for course and fine motor control is a planetary gear train providing two ratios with singular input. It may be possible to use such a system rather than separate actuators for course and fine motion.

4.5.6 *Vibration Control*

The LDA system will have to have some vibration control capabilities. Disturbance inputs to this system will come from its own required motion as well as from the motions of the space platform to which it is attached. The actuators envisaged for use in producing the required LDA motions can also be utilized to attenuate vibration. It will be important to have as many practical motion inputs as possible to insure controllability.

Many of these vibration control concepts have been demonstrated in laboratory experiments. Juang [4.5-21] uses a rotary actuator to control the vibration of a continuum attached to it. Fanson [4.5-22] describes an active member truss concept for controlling vibrations of the precision structure. Additionally, there is a whole body of knowledge concerning the addition of proof mass and reaction wheel type actuators for vibration suppression. Clark [4.5-23] performed an analytical (parametric) comparison study of three inertial actuator concepts and an active truss concept for controlling the vibrations of the (so-called) mini-mast at NASA LaRC.

The LDA vibration control task could be formidable. For example, the trusses connecting the main reflector and the subreflector could be 45-50m long. There do not seem to be any experiments with vibration control of truss beams that long where travelling wave effects will be come significant. Von Flotow ([4.5-24] and other publications) has investigated this problem in a controls context.

Stiffening the structure is certainly a time-tested method for providing passive vibration control. This method results in decreased vibrational amplitude as the structural frequencies increase. However, the level of accuracy needed from the sum of all the individual component and phenomenologial accuracies is the same as that given in Table 4.5-1. This is the concept of an *accuracy budget*. If, then, there are structural vibrations that result, for example, in a feed angle deviation of ±0.006° (see Table 4.5-1), then the allowable deviations resulting from all other effects: actuators, thermal effects, structural inaccuracies, gravity gradient loading, etc. must all

be zero.

The concept of *vibration control* can be broadened to cover a range of time scales that coincide with the forcing functions that the LDA will experience. This will then lead to the idea that vibration control in this case will become *metric control and compensation.* The motion actuator systems discussed in this section can be used to perform large structure compensation over a wide range of time scales (from solar loading cycles to higher modes of the structure). These actuators are already in place; the ingredient missing for control is that of measurement--it seems to be unavoidable.

4.5.7 *Summary of Motion Technology*

The technology issues relating to moving the subassemblies of the LDA system have been discussed. The general requirements stated in Table 4.5-1 are in the same ranges as some systems that have been proposed and tested (and discussed in the open literature). It appears then, that this motion control will be possible, especially if some technology from presently classified projects is released. The needed motions may be possible with motion control systems using direct or geared drives and mechanical rolling element bearings rather than magnetic or flexural bearings. This would be the preferred approach. The need for a high number of degrees-of-freedom in the motion control system for one of the point designs may lead to some unique configurations for the motion control hardware. This high degree-of-freedom will be an advantage in the vibration control task.

Vibration control has been generalized here to the concept of metric control and compensation for the LDA system. If the structure can be made relatively stiff so that characteristic structural frequencies are high and the concomitant vibration amplitudes are low, then the motion control system may also be utilized to perform large structure compensation.

4.5.8 *Scan Kinematics*

Two scanning schemes for the LDA radiometer were investigated; first, a raster scan; second, a spiral scan. The time to perform the scan of a circular area for the different schemes was determined to compare the two methods. It was found that a spiral scan, starting at the center and spiraling outward, requires approximately 85 percent of the time required the raster scan. The raster scan involves starting at an edge and scanning across the circular spot. The time for the scanning was determined by the relationships between maximum angular velocity, maximum acceleration, size of scan spot and angular size of scan area.

For a sample circular area of 7.5 degrees or 0.13 radians, dwell time at each small section of the scan area of 0.001 seconds, scan sections of radius 2.38×10^{-4}, and a angular acceleration of 10^{-6} rad/sec^2, the total scan time was determined for the two different schemes. With an electronic scan capability of ±25 beam widths a 3-hour scan time would be possible for the raster scan. The disturbing torque for a 3,000 kg antenna with a radius of gyration of 10 m would be only 0.3 N-m.

Although the spiral scan is only 15 percent faster than the raster scan, it may have the great advantage that the motion is smooth; the "jerk" (third time derivative) is small. It should be easy

to provide a lightweight, simple, self-contained control system that can steer the antenna independently from the spacecraft on which it is mounted.

On the other hand, the raster scan has the advantage that the electronic scan could be designed so that it is only single-dimensional. This could greatly ease the complexity and size of the feed system, enable a refined phased-array feed with a reasonable number of elements (hence, reasonable cost), and reduce the focal length and height of the antenna system. The self-contained control system for steering would be more complex, but still feasible.

Of course, if mission requirements dictate a two-dimensional electronic scan (for example, in order to dwell on a moderate-scale interesting feature), then the spiral mechanical scan would be preferred.

4.5.9 *A Scan Scenario*

A possible scan scenario which has received support is described here. Slow mechanical slewing of the entire antenna assembly (or the spacecraft) offers several advantages. It reduces difficulties associated with other types of mechanical scan. In particular, relative motions such as translating and/or rotating subreflectors and/or feed assemblies with many potential misalignment problems. For such relative motion schemes to be workable and accurate, on-board sensing and control subsystems may be necessary. If extensive electronic scan approaches are used, the feed system becomes complex and lossy compromising radiometric performance.

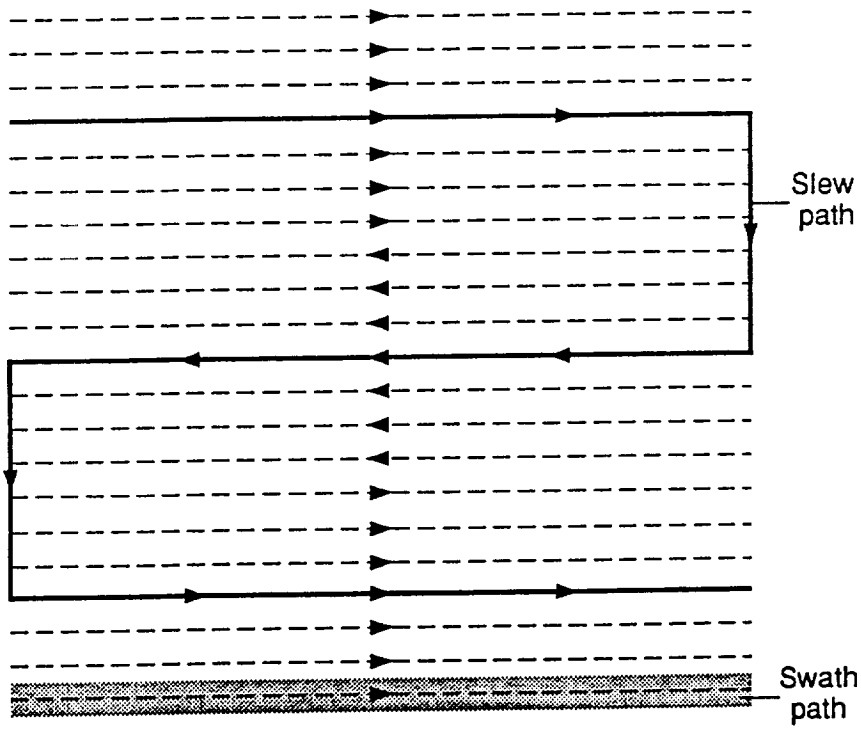

Figure 4.5-1. A Scan Scenario. Slow coarse scan is by mechanical slewing of the entire antenna (or spacecraft).

Figure 4.5-1 illustrates the concept. The slew path is the path of the boresight axis of the reflector system as it is mechanically slewed. Individual swaths are from multiple feeds with individual radiometers or a single feed which is electronically scanned (or mechanically moved). It is a raster type of coarse scan. At the same time, there are several feeds (six shown in the figure) in the reflector each with its own radiometer displaced to produce swatch paths that fill in between coarse scans. Alternatively, a feed array could be electronically scanned rapidly during slow mechanical scan. This, however, may not have sufficient dwell time. Several variations on this theme are possible as well.

To generate some numbers, let there be

N_r = Number of simultaneous radiometers
N_s = Number of slews
$N = N_r N_s$ = Number of swaths

For a 20 km (half power beamwidth footprints) swath width using a 40-m reflector at 18 GHz, the half power beam width (HP) is 0.0272 degree (see Table 2-1). Then

$$\frac{Earth\ extent}{HP} = \frac{17.2°}{0.0272°} = 632\ swaths$$

are required. This can be generated by various combinations of slews and simultaneous radiometers, i.e., $632 = N_r N_s$. For example, six radiometers (as shown in Fig. 4.5-1) would require 105 slewings.

4.6 Electromagnetic Designs

In Section 3.2 several reflector configurations were presented. Figures 3.3-1 through 3.3-10 show the configurations together with remarks on scan performance. In this section, we select those configurations which should continue to be studied from an electromagnetic standpoint and present more detailed comments on the configurations.

4.6.1 *Selected Electromagnetic Configurations*

Bifocal Dual Reflector Antenna: The bifocal, offset dual reflector antenna (Concept 1.1) is constructed of two shaped reflectors such that their combination produces two perfect focal points corresponding to the ± angular limits of scan. The impetus behind this design is the observation by Rao [4.6-3] that a bifocal dielectric lens has a wider angle scan capability than a dielectric lens with a single focus [4.6-1,2]. Therefore, it is reasonable to assume that a bifocal, dual reflector antenna will have better scan capabilities than a single focus dual reflector antenna. The superior scan capabilities of the bifocal dual reflector have been documented [4.6-3,4].

Rao [4.6-3] designed the bifocal dual reflector by starting with a bifocal cylindrical reflector, and then revolving the cross sectional curve to form a surface of revolution. A representation of the two dimensional surface is shown in Fig. 4.6-1 where focal point B(0,d) corresponds to the $-\alpha$ direction of scan and focal point A(0,-d) corresponds to the $+\alpha$ direction of scan. A disadvantage of this procedure is that by rotating the two dimensional structure to form a three dimensional structure, the two perfect focal points are spread into an imperfect focal ring. Also it should be noted that only axially symmetric structures can be designed by this method leading to aperture

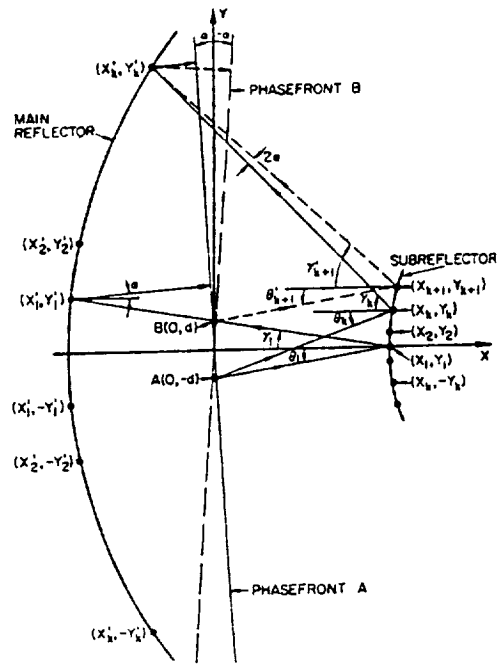

Figure 4.6-1. Cross-Section of Bifocal Dual (Axisymmetric) Reflector [4.6-3]

blockage. Despite these short comings, theoretical analysis of a bifocal dual reflector antenna designed by this technique to have a scan range of ±6° with a main reflector diameter of 6.48 m and a subreflector diameter of 1.25 m showed considerable scan improvement over an equivalent Cassegrain reflector [4.6-3]. The radiation patterns of the bifocal reflector versus those for an equivalent Cassegrain reflector were calculated at 4 GHz over a scan range of 0° to 6° [4.6-3]. The variation in gain and half-power beamwidth of the bifocal reflector, as compared to that of the Cassegrain reflector, is 1.5 dB versus 5.8 dB and 0.8°-0.9° versus 0.8°-1.5°, respectively. The sidelobes are lower for the bifocal reflector except for radiation patterns which are close to or on boresight. The peak gain of the bifocal reflector on boresight is several dB lower than that of the Cassegrain. The theoretical radiation patterns for the same example at a frequency of 6 GHz were also calculated. In this case, the variation in gain and half-power beamwidth of the bifocal reflector compared to that of the Cassegrain reflector is 2 dB versus 9.3 dB and 0.6°-0.7° versus 0.6°-1.2°, respectively.

Rappaport [4.6-4] presented a method of generating three dimensional bifocal reflector surfaces with two perfect focal points. An advantage of this method is that it allows for the design of offset configurations leading to reduced aperture blockage. A disadvantage of this method is that improved scan capabilities are only obtained in the plane containing the two focal points (in [4.6-3], improved scan characteristics are obtained in all directions due to the axially symmetric structure).

Using his method, Rappaport designed and constructed an offset bifocal reflector antenna with a scan capability of ± 8°. To obtain a transverse polynomial for this design, Rappaport first found a two dimensional configuration in which the main reflector approximated a paraboloid.

Then, given the bifocal's main reflector, the unscanned system focal point, and the z-intercept of the subreflector, the closest Cassegrain was found (the hyperbolic subreflector corresponding to the parabolic main reflector). Next, the Cassegrain subreflector's projection onto the yz-plane was identified as its transverse polynomial p(y). This polynomial was then used for the bifocal transverse polynomial to form a three dimensional dual reflector with an approximately parabolic main reflector. This design technique was used so that a parabolic main reflector could be used to simplify construction, and is not meant to be an optimum design [4.6-1].

The offset bifocal reflector designed by Rappaport had a main reflector diameter of 130 λ, a subreflector diameter of 47.5 λ, and a feed-to-subreflector distance minimum of 139.7 λ and maximum of 188.0 λ. Figure 4.6-2 is a comparison of the theoretical scanned peak gain for an offset bifocal, offset paraboloid, most efficient Cassegrain and optimum scanning Cassegrain (the optimum scanning Cassegrain is the closest fit Cassegrain to the offset bifocal from which the polynomial P(y) was taken), each constrained to fit within the same volume and have a 130 λ diameter circular aperture.

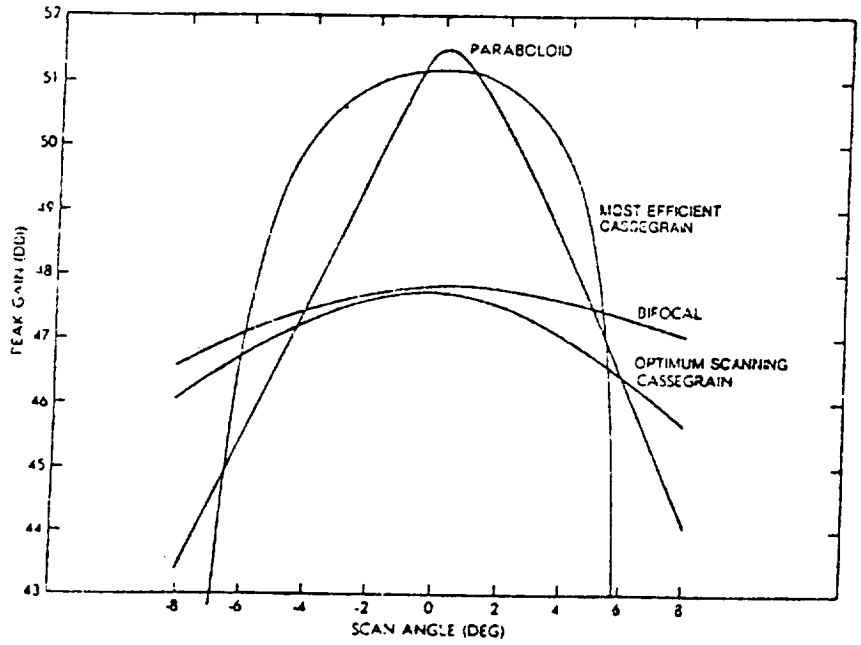

Figure 4.6-2. Comparison of the Scanned Peak Gain for an Offset Bifocal, Offset Paraboloid, Most Efficient Cassegrain, and Offset Cassegrain (each constrained to fit within the same volume and have a 130 λ diameter circular aperture) [4.6-4].

Rappaport constructed a model of this offset bifocal antenna to operate at 36 GHz. Measured versus calculated radiation patterns for scan angles of 8°, 0°, and -8° were determined from the model. The offset bifocal dual reflector achieved a scan angle of ± 8° with a peak gain variation of only 3 dB and a first sidelobe level of at least 15 dB below maximum, with no apparent aperture blockage for any scan direction.

It has been shown that the bifocal dual reflector demonstrates significantly improved scan

characteristics [4.6-3,4]. For this reason, this concept is currently being studied at Virginia Tech. Toward this end, a computer program based on the algorithm of Rappaport's method has been written, and several configurations have been studied. To date only two dimensional configurations have been analyzed, however we expect to be able to analyze full three dimensional configurations in the near future. Our emphasis is on finding a configuration which reduces both sidelobe levels and cross polarization.

Parabolic Torus: The parabolic torus (Concept 1.4 of Table 3.2-1) offers advantages of low feed assembly complexities and (ideally) undistorted azimuth scan. LEO orbit with spacecraft motion providing one direction of scan (elevation) is an excellent application for this antenna [4.6-5]. Feed antennas disposed along the focal arc can be switched individually or in combination to scan the main beam. The penalty paid is reduced aperture efficiency. However, the bottom line is total cost and complexity of the system from concept to space realization. Chu and Iannone [4.6-6] have examined a earth terminal parabolic torus that is 2.5 m wide, 1.25 m high. Tests were performed at 22 GHz where the beamwidth is 0.8° ($F/D_p = 1$). Measurements were made for feed movement along the focal arc giving ±15° FOV (field of view) that was extended to ±20° by squinting the feed after reaching the ±15° limit. Only 1.4 dB gain loss was experienced at ±15°. Scan in the elevation (parabolic curvature) plane was +3.3°/-5.7°. Aperture efficiency was 26%.

A subreflector can be added to an offset parabolic torus to correct for aberrations [4.6-7]. This is shown in Fig. 4.6-3. Scanning in this case is achieved by movement of the feed/subreflector assembly

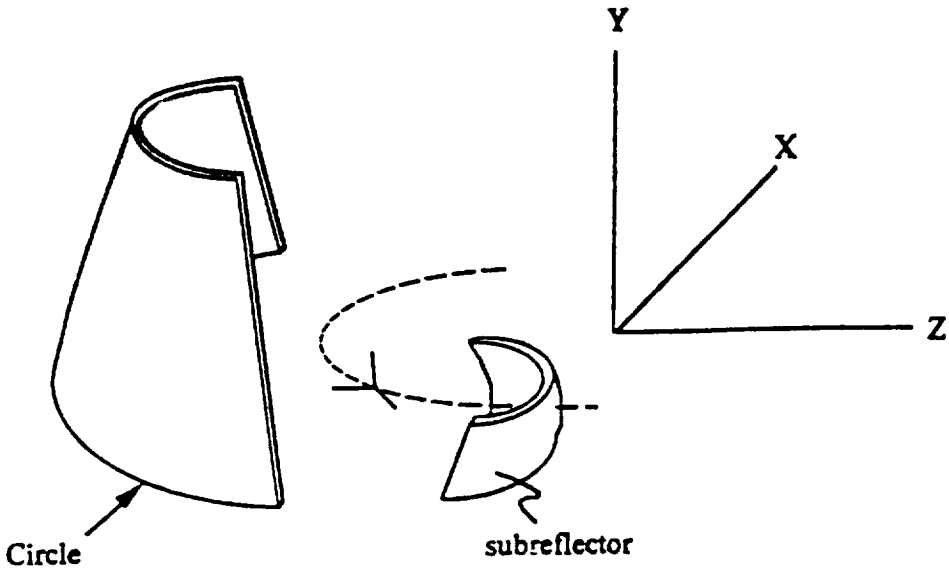

Figure 4.6-3. Dual parabolic torus antenna with a moveable feed assembly for scan

Cylindrical Reflector: The cylindrical reflector (Concepts 2.3 and 3.3 of Table 3.2-1) uses a phased array along the focal line to scan the beam in azimuth. Simple theory for a very long parabolic cylinder and a continuous line feed predicts undistorted scan. However, no results have been reported for the practical case of an array-fed finite cylinder. Therefore, computer analysis

employing physical optics was used to evaluate such an antenna. The results show that the beam is nearly undistorted and experiences very low gain loss during scan.

Spherical Reflector: While spherical reflectors (see discussion in Sec. 3.2.2 and Fig. 3.2-10) have lower aperture efficiency than a paraboloid, it is potentially useful in scanned systems. With a diffuse focal region, the feed system can be moved to scan the main beam with less gain loss than with a paraboloid. Recent research with folded optics feed systems for a spherical reflector to correct for aberrations show much promise. The feed system for the Arecibo 1000-foot diameter spherical reflector is currently being fitted with such a feed [4.6-8]. Both theoretical and experimental results from two multi-reflector feed systems for a spherical reflector have been reported from Japan [4.6-9,10]. They constructed and tested feed systems with two and four subreflectors. The main reflector (effective radius = 3.95 m) was 2.8 m x 1.9 m. The three reflector system had a subreflector of elliptical perimeter (16% x 10% of main reflector) and a circular auxillary reflector (8% of the main reflector size). Scanning was achieved in any direction by rotation of the feedhorn and subreflector about the sphere center. Spherical aberration and crosspolarization correction were obtained along with a 68% aperture efficiency. Tests at 34 GHz gave ±8° by ±2° (±30 BW by ±7.5 BW) of scan with crosspolarization below -28 dB. At 12° of azimuth scan gain was down 1.8 dB.

Watanobe et al. [4.6-10] also designed and tested a five reflector system in which four subreflectors acting as a beam waveguide move, but the feed horn (and main reflector) remain stationary. Measured results similar to those for the tri-reflector were obtained.

Dual Parabolic, Array-Fed Reflector Antenna: For scanning purposes, a large aperture phased array offers many advantages over a reflector antenna system with an equivalent aperture size. Advantages include the speed of electronic scanning and more efficient use of aperture area. A disadvantage of large aperture phased arrays is increased weight and the increased loss and complexity associated with the long interconnections required by large spacing between array elements. A possible compromise involves the use of a small phased array, a large main reflector, and an imaging arrangement of subreflectors. Using these elements, it is possible to form a "magnified" image of the small array in the aperture of the main reflector [4.6-11,12,13].

In the following, a two dimensional array-fed, dual parabolic reflector system (similar to Concept 3.1) is analyzed. Radiation patterns are calculated using the Multiple Reflector Antenna Program for Cylindrical Antennas (MRAPCA), which was developed at Virginia Tech. MRAPCA uses physical optics to approximate the current on the surface of all reflectors in a given antenna configuration.

It is shown that the radiation patterns calculated using MRAPCA can be predicted with reasonable accuracy by modeling the entire reflector antenna system with a large array (called the image array). The element positions in the image array are a magnified image of the element positions in the feed array with relative element phasings preserved. The element patterns in the image array are equivalent to the corresponding element patterns in the feed array after being transformed by the optics. This in itself is not a particularly important result as the effect of the optics on the element patterns of the feed array must still be calculated and hence the procedure saves no computation time while accuracy is lost. Where this result is important is in the insight it gives into the underlying principles behind the array-fed dual parabolic reflector (and by

extension other similar array feed reflector systems). The observation is made that one could design a large array using pattern synthesis techniques and then by using the proper magnification factor, find an array fed reflector system with similar characteristics. Also, if array thinning techniques are employed in the design of the large array, then the number of elements in the corresponding feed array may likewise be reduced.

In order to highlight the ideas presented above, two examples are presented in appendix 2 using a simple two dimensional axisymmetric array-fed dual parabolic reflector. The geometry used is shown in Fig. 4.6-4. It is noted that the high aperture blockage of this configuration makes it impractical for use as an actual antenna configuration. Aperture blockage effects are not accounted for in this study so that the basic capabilities of each concept can be observed. With reference to Fig. 4.6-4, the principle behind the array fed dual reflector can be explained as follows: The feed array excites a plane wave which reflects off of the subreflector and is focused to point F. The waves then spread spherically from F to reflect off of the main reflector and form a plane wave in the aperture of the main reflector.

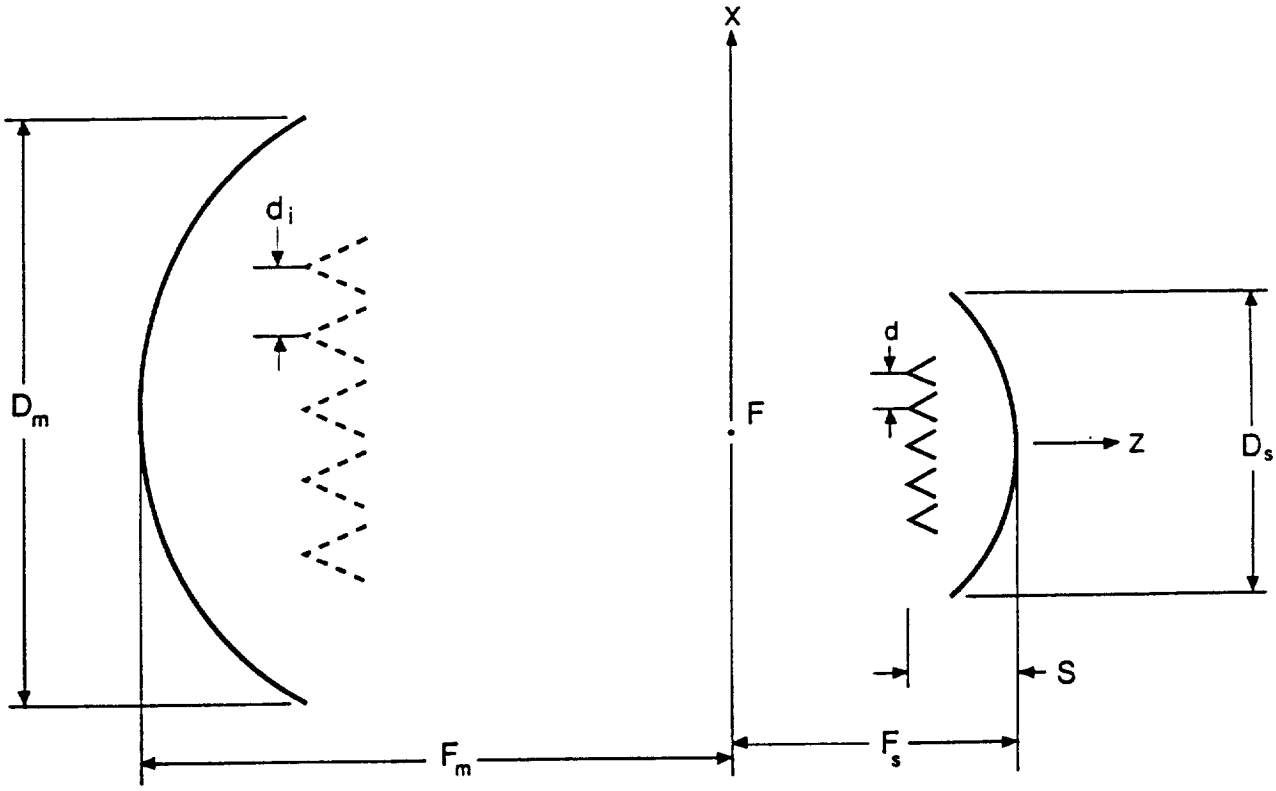

Figure 4.6-4. Cylindrical array feed dual parabolic reflector antenna. The dashed elements in the aperture of the main reflector represent the magnified image of the feed array

The dashed array elements shown in Fig. 4.6-4 represent the element positions of the image array. If the interelement spacings in the feed array is d and the magnification factor for the system is M, then the interelement spacings in the image array can be approximated by Md [4.6-12,13]. In several cases, the effect of a linear phase tilt on the feed array will be considered; therefore, let α denote the relative phase between adjacent elements.

In the following examples, the diameter of the subreflector is $D_s = 50\ \lambda$, and the focal length of the subreflector is $F_s = 50\ \lambda$. The distance from the plane of the feed array to the apex of the subreflector is $S = 6.25\ \lambda$. The distance between elements in the feed array is denoted by d, this value, along with the number of elements in the feed array, will be varied in the following examples. The diameter of the main reflector is $D_m = 100\ \lambda$, and the focal length of the main reflector is $F_m = 100\ \lambda$. The magnification factor for this reflector configuration is $M = F_m/F_s = 2$.

Example 1: Comparison of Radiation Patterns of the Reflector System and Corresponding Image Array

In this example a 15 element feed array with interelement spacings of $d = \lambda/4$ and $\cos^2(\theta)$ element patterns is used. Radiation patterns were calculated using MRAPCA for interelement phase shifts of $\alpha = 0°$ and $\alpha = 10°$. The pattern for the $\alpha = 0°$ is shown in Fig. 4.6-5. It is noted that in both cases, the patterns die off rapidly after $\theta \approx 7.5°$. The radiation pattern for the $\alpha = 10°$ has a beam maximum at $\theta \approx 3°$ and shows a distinct asymmetry about the main beam.

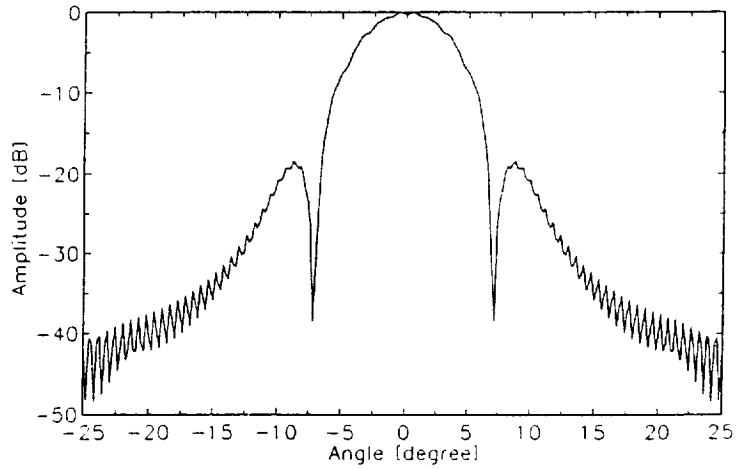

Figure 4.6-5. Radiation pattern of Array-fed Dual Parabolic Reflector, calculated by MRAPCA, 15 element feed array, interelement spacings of d=λ/4.

Using the magnification factor of M = 2, the interelement spacing of the image array is Md = $\lambda/2$. The radiation pattern of this image array, for the phase factor of $\alpha = 0°$, and element patterns of $\cos^2(\theta)$, is shown in Figs. 4.6-6. The gross features of the pattern (the $\alpha = 10°$ pattern as well), null locations and beam pointing angles, agree quite well with those calculated by MRAPCA. However, the finer features of the patterns, such as first side lobe levels and the rapid decrease in amplitude after $\theta \approx 7.5°$, are not present. Because these features are dependent on the element patterns, it is reasoned that the element patterns used with the image array were not correct.

A typical radiation pattern from the reflector system when fed by only one element in the feed array, was calculated by MRAPCA. This pattern, which dies off rapidly at $\theta \approx 7.5°$, shows promise as a potential element pattern for the image array. Therefore, the radiation pattern from the image array with each element pattern equal to the radiation pattern of the corresponding element in the feed array, after being transformed by the optics, was calculated for $\alpha = 0°$ and

$\alpha = 10°$. The case for $\alpha = 0°$ is shown in Figs. 4.6-7. As may now be expected, the pattern agrees quite well with that calculated by MRAPCA.

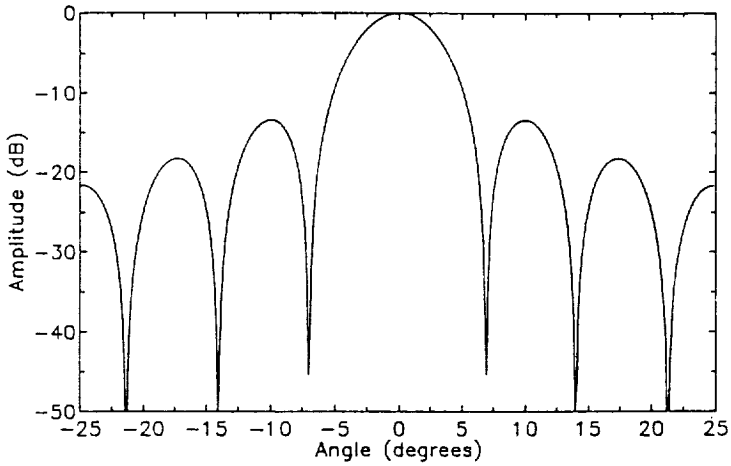

Figure 4.6-6. Radiation pattern of 15 element image array with interelement spacings of md = λ/2. Element patterns are $\cos^2(\theta)$. Relative element phases are $\alpha = 0°$

Example 2: Application of Pattern Synthesis to Feed Array Design

This example demonstrates how pattern synthesis techniques may be used to improve the characteristics of an array-fed parabolic dual reflector. For this example, a 51-element feed array with interelement spacings of λ/4 and $\cos^2(\theta)$ element patterns is used. The radiation patterns were calculated by MRAPCA for $\alpha = 0°$, 10° and 20°. The pattern for the $\alpha = 10°$ is shown in Fig. 4.6-8. It is noted that the first sidelobe levels for these patterns are approximately -12 dB below the main beam peak. In order to reduce the sidelobe levels, a Dolph-Chebyshev technique is used. A sidelobe level of -40 dB was specified, and the corresponding relative element

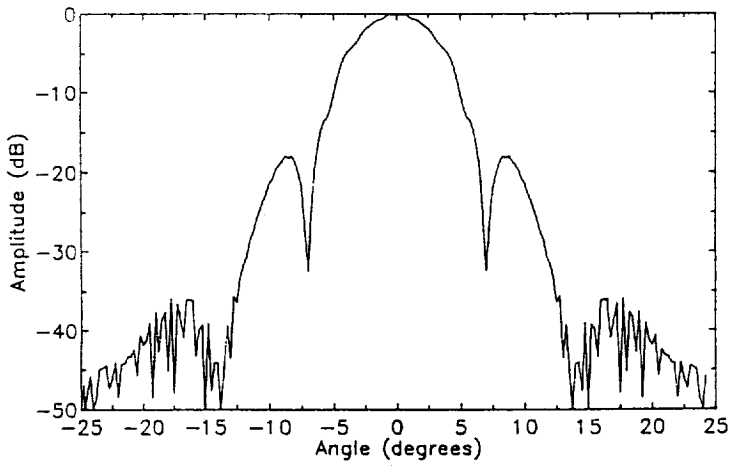

Figure 4.6-7. Radiation pattern of 15 element image array with interelement spacings of md = λ/2. Element patterns match the corresponding elements in the feed array after being transformed by the optics.

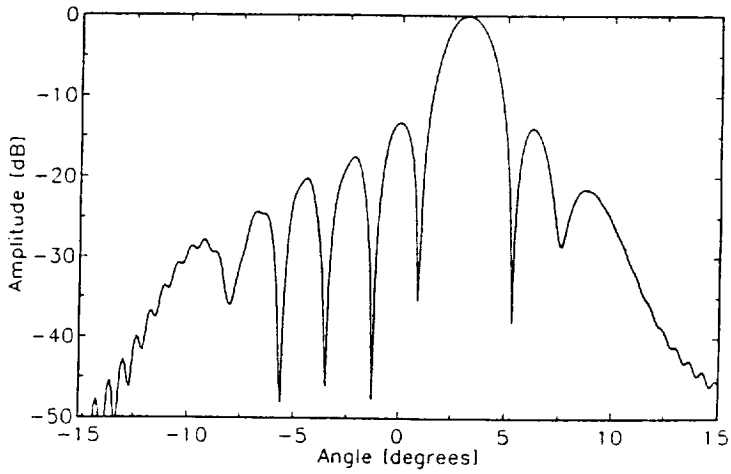

Figure 4.6-8. Radiation pattern of an array-fed dual parabolic reflector, calculated by MRAPCA, for a 51 element feed array. The relative element phases are α = 10°.

amplitudes calculated for the image array of 51 elements spaced $\lambda/2$ apart. These element amplitudes are then applied to the elements of the feed array such that the element patterns are now given by $A_n\cos^2(\theta)$, where A_n represents the amplitude of the n^{th} array element as calculated by the Dolph-Chebyshev technique. The radiation patterns were calculated by MRAPCA for this case, with α = 0°, 10° and 20°. The pattern for α = 10° is shown in Fig. 4.6-9. For the unscanned case (α = 0°) the -40 dB sidelobe level goal is achieved. For the case of α = 10°, a scan of $\theta \approx 3°$ is achieved with a sidelobe level of about -37 dB. For α = 20°, a scan of $\theta \approx 6°$ is achieved with a sidelobe level of about -29 dB. The increase in sidelobe level of the scanned cases may be accounted for by the element patterns which reduce the peak gain of the main beam for these cases.

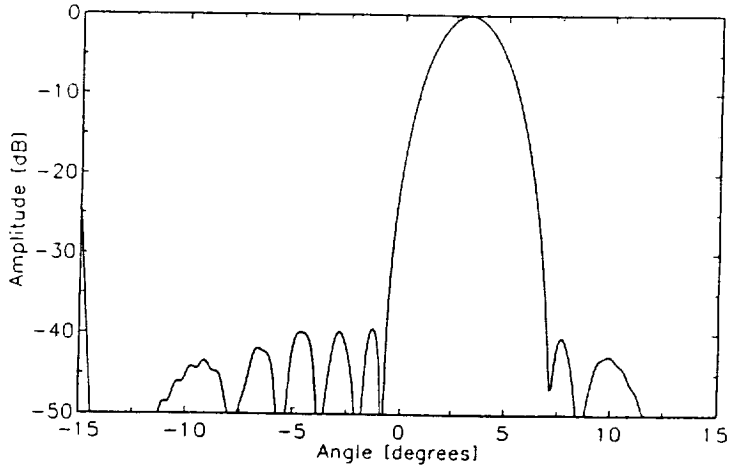

Figure 4.6-9. Radiation pattern for same configuration as shown in Fig. 4.6-8, but element amplitudes are based on a Dolph-Chebyshev array of 51 elements spaced $\lambda/2$ apart.

To conclude, it has been shown that the radiation patterns of an array-fed dual parabolic reflector antenna can be approximated by the radiation pattern of an image array with the relative phase between elements in the image array equal to the relative phase between elements in the feed array. The element patterns in the image array can be approximated by the element patterns of the corresponding elements in the feed array after being transformed by the optics. Using this concept, a Dolph-Chebyshev synthesis procedure was used to find the relative amplitudes of the elements in the image array to produce a sidelobe level maximum of -40 dB below the main beam peak. Feeding the dual parabolic reflector with an array whose elements possess the calculated amplitude distributions, produced a radiation pattern with a -40 dB sidelobe level for the unscanned case, and a -30 dB sidelobe level for a theta $\approx 6°$ scanned case.

Summary

The following areas are targeted for future investigation:

1. The development of a more reasonable offset dual parabolic configurations.
2. Evaluation of the effect of reflector size on the element patterns in the image array.
3. Evaluation of the effects of increasing the interelement spacings of the feed array.
4. Exploring the applications of pattern synthesis and array thinning techniques in the design of array-fed dual parabolic reflector antennas.

5. SUMMARY AND CONCLUSIONS

1. Structural Designs and Configurations

   a. Several structural design approaches were conceptualized and evaluated (Chap. 4).

   b. Parametric studies were calculated; they showed the need for "thick" reflector facets supported by a "deep" truss structure for configurations approaching 40 m diameter antennas (Sect. 4.2.3).

2. Reflector Surfaces

   a. Evaluated three reflector surface concepts: rigid facet, furlable surfaces, and membrane surfaces. Of these the rigid facet approach appears most capable of meeting inplane requirements (Sects. 4.3, 4.4).

   b. Preliminary studies indicate that an areal density of 2 kg/m^2 for a rigid facet is reliable this close to the initial goal of 1 kg/m^2 (Sect. 4.3.1).

   c. The total thickness of rigid facets 2.0- and 3.1-m square facets to accommodate ground testing and demonstrate a surface accuracy of 0.1 mm RMS are 7.26 cm and 14.02 cm, respectively (Sect. 4.3.1).

   d. Analysis of square rigid facts was based on a four-point support. Additional facet-truss interface points could reduce the above mentioned facet areal density and thickness values (Sect. 4.3.1.1).

   e. Two design concepts were developed and evaluated for utilizing furlable reflector surfaces on square and gored Pactruss configurations (Sect. 4.3.3).

   f. An experimental investigation of deployment repeatibility was conducted with 0.0006 inch maximum variation over three deployment of a one-meter furlable reflector (Sect. 4.3.3.1).

   g. The influence of a 0.05 inch-thick, 0.5-wide shim on the reflector support interface was measured and showed a 0.0025 inch increase in surface rms deviation on the one-meter furlable reflector (Sect. 4.3.3.1).

   h. Detailed design concepts were developed for controllable deployment and registration of furlable segments on to a support structure (Sect. 4.3.3.1).

   i. Manufacturing techniques were conceived for fabricating large furlable segments. A single mold concept was developed as well as mold fabrication techniques (Sect. 4.3.3.2).

   j. In order to meet the design goal of 0.1 mm RMS surface accuracy in a 1-g environment, the maximum size is 12 m for the furlable configurations studied (Sect. 4.3.2).

   k. A new membrane concept utilizing practically inextensible molded membranes was

studied (Sect. 4.4.1). Included in this study was a new hybrid composite material composed of silicon chopped glass fiber with Kevlar reinforcement (Sect. 4.4.2).

l. Preliminary analysis of the practically inextensible membrane concept indicated that a 15 m reflector may be possible.

3. Materials and Controls

a. We performed a materials technology review for precise reflector applications (Sect. 3.5).

b. A motion and controls study was performed to determine LDA motion requirements and evaluate actuator technology (Sect. 4.5).

c. Scan scenarios and their implications on revisit time and acceleration/deceleration requirements were examined (Sects. 4.5.8,9).

d. SMA actuated hinge concept for deployment of rigid facets on a support truss was developed.

4. Electromagnetic Results and Antenna Configurations

a. The desired full range of frequencies (6 to 220 GHz) was determined with input from the Electromagnetic Advisory Committee (EMAC) to not be addressable at this stage. This is because feed array technology above 60 GHz for space radiometers is not considered available in the near term. Also, all frequency bands from 6 to 220 GHz in a single antenna is not practical. Instead, we consider here a 6 to 60 GHz design and leave the 60 to 220 GHz for further development (Chapter 2).

b. Antenna concept trade-offs were examined carefully. The types considered were full mechanical slewing, full electronic scanning, and hybrid configurations of partial mechanical and partial electronic. Hybrid configurations are attractive, but selection of a specific design await further mission requirements definition and detailed EM analysis (Sect. 3.2).

c. The feed will, of necessity, be physically large. This dictates an offset-fed reflector to reduce aperture blockage.

d. The design of an offset multiple reflector system, with several alternative configurations, which can be either scanned electromagnetically or mechanically slewed is the baseline design (Fig. 3.3-2).

e. The typical radiometer flown to date employs a 1-meter class reflector operating above 10 GHz in a LEO orbit with a resolution of 15 to 100 km (Sect. 3.4).

f. A detailed study of previous deployable antenna concepts and prototype hardware was conducted.

g. The baseline design requires detailed electromagnetic analysis and mechanical implementation study.

h. In parallel with the baseline design efforts, several alternative concepts were considered potentially suitable for wide scanning radiometric application. These include: the bifocal, offset dual reflector; the parabolic torus, the cylindrical reflector; the spherical reflector; and the dual parabolic, array-fed reflector (Sect. 4.6).

   Computations on the finite cylinder reflector with a linear array feed showed excellent scan performance. Computations for cylindrical array-fed dual parabolic reflector antenna also indicate potential value.

i. The alternative concepts are necessary for two reasons. First, mission contraints as they unfold may dictate, for example, that mechanical slewing is not permitted. Second, wide scanning with approporiate realization (undistorted beam scanning, feed implementation, etc.) remain to be demonstrated.

j. Other electromagnetic issues were not addressed including radiometric system design and feed realization.

6. REFERENCES

1-1 Ride, S.K., "Leadership and America's Future in Space - A Report to the Administrator", NASA, Aug. 1987.

1-2 Ad Hoc Review Team on Space Technologies, "Technology for the Mission to Planet Earth,"

2-1 A. J. Gasiewski and D. H. Stalin, "Science Requirements for Passive Microwave Sensors on Earth Science Geostationary Platforms," *Proceedings of the NASA Technology Workshop for Earth Science Geostationary Platforms*, NASA CP-3040, July 1989.

4.2-1 Thompson Ramo Wooldridge, Inc., "Sunflower Solar Collector," NASA CR-46, May 1964.

4.2-2 Ard, K.E., "Design and Fabrication Study for Extreme Precision Antenna Structures," NASA CR-174861, August 1985.

4.2-3 Hedgepeth, John M., and Louis R. Adams, "Design Concepts for Large Reflector Antenna Structures," NASA CR-3663, January 1983.

4.2-4 Hedgepeth, John M., "Critical Requirements for the Design of Large Space Structures,"NASA CR-3484, November 1981.

4.2-5 Hedgepeth, John M., "Influence of Fabrication Tolerances on the Surface Accuracy of Large Antenna Structures," *AIAA Journal*, Vol. 20, No. 5, pp. 680-686, May 1982.

4.2-6 Hedgepeth, John M., "Accuracy Potentials for Large Space Antenna Reflectors with Passive Structure," *J. Spacecraft and Rockets*, Vol. 19, No. 3, pp. 211-217, May-June 1982.

4.2-7 Hedgepeth, John M., "Support Structures for Large Infrared Telescopes," NASA CR-3800, July 1984.

4.2-8 Dyer, J.E., "Development of a Verification Program for Deployable Truss Advanced Technology," NASA CR-181703, September 1988.

4.2-9 Ribble, J.W. and Woods, A.A., "On the Design of Large Space Deployable Modular Antenna Reflectors", *15th Aerospace Mechanisms Symposium*, Marshall Space Flight Center, AL, May 14-15, NASA CP-2181, 1981.

4.2-10 Kellermaier, H., Vorbrugg, H., and Pontoppidan, K., "The MBB Unfurlable Mesh Antenna (UMA) Design and Development," *AIAA 11th Communication Satellite Systems Conference*, San Diego, CA, March 17-20, 1986.

4.2-11 Hedgepeth, John M., "Sequential Deployment of Truss Structures; Large Space Systems Technology - 1981," NASA CP-2215, Part 1, pp. 179-192, 1982.

4.2-12 Coyner, J.V., "Box Truss Development and Its Applications", NASA CP-2368, *Large Space Antenna Systems Technology - 1984*, 1985.

4.2-13 Batchell, E.E., Bettadapur, S.S. and Coyner, J.V., "Integrated Analysis System for Box Truss Antenna Mech Performance," *AIAA 11th Communication Satellite Systems Conference*, San Diego, CA, March 17-20, 1986.

4.2-14 Coyner, J.V., and Batchell, E.E., "Box Truss Antenna Technology Status," NASA/DoD Control/Structures Interaction Technology - 1986, Norfolk, VA, November 18-21, 1986, NASA CP-2447, part 2, 1987.

4.2-15 Coyner, J.V. and Tobey, W., "Space Deployable Box Truss Structure Design," *15th Aerospace Mechanisms Symposium*, Marshall Space Flight Center, AL, May 14-15, 1981, NASA CP-2181, 1981.

4.2-16 Hedgepeth, John M., "Pactruss Support Structure for Precision Segmented Reflectors: Final Report," AAC-TN-1153, Astro Aerospace Corporation, Carpinteria, California, September 1988.

4.2-17 Bernasconi, M.C., and G.G. Reibaldi, "Inflatable, Space-Rigidized Structures: Overview of Applications and Their Technology Impact," preprint IAF 85-210, *36th Congress of the International Astronautical Federation*, Stockholm, Sweden, October 1985.

4.2-18 Bernasconi, M.C., and G. G. Reibaldi, "Large Inflatable Space-Rigidized Antenna Reflectors," International Astronautical Federation, Paper IAF-87-315, *38th IAF Congress*, Brighton, United Kingdom, October 1987.

4.4-1 Veal, G. and Thomas, M., "Highly Accurate Inflatable Reflectors," Air Force Rocket Propulsion Laboratory Technical Report 84-021. Edwards Air Force Base, CA., May 1984.

4.4-2 Goslee, J.W., Hinson, W.F., and Davis, W.T., "Electrostatic Forming and Testing of Polymer Films on a 16-Foot Diameter Test Fixture," NASA Technical Memorandum 86328, Langley Research Center, Feb. 1985.

4.4-3 Kato, S., Takeshita, Y., Sakai, Y., Muragishi, O., Shibayama, Y., and Natori, M., "Concept of Inflatable Elements Supported by Truss Structure for Reflector Application," *39th Congress of the International Astronautical Federation*, Oct. 8-15, 1988, Bangalore, India.

4.4-4 Natori, M., Shibayama, Y., and Sekine, K., "Active Accuracy Adjustment of Reflectors Through the Change of Element Boundary," *30th Structures Structural Dynamics and Materials Conference*, Mobile, Alabama, April 3-5, 1989.

4.4-5 Leonard, L., "Composites in Space-Durability is a Major Concern," Advanced Composites, November/December 1986, pp 35-39.

4.4-6 "Hitchhiker Shuttle Payload of Opportunity Carrier Customer Accommodations and Requirements Specification," Goddard Space Flight Center, Greenbelt, Maryland, July 1988, HHG-730-1503-04.

4.4-7 Hedgepeth, J. M., "Dynamics of a Large Spin-Stiffened Deployable Paraboloidal Antenna," *Journal of Spacecraft and Rockets*, Vol 7, No. 9, September 1970. pp 1043-1048.

4.4-8 Dyer J. E. and Dudeck, M. P., "Deployable Truss Structure Advanced Technology," *First NASA/DoD CSI Technology*. NASA CP-2447, Part 1, 1986, pp. 111-124.

4.4-9 Miller, J. B., Ahl, E. L., Butler, D. H., and Peri, F., "Surface Control System for the 15 Meter Hoop-Column Antenna," *NASA/DOD CSI Technology*. NASA CP-2447, Part 1, 1986, pp. 533-545.

4.5-1 Hedgepeth, J.M., "Analysis of Scanning From a Geosynchronous Platform", Report AAC-TN-1156, Astro Aerospace Corporation, Carpinteria, CA, February 1990.

4.5-2 Emerick, K.S., "Design of a 60 GHz Waveguide Antenna Positioner", *23rd Aerospace Mechanisms Symposium*, NASA CP-3032 (1989).

4.5-3 Lightsy, E. and F. Bauer, "Design and Analysis of a Flexible Body Instrument Pointing System for the GOES Meteorological Satellites", *27th Aerospace Sciences Meeting*, Jan 9-12, 1989, Reno, AIAA Paper 89-0542.

4.5-4 Heimerdinger, H., "An Antenna Pointing Mechanism for Large Reflector Antennas", *15th Aerospace Mechanisms Symposium*, NASA CP-2181 (1981).

4.5-5 Wiktor, P., "A Reactionless Precision Pointing Actuator", *21st Aerospace Mechanisms Symposium*, NASA CP-2470 (1987).

4.5-6 Hubert, B., and P. Brunet, "SOFA: An Antenna Fine Pointing Mechanism", *15th Aerospace Mechanisms Symposium*, NASA CP-2181 (1981).

4.5-7 Cunningham, D.C., T.P. Gismondi, and G.W. Wilson, "Control System Design of the Annular Suspension and Pointing System", *Journal of Guidance and Control*, Vol. 3, No. 1, Jan.-Feb. 1980, AIAA.

4.5-8 Takahara, K., T. Ozawa, H. Takahashi, S. Shingu, T. Ohashi, and H. Sugiura, "Development of a Magnetically Suspended, Tetrahedron Shaped, Antenna Pointing System", *22nd Aerospace Mechanisms Symposium*, NASA CP-2506, (1988).

4.5-9 Wyn-Roberts, D.,"The Evolution of Space Mechanisms in the ESA R&D Program", *23rd Aerospace Mechanisms Symposium*, NASA CP-3032 (1989).

4.5-10 Lorell, K.R., J-N. Aubrun, D.F. Zacharie, and E.O. Perez, "Development of a Precision, Wide-Dynamic-Range Actuator for Use in Optical Systems", *23rd Aerospace Mechanisms*

Symposium, NASA CP-3032 (1989).

4.5-11 Rhodes, M.D., and M.M. Mikulas, "Deployable Controllable Geometry Truss Beam", NASA Technical Memorandum 86366, June 1985.

4.5-12 Warrington, T.J. and C.G. Horner, "Flexible Beam Control Using an Adaptive Truss", To be Presented at the *1990 American Control Conference*, San Diego, CA, May 23-25, 1990.

4.5-13 Reinholtz, C.F., and D. Gokhale, "Design and Analysis of Variable Geometry Truss Robots", *Proceedings of the 10th Applied Mechanisms Conference*, New Orleans, Louisiana, Dec. 6-9, 1987.

4.5-14 Lovejoy, V.D., H.H. Robertshaw, W.N. Patten, and G.C. Horner, "Dynamics and Control of a Planar Truss Actuator", *Vibration Control and Active Vibration Suppression*, DJ Inman Ed., DE-Vol 4, ASME, Sept 1987, pp 47-55.

4.5-15 Robertshaw, H.H., R.H. Wynn, Jr., H.F. Kung, S.L. Hendricks, and W.W. Clark, "Dynamics and Control of A Spatial Active Truss Actuator", *30th SDM Conference*, AIAA Paper #89-1328, pp 1473-1479, April 1989.

4.5-16 Natori, M., K. Muira and H. Furuya, "Deployable Surface Truss Concepts and Two-Dimensional Adaptive Structures", *Proceedings of the 15th International Symposium on Space Technology and Science*, Tokyo, 1986.

4.5-17 Loewenthal, S.H., "Two Gimbal Bearing Case Studies: Some Lessons Learned", *22nd Aerospace Mechanisms Symposium*, NASA CP-2506, (1988).

4.5-18 Geirsson, A. and D.B. DeBra, "Kinematic Support Using Elastic Elements", *22nd Aerospace Mechanisms Symposium*, NASA CP-2506, (1988).

4.5-19 Williams, D.M. and D.P. Kuban, "Traction-Drive Force Transmission for Telerobotic Joints", *23rd Aerospace Mechanisms Symposium*, NASA CP-3032 (1989).

4.5-20 Steinetz, B.M. and D.A. Rohn, "Evaluation of a High-Torque Backlash-Free Roller Actuator", *23rd Aerospace Mechanisms Symposium*, NASA CP-3032 (1989).

4.5-21 Juang, J-N., L.G. Horta and H. H. Robertshaw, "A Slewing Control Experiment for Flexible Structures", *Journal of Guidance and Control*, AIAA, Sept-Oct 1986.

4.5-22 Fanson, J.L., G. H. Blackwood and C-C. Chu, "Active-Member Control of Precision Structures, *30th SDM Conference*, Mobile, April 1989, AIAA Paper #89-1329-CP.

4.5-23 Clark, W.W., H.H. Robertshaw, and T.J. Warrington, "A Planar Comparison of Actuators for Vibration Control of Flexible Structures", *30th SDM Conference*, Mobile, AIAA Paper # 89-1330, April 1989.

4.5-24 von Flowtow, A.H., and B. Schaefer, "Wave Absorbing Controllers for a Flexible Beam", *Journal of Guidance, Control and Dynamics*, Vol. 9, No. 6, AIAA, Nov-Dec 1986.

4.6-1 R. M. Brown, "Dielectric Bifocal Lenses," *IRE Nat. Convention Rec.*, pp. 180-187, 1956.

4.6-2 F. S. Holt and A. Mayer, "A Design Procedure for Dielectric Microwave Lenses of Large Aperture Ratio and Large Scanning Angle," *IRE Trans. Antennas Propagation*, Vol AP-5, pp. 25-30, Jan. 1957.

4.6-3 B. L. J. Rao, "Bifocal Dual Reflector Antenna," *IEEE Trans. Antennas Propagation*, Vol., pp. 711-714, Sept. 1974.

4.6-4 Carey M. Rappaport, "An Offset Bifocal Reflector Antenna Design for Wide-Angle Beam Scanning," *IEEE Trans. Antennas Propagation*, Vol. , pp. 1196-1204, Nov. 1984.

4.6-5 H. Nakaguro, et al., "Development of Cenical Scanning Torus Antenna for Advanced Microwave Scanning Radiometer," *Proceedings of ISAP (Japan)*, pp. 651-654, 1989.

4.6-6 T-S Chu and P. P. Iannone, "Radiation Properties of a Parabolic Torus Reflector," *IEEE Trans. Antennas Propagation*, Vol. 37, pp. 865-874, July 1989.

4.6-7 C. Sletten, ed., *Reflector and Lens Antennas*, p. 355, 1988.

4.6-8 P. S. Kildal, "Exact Synthesis of Offset Multi-Reflector Antennas Using Dynamic and Kinematic Ray Tracing," *International Conference on Antennas and Propagation*, 1989.

4.6-9 F. Watanobe and Y. Mizugutch, "A Offset Spherical Tri-Reflector Antenna," *Trans. IECE of Japan*, Vol. 66, pp. 108-119, Feb. 1983.

4.6-10 F. Watanobe, Y. Mizugutch, and M. Yamada, "A Beam-Steerable Antenna with an Offset Spherical Reflector for Earth Station," *AIAA Comm. Sat. Sys. Conf.*, 1984.

4.6-11 G. Skahill, "A Dual Reflector Antenna Scans Many Beamwidths Without Loss of Gain, Resolution or Sidelobe Level," *Microwave Journal*, pp. 129-139, March 1988.

4.6-12 C. Dragone and M. J. Gans, "Imaging Reflector Arrangements to Form a Scanning Beam Using a Small Array," *Bell System Tech. Journal*, Vol. 58, No. 2, pp. 501-515, Feb. 1979.

4.6-13 A. Kumar, "An Array Fed Dual Reflector Antenna at 36 GHz," *IEEE APS Symposium Digest*, June 1989.

4.6-14 W. L. Stutzman and G. A. Thiele, *Antenna Theory and Design*, John Wiley: New York, 1981.

NASA
National Aeronautics and Space Administration

Report Documentation Page

1. Report No.	2. Government Accession No.	3. Recipient's Catalog No.
NASA CR-4410		

4. Title and Subtitle	5. Report Date
Large Deployable Antenna Program Phase I: Technology Assessment and Mission Architecture	October 1991
	6. Performing Organization Code

7. Author(s)	8. Performing Organization Report No.
Craig A. Rogers Warren L. Stutzman	
	10. Work Unit No. 590-41-14-03
9. Performing Organization Name and Address Virginia Polytechnic Institute and State University Blacksburg, Virginia 24061-0111	11. Contract or Grant No. NAS1-18471
12. Sponsoring Agency Name and Address National Aeronautics and Space Administration Langley Research Center Hampton, Virginia 23665-5225	13. Type of Report and Period Covered Contractor Report
	14. Sponsoring Agency Code

15. Supplementary Notes

Technical Monitor: Lyle C. Schroeder
NASA Langley Research Center
Hampton, VA 23665-5225

Task 18 Report

16. Abstract

This program was initiated to investigate the availability of critical large deployable antenna technologies which would enable microwave remote sensing missions from geostationary orbits as required for Mission to Planet Earth. Program goals for the large antenna were: 40-meter diameter, offset-fed paraboloid, and surface precision of .1mm rms. Phase I goals were to review the state of the art for large, precise, wide-scanning radiometers up to 60 GHz; to assess critical technologies necessary for selected concepts; to develop mission architecture for these concepts, and to evaluate generic technologies to support the large deployable reflectors necessary for these missions. Selected results of the study show that deployable reflectors using furlable segments are limited by surface precision goals to 12 meters in diameter, current launch vehicles can place in geostationary only a 20-meter class antenna, and conceptual designs using stiff reflectors are possible with areal densities of 2.4 deg/m^2.

17. Key Words (Suggested by Author(s))	18. Distribution Statement
large aperture antenna deployable structure geostationary orbit radiometer sensor	unclassified - unlimited subject category 15

19. Security Classif. (of this report)	20. Security Classif. (of this page)	21. No. of pages	22. Price
unclassified	unclassified	88	A05

NASA FORM 1626 OCT 86

For sale by the National Technical Information Service, Springfield, Virginia 22161-2171

NASA-Langley, 1991